Università degli Studi di Udine

Dottorato di Ricerca in
Tecnologie Chimiche ed Energetiche

DESIGN OF NH_3-H_2O ABSORPTION CHILLER FOR LOW GRADE WASTE HEAT RECOVERY

Dr. Marco CEFARIN

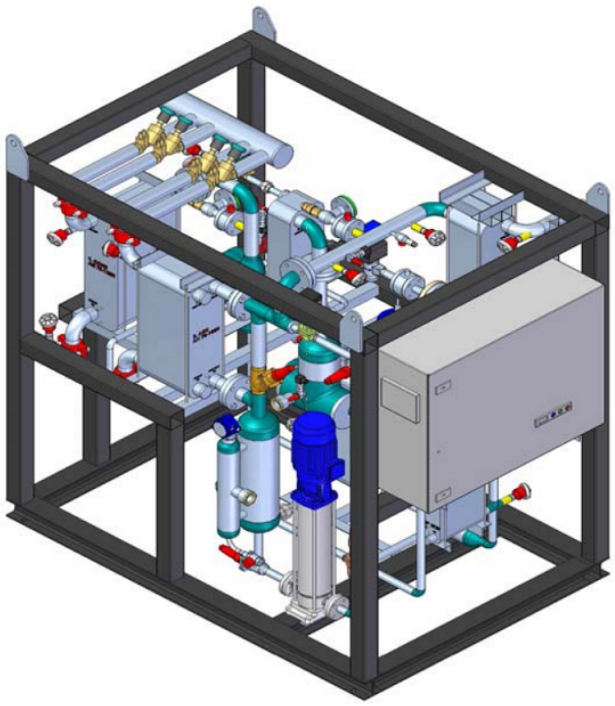

COMMISSIONE

Ing. Sergio BOBBO	Revisore
Prof. Fabio POLONARA	Revisore
Prof. Piero PINAMONTI	Commissario
Dott.ssa Monica FABRIZIO	Commissario
Prof. Giuseppe SPAZZAFUMO	Commissario
Prof. Diego MICHELI	Supervisore
Prof. Mauro REINI	Co-Supervisore
Prof. Alfredo SOLDATI	Coordinatore del Dottorato

Author's Web Page: www.ing.units.it

Author's e-mail: marco.cefarin@gmail.com

Author's address:

Dipartimento di Ingegneria e Architettura
Universit'a degli Studi di Trieste
Via A. Valerio, 10
34127 Trieste Italia
tel.: +39 040 5583051
fax: +39 040 5583812
web: http://www.units.it

Abstract

Absorption refrigeration technology is a well known subject that has been studied for a long time. The Absorption Refrigeration Cycle uses as primary energy source the heat which drives the cooling process, instead of electricity as in vapor compression cycle. Despite different technologies can be used to design an absorption chiller, the most common available on market are based on ammonia-water (NH_3 - H_2O) and water - lithium bromide (H_2O - LiBr) mixtures. The absorption cycle heat requirement is a characteristic that increase overall efficiency of the system when applied to industrial processes where wasted heat is available. The aim of this project is to investigate the NH_3 - H_2O technology and suitability for heat recovery applications.

Moreover, this project is focused oin the development of an analytical feasibility study method to evaluate the application of this technology to industrial processes, with a particular focus on below 0 °C cooling applications.

This method is based on a numerical model of the system that analyses the cycle temperature influence on the overall cycle performance. The heat source is a flow of hot water (90°C - 120°C). The analysis shows that a Coefficient Of Performance (COP) of 0.521 has been obtained for a configuration with a pre-condenser heat exchanger rectifier.

This method is focused on reducing the desorber temperature required to operate the chiller for a fixed evaporation temperature. The parametric study at constant condensation and evaporation temperature shows high gradient COP drop for low values of generation temperatures. The optimal minimum generator temperature is a result of balance of many parameters, such as heat exchangers dimensions and solution flow.

Differential ammonia concentration (between weak and strong solution) is also considered as a further design criteria to evaluate heat recovery application feasibility. This parameter affects directly the system operative design in terms of heat exchanger dimensions, installed pump size and the cycle performance. The operating design is obtained considering also local robustness, to reduce system instability if fluctuation of functional parameters occurs. Charts for easy first sizing of a new chiller has been developed.

Furthermore, a 75 kW ammonia-water absorption chiller operated by waste heat has been designed and tested. The prototype is operated with a glycol-water solution at approximately 105°C, evaporation is fixed to -3.5°C to cool glycol-water solution down to 0.5°C and condensation temperature for summer working period is assumed as 35°C. The prototype has been built to test different technical solutions. The pump is a critical component in absorption chillers. In order to reduce cost and complexity of the system a centrifugal water pump is installed and tested, instead of more complex and costly membrane pumps. Moreover, Plate Heat Exchangers are used to obtain a compact system design, instead of Tube Heat exchangers , commonly used in the industrial refrigeration sector.

The results obtained from the apparatus test confirm that the design process and all the assumptions are correct. The COP value obtained during the tests is 0.413, in line with the expected theoretical figures. All the problems encountered during the design process are reported in the Conclusions section. This section includes also some suggestions on features that can be implemented to enhance the overall chiller design and performances.

Sommario

La refrigerazione ad assorbimento una tecnologia ben nota e studiata da lungo tempo. Il ciclo di refrigerazione ad assorbimento, a differenza del ciclo a compressione del vapore che usa lelettricit, permette di utilizzare come fonte primaria di energia il calore come motore per il processo di raffreddamento. Esistono diverse tecnologie che possono essere impiegate per la costruzione di un frigo ad assorbimento, ma quelle basate su miscele di ammoniaca-acqua e acqua-bromuro di litio sono le pi comuni e disponibili sul mercato.

La richiesta di calore del ciclo ad assorbimento una caratteristica che pu rendere questo sistema molto efficiente se applicato a processi industriali laddove il calore di scarto disponibile. Lobiettivo di questo progetto di ricerca studiare la tecnologia basata sulla coppia NH_3 - H_2O e la sua compatibilit per applicazioni di recupero di calore. Questo progetto inoltre incentrato sullo sviluppo di un metodo analitico di valutazione di fattibilit per stimare limpiego della tecnologia ad assorbimento a NH_3 - H_2O in differenti processi industriali, in particolare considerando applicazioni di raffreddamento con temperature inferiori allo 0°C.

Questo metodo basato su un modello numerico del sistema che analizza linfluenza delle temperature nel ciclo sulla complessiva prestazione del sistema. Come fonte di calore stato considerato un flusso di acqua calda di 90-120°C. Lanalisi mostra che quando si ha una configurazione con uno scambiatore di condensazione parziale il coefficiente di prestazione (COP) pari a 0.471. Inoltre, con questo metodo si vuole ridurre la temperatura di generazione richiesta per azionare il frigo a temperature di evaporazione fisse. Lo studio parametrico fatto a temperature di condensazione ed evaporazione costanti, mostra un marcato gradiente nel calo del COP per bassi valori di temperature di generazione. La temperatura di generazione minima ottimale il risultato dellequilibrio di diversi parametri che comprendono le dimensione degli scambiatori di calore e la portata della soluzione.

Come ulteriore criterio di progettazione sono state considerate concentrazioni diverse di ammoniaca (tra le soluzioni ricca e povera) per stimare la fattibilit di applicazione

nal caso di recupero del calore. Questo parametro influenza direttamente la progettazione del sistema in termini di dimensioni degli scambiatori di calore, della potenza della pompa installata e della prestazione del ciclo. Il punto di funzionamento stato ottenuto considerando anche la robustezza locale per ridurre linstabilit del sistema nel caso in cui siano presenti fluttuazioni dei parametri funzionali. Grafici per un iniziale dimensionamento del nuovo frigo sono stati sviluppati.

Inoltre, un frigo ad assorbimento ammoniaca-acqua della potenza di 75kW azionato tramite calore di scarto stato progettato e testato. Il prototipo attivato con una soluzione di acqua e glicole ad una temperatura di circa 105°C, levaporazione fissata a -3.5°C per raffreddare la soluzione acqua e glicole a 0.5°C e la temperatura di condensazione fissata a 35°C per il periodo lavorativo estivo. Il prototipo stato costruito per testare diverse soluzioni tecniche. Considerando che la pompa una componente critica nei frighi ad assorbimento, per ridurre i costi e la complessit del sistema stata installata e successivamente testata una pompa centrifuga per acqua invece di pompe a membrana che sono pi complesse e costose. Scambiatori di calore a piastre sono stati utilizzati per ottenere un design compatto del sistema, invece di scambiatori di calore a fascio tubiero, che sono comunemente usati nel settore della refrigerazione industriale.

I risultati riportati dal test dellapparato confermano che il processo di progettazione e tutti le ipotesi di lavoro sono corretti. Il valore di COP ottenuto durante il test pari a 0.421 che in linea con i valori teorici previsti. Tutte le difficolt riscontrare durante il processo di progettazione si possono trovare nella sezione delle conclusioni, dove sono anche enunciati suggerimenti su caratteristiche che possono essere implementate per incrementare la progettazione complessiva del frigo e le sue prestazioni.

Acknowledgments

This research project has been supported and sponsored by Zudek srl, Muggia(TS).

Contents

List of Figures

List of Tables

1

INTRODUCTION

1.1 Background

Environmental awareness is increasingly arising and it is pushing for a more sustainable and less polluted world. Reduction of the of primary energy consumption and lowering green house gases emissions are the principal objectives fixed by international agreements such as Kyoto protocol. To reach this goals, many governments and international organizations are introducing economic incentives and feed in tariffs. Along these factors, the increment of the raw resources prices make the energy efficiency one of the principal research topics in the industry.

As a matter of fact, energy is often improperly used due to aged and poorly designed industrial facilities. Therefore, design of effective devices is essential to shift to more efficient and conscious energy consumption.

Indeed, heat recovery in industry is one of the most investigated topic in many researches. In fact, in industrial processes, there is a large amount of waste energy that is not exploited. A typical case of energy recovery is heat recovery from combustion exhausted gases. The recovered heat can be used to pre-heat a process flow or used for space heating. Furthermore, recovered heat cannot be always completely exploited,like the case where heat load demand is not uniformly time distributed, i.e. seasonal load variation or non uniform industrial processes.

Converting unused heat in cold is an effective way to increase the recovered heat utilisation rate. Heat activated refrigeration systems, such as absorption cooling heat pumps permit to exploit unused heat.

Many technologies are available both on market or as experimental prototypes; they mainly differ for the refrigerant mixture employed. As already stated, the most common absorption systems are based on ammonia - water (NH_3/H_2O) and water - lithium bromide (H_2O/LiBr). The main difference between these two systems is that only the

NH_3/H_2O system is suitable for applications below 5°C, while lithium bromide mixture based cycle is usually limited to air-conditioning applications, due also to a slightly higher performance figure.

The CFCs and HCFCs were the most common refrigeration fluids up to early 1990s. In 1987 the Montreal protocol banned the production and use of ozone depleting substances. Indeed the HFCs became the most used for their non-ozone depleting characteristic. At the moment many of these refrigerants are being removed from the market. Consequently, a new interest in natural refrigerants as CO_2 or NH_3 for refrigeration applications is growing.

The NH_3/H_2O couple is composed by natural refrigerants with ODP=0, a fundamental characteristic, as the actual regulations are phasing out all CFC refrigerants.

1.2 Objectives

The aim of this research project is to study a single stage absorption chiller that uses a mixture of ammonia and water as working fluid. The study consist of a theoretical analysis followed by the design, construction and test of an operative prototype to confirm the theoretical results and the design process. Moreover it is designed to be used for further studies. To realize the described objective the work is organized in the following stages:

- Develop numerical model to describe the operation of an absorption cooling heat pump that uses ammonia-water solution
- Identify the principal system parameters values in order to find the optimal working condition with high global system performance
- Using the obtained numeric values, sizing charts are created in order to identify the space of solutions where an absorption chiller can operate
- Design, build and test an ammonia absorption chiller prototype
- Anlyse and compare the experimental data with the theoretical values obtained from the numerical simulations

1.3 Outline of thesis

The thesis is organized according to the following outline:

Chapter 2 contains a detailed introduction on the absorption cycle, giving an overview of thermodynamic fundamentals and theoretical basis for its comprehension. The main modified cycle are reported and analysed. The mixture characteristics in absorption cycles are discussed; H_2O/LiBr and NH_3/H_2O mixtures are compared.

Chapter 3 reports the state of the art of the technology. The literature is investigated and reviewed: the most recent and promising topics are explained and discussed. The critical aspects of some component of an absorption chiller are reported and discussed. Performance enhancement through surfactants and nano-particles is described. Typical installations and applications are reported.

Chapter 4 describes the numerical model that has been developed to evaluate the absorption chiller operating conditions. The equations and their implementation in EES are reported. The obtained results are analysed and commented. Some comparisons between different cycle configurations are investigated and discussed.

Chapter 5 goes through design process of the prototype. The cycle design criteria are explained and the component selections are discussed. The main issues faced during the process are explained. There is also a brief overview of P&ID, piping and mechanical design from 3D modelling, through construction, to site installation.

Chapter 6 reports the tests carried out on the prototype. The test facility and plant P&ID are described. The prototype commissioning , test settings, test procedure and data acquisition are described. The obtained data are shown and analysed. Results are compared with numerical figures.

Chapter 7 is the end chapter where the conclusions are drawn. The results of present research are discussed along with issues and problem faced during the design process. Some comments on achieved results are made and some suggestions on possible future development are given.

2

ABSORPTION CYCLE

2.1 Bithermal Heat Pump Cycles

For claim of clarity some concepts will be defined to permit a better understanding of theory that underlay the absorption chiller technology. Following will be exposed the basic ideas that will be used to characterize and describe the absorption cycles. It is fundamental to start with classification of the absorption cycle and its relationship with other thermodynamic cycles. Thermal source designation is used for a body capable of giving or receiving heat at a constant temperature. In practice, a thermal source is realized either by a body of sufficient large dimensions so that heat transfer do not affects its temperature (e.g., the atmosphere or the ocean), or by a body maintained at a constant temperature by another heat transfer of opposite sign (e.g. tube of a boiler, radiator or cooler). It is employed the term thermal machine for the devices in which during a thermodynamic process from a state 1 to a state 2 , various transfers (work, heat, mass) take place with the considered system. It can be also defined closed system, without fluid transfer as a system in which fluids practically do not move in space. The system thermodynamic state evolves in time, on the one hand according to the work transfers occurring from the motion of certain solid walls, and on the other hand according to heat transfers that take place by conduction across other solid walls. It is important to note that these energy transfers can be simultaneous or successive. Since all cycles that occur one after the other in time are identical, it is obvious that the operation of a system without fluid transfer is necessary periodical.[1]

A closed system, undergoing a bithermal cycle, can receive work (or work power) and supply heat (or heat power). Such a cycle is called a heat pump cycle. So they transfer heat from a source at a lower temperature to another at a higher temperature, through the supply of work from the outside.

Depending on the effect to achieve, they are divided in :

- HEATING HEAT PUMP CYCLE = heating by transfer of heat to a source at a higher temperature (Thermopump). It is a bithermal heat pump cycle with atmosphere as the cold source at temperature T_a, and delivering heat to a hot source at a higher temperature T_h.
- REFRIGERATION HEAT PUMP CYCLE = cooling by removing heat from a source at a lower temperature source (Frigopump). It is a bithermal heat pump cycle which employ the atmosphere at temperature T_a as a hot source and a source at lower temperature T_f as the cold source.

In order to realize the cycle, input energy is required in the form of mechanical energy, chemical, electrical, thermal , etc.

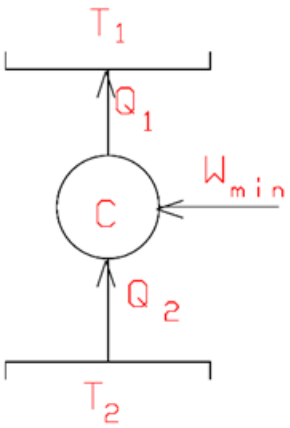

Figure 2.1: Schematic representation of heat pump cycle

The thermodynamic comparison basis is given by reversed Carnot cycle used as heat pump cycle. The reversed Carnot cycle is a reversible bithermal heat pump cycle, defined in the same way as the Carnot power cycle. The difference lies in the fact that it operates counter clockwise in the p-v and T-s diagrams. The main characteristics are listed below, referring to Fig. 2:

- It absorbs the least amount of mechanical energy (reversible process)
- Subtract heat Q_2 to cold source at temperature T_2
- It transfers heat Q_1 to the hot source at temperature T_1

The Carnot cycle is defined by:

- 2 Isothermal heat exchanges = transformations at constant temperature to reduce the irreversibilities; it occurs in phase transitions systems
- 2 isentropic adiabatic transformations (compression and expansion)

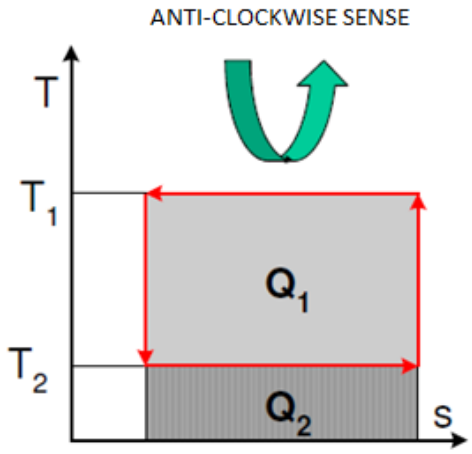

Figure 2.2: Schematic representation of heat pump cycle

2.2 Performance Indexes

In general way, it can be denoted as effectiveness the ratio between the useful energy and the used or dispersed energy. For the heat pump cycles effectiveness can be estimated with a performance index called COP (Coefficient of Performance).

In heating heat pump (thermopump), useful heat Q_1^- is transferred to the a higher temperature source T_1(condenser). For a heat pump used for heating we have the following energy rate balance such that:

$$W^+ + Q_2^+ + Q_1^- = 0 \tag{2.1}$$

or

$$|W^+| + |Q_2^+| = |Q_1^-| \tag{2.2}$$

Where the terms are:

- W^+ = is the mechanical power input received by the compressor

- Q_2^+ = is the heat transfer rate draw from the atmosphere
- Q_1^- = is the heat transfer rate moved to the hot source, i.e. heating network (heating service)

It is possible to define the heating effectiveness, called heating coefficient of performance COP_H by the relation:

$$COP_H = \frac{Q_1^-}{W^+} = \frac{|W^+| + |Q_2^+|}{|W^+|} = 1 + \frac{Q_2^+}{W^+} \tag{2.3}$$

The value of effectiveness COP_H is always superior to 1,0.

In cooling heat pump cycle, useful heat removed from the cold source (evaporator) is Q_2; energy rate balance is given by:

$$W^+ + Q_2^+ + Q_1^- = 0 \tag{2.4}$$

Where the terms are:

- W^+ = is the mechanical power input received by the compressor
- Q_2^+ = is the heat transfer rate drawn from the source to be cooled (cooling service)
- Q_1^- = is the heat transfer rate rejected in atmosphere

It is possible to define the cooling effectiveness, called cooling coefficient of performance COP_C by the relation:

$$COP_C = \frac{Q_2^+}{W^+} \tag{2.5}$$

This definition results in an effectiveness that can be either lower or higher than 1,0. The two coefficients of performance COP_C and COP_H are related. From their definitions we can also write:

$$COP_H = \frac{Q_1^-}{W^+} = \frac{|W^+| + |Q_2^+|}{|W^+|} = 1 + \frac{Q_2^+}{W^+} = COP_C + 1 \tag{2.6}$$

The COP_H of the heating heat pump (for the same cycle) is higher by 1,0 to the COP_C of cooling heat pump, if comparing two cycles operating between the same two heat source temperatures . The same cycle can have two COP values depending on which heat rate is considered as useful. [1]

2.3 Compression refrigeration heat pump cycle

In Figure 2 it is represented a schematic compression refrigeration heat pump. Its main features are:

- a compressor (usually reciprocating, screw or centrifugal type) driven by an electric motor absorbing power W^+
- a condenser cooled by a cooling network, eliminating the heat power Q_1^- at atmospheric temperature T_1
- a throttling valve
- an evaporator cooling a cold heat source, drawing the heat power Q_2^+ at the temperature T_2
- pipes linking all the above components

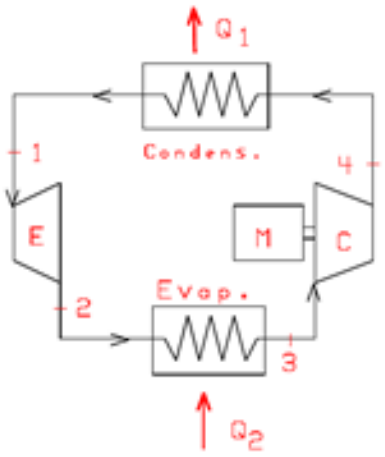

Figure 2.3: Schematic representation of compression refrigeration cycle

The system can be described as a bithermal closed heat pump cycle on T-s diagram like in Figure 2. The transformations occurring in the cycle are:

- Adiabatic expansion 1-2: isentropic transformation, from pressure p_1 to p_2, starts at the point 1 (saturated liquid) and it ends in point 2 in conditions of wet steam (in large facilities it is conveyed in a turbine to recover expansion work). In most

cases, the expansion happens in a throttling valve or in a capillary. Expansion occurs without work exchange at constant enthalpy. The liquid has a higher vapor fraction after expansion.

- Isobaric evaporation 2-3: it occurs inside the liquid vapor dome on T-s diagram representation of the fluid at a constant temperature, it exploits transition phase heat. Point 3 is usually located on saturated steam curve of the liquid vapor dome. In the refrigeration cycle, the evaporation heat rate is the useful heat power.

- Adiabatic compression 3-4: in the ideal cycle, it is an isentropic process from p_2 to p_1. In a real cycle it is an irreversible adiabatic transformation (not isentropic.) The transformation starts in point 3 (saturated vapor) and ends in point 4 (superheated gas).

- Isobaric condensation 4-1: inside the liquid vapor dome on T-s diagram. The transformation occurs at a constant temperature in conditions of saturated vapor. For heating heat pumps, the condensation heat rate is the useful heat power.

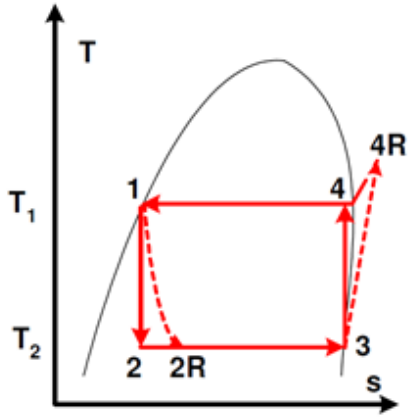

Figure 2.4: Representation of compression refrigeration cycle on T-s diagram

2.4 Absorption refrigeration heat pump cycles

The absorption cycle is a compression heat pump cycle in which the compressor is replaced by the absorber and the generator. In Figure 3 an absorption heat pump cycle employing NH_3/H_2O mixture is taken as example. The generator is flooded by the rich

in NH3 composition mixture. Supplying heat Q_1 in the generator it occurs the partial evaporation of the more volatile fraction (NH_3) with a consequent enrichment of water in the mixture (point 8). The vapor phase, is rich in NH_3 component and it is flows (point 1) to the condenser where it transfers phase transition heat Q_C to the ambient becoming liquid. The liquid NH_3 is laminated through an expansion valve. After lowering pressure NH_3 subsequently evaporates transferring phase transition heat Q_2 from the cold source to the evaporator.

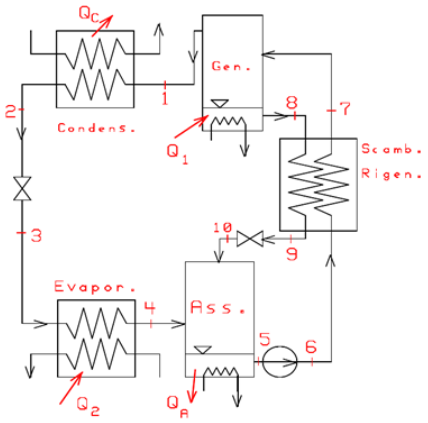

Figure 2.5: Schematic representation of a NH_3/H_2O absorption refrigeration heat pump cycle

The useful heat power Q_2 is clearly proportional to the amount of working fluid circulating inside the evaporator. An absorption cycle is more efficient when it can transfer more working fluid from absorber to generator for the same heat power input. So it depends on the absorption rate of ammonia in the poor solution and on the rate of separation of ammonia from rich solution in the generator.

A simple way to increase the efficiency of the cycle is to insert a regenerative heat exchanger between the two streams of rich and poor solution. The rich solution coming from the absorber is pre-heated by the poor solution coming from the absorber. It permits to reduce the heat needed in the absorber to separate the same amount of ammonia. Beside this it is common to find a pre-cooler heat exchanger which sub-cool the ammonia liquid from condenser and superheat the ammonia vapor from the evaporator.

Ammonia-water cycles usually require an additional heat exchanger to rectify (purify) the NH_3 vapor output from the generator, before entering the condenser. It can also be

a pre-condenser (or partial condenser) which separate the liquid from the vapor phase enriched in ammonia.

The cycle has the same mechanical components which can be commonly seen in a compression refrigeration equipment (condenser, expansion device, evaporator). The advantage of absorption cycles is to avoid the direct compression of the gaseous refrigerant (ammonia, in the present case). The pressure increase is performed on the liquid phase by a pump; the refrigerant is solved in a liquid mixture with an appropriate solvent (water). This allows to perform a considerable savings in mechanical power required to operate the cycle. [1]

2.5 Absorption heat pump Coefficient Of Performance COP

The absorption heat pump performance can be evaluated in the same way as previously done in *Section 2.2*. For a cooling heat pump, the COP_{FR} of an absorption system can be defined as:

$$COP_{FRass} = Q_2/(Q_1 + W_p) \tag{2.7}$$

Where the terms are:

- $Q_1^- =$ is the heat transfer rate supplied to the generator
- $W_p =$ is the mechanical power input received by the pump

The heat Q_1 is often provided by waste heat from combustion or low pressure steam. Heat recovery at low temperatures is interesting:

- 120-150°C are sufficient to operate, against a high exchange surface.
- Use of huge amounts of heat that are available in industrial facilities that cannot be exploited in other ways.
- Pairing a absorption plant to a cogeneration system opens up to interesting alternative for summer operation (space cooling, power supply of cold storage); the recovery heat of cogeneration plant can be directly used during winter.

The design of an absorption system requires the knowledge of thermodynamics properties of the mixture. To evaluate them state diagrams are needed (or spreadsheet programs , for example EES that has internal routines with properties of many mixtures).

An upper limit to COP_{FRass} can be calculated neglecting the pumping work (the value is very small compared to the heat transferred in the heat generator). Referring to ideally reversible transformations , the system interacts only through the heat exchanges that take place at a constant temperature , so the entropy changes are calculated for the flow of heat (+ or -) :

$$\frac{Q_2}{T_{evap}} + \frac{Q_1}{T_{gc}} = \frac{(Q_C + Q_A)}{T_a} \tag{2.8}$$

Where the terms are:

- T_{evap} is the temperature of the evaporator
- T_{gc} is the temperature to the heat generator (related to the availability of thermal energy from recovery, or the choice of the operating pressure of the generator)
- T_a is the temperature of the external refrigerant used for both the condensing and the absorber (usually equal to the ambient temperature)

The heat transfer rates are taken in absolute value so that the entropy changes expressed to the first and second member are equal in sign.

$$\frac{|Q_2|}{T_{evap}} + \frac{|Q_1|}{T_{gc}} = \frac{|Q_C| + |Q_A|}{T_a} \tag{2.9}$$

From the first law (conservation of energy) it is (neglecting W_p) :

$$Q_1 + Q_2 = Q_C + Q_A \tag{2.10}$$

for which , by substitution:

$$\frac{Q_2}{T_{evap}} + \frac{Q_1}{T_{gc}} = \frac{(Q_1 + Q_2)}{T_a} \tag{2.11}$$

namely:

$$COP_{FRass} = \frac{Q_2}{(Q_1 + W_p)} = \frac{Q_2}{Q_1} = \frac{\frac{1}{T_a} - \frac{1}{T_{gc}}}{\frac{1}{T_{evap}} - \frac{1}{T_a}} \tag{2.12}$$

- This expression tends to T_{evap} / (T_a - T_{evap}) for T_{gc} tending to infinity , which is equal to COP_FR a reverse Carnot cycle operating between T_{evap} and T_a - The COP_{FRass} value, in the case of cycles fed by low temperature recovery heat, is usually close to one, considerably lower than the one that is typical for a compression cycle (COP = 3-4) .

2.6 Refrigeration working fluids

Heating and cooling devices based on bithermal heat pump cycle are widely adopted in industrial and residential applications. Therefore the working fluids used should have some desirable characteristics that make them easier to exploit:

- Condensing pressure is not too high for the corresponding heat rejection temperature
- Evaporation pressure is not too low for the corresponding cooling heat temperature
- High value of transition phase heat(reduced amount of working fluid for same heat rate at evaporator).
- Low saturated vapor specific volume to reduce volumetric flow. Higher mass flow for the same volume flow enable to reduce compressor size.
- No toxicity.
- Not inflammable and not explosive in case of leakage in the atmosphere.
- Compatibility with the construction materials used in heat pump equipment (copper, brass, stainless steel, aluminium, ...).
- Environmentally friendly in event of accidental leakage.

Traditionally, CFCs (chlorofluorocarbons) were the most common choice, which are now being replaced progressively according to Montreal Protocol (1976 , 1987). They have been recognized as major contributors to the ozone depletion and - then - of substantial damage to the environment.

The working fluids for refrigeration are usually divided into:

- CFC : hydrocarbons of the paraffin series in which the hydrogen atoms are replaced with atoms of chlorine and fluorine : R12 (CF_2Cl_2), R11 ($CFCl_3$), R13 (CF_3Cl), R113 (CF_3Cl_3), R114 (CF_4Cl_2) (all of them are banned);
- HCFC: Chlorofluorocarbons are still in use and they are being progressively replaced (production has been stopped, only stocks remaining): R21 ($CHCl_2F$) , R22 (CHF_2Cl). They are 10 times less harmful for environment than previous group (not allowed since 2002);
- HFC: Fluorocarbon without chlorine;

- Natural Refrigerants: R717 Ammonia NH_3, R744 Carbon Dioxide CO_2, R718, H_2O, Water, Air;
- Hydrocarbons: R290 Propane (C_3H_8), R600 Butane.

2.7 Environmental compatibility

There were defined many indicators to evaluate the potential harmfulness for environment. The most relevant are:

- ODP (Ozone Depletion Potential): indicates the destructive capacity of a gas to deplete the ozone layer.It is a relative value and it is referred to trichlorofluoromethane (CFC-11 or R11), which has ODP = 1. The ideal refrigerant has ODP=0;
- GWP (Gross Warming Potential): it is the amount of radiant energy in the infrared band that gas can absorb in a time frame of 100 years , yield compared to the non-dimensional figure of the carbon dioxide ($GWPCO_2 = 1$) . The GWP (or DGWP , Direct Gross Warming Potential to distinguish from IGWP) is an indicator of the effect, the emission of a refrigerant in the environment, has on global warming;
- IGWP (Indirect Gross Warming Potential) and TEWI (Total Equivalent Warming Impact) : beside direct emission effect, a refrigerant can impact the heating effect on environment through its working characteristics. During the operation of a plant, the work absorbed by the compressor must be provided by a system of energy conversion which generally produces CO_2 during energy transformation.

  It is clear that the best practice requires refrigeration systems with high efficiency COP values. The global result also depends very much on "production mix" of energy taken as reference for a specific regional area (eg, combustion, hydro, nuclear, renewable, etc.). The indices IGWP and TEWI quantify this aspect related to primary energy transformations;

2.8 Absorption heat pump cycles

It is possible to realize refrigeration cycles that do not require mechanical energy input; heat can be employed, even at relatively low temperature, by means of the absorption cycles. In an absorption system a mixture of two fluids is employed: one with a higher vapor pressure (solute), another with a lower vapor pressure (solvent). Typical

couples are ammonia - water (NH_3 - H_2O) and water - lithium bromide (H_2O LiBr) (solute - solvent). Only the first pair allows to drop cooling fluid below 0°C (the water solidifies below this limit), instead the pair H_2O - LiBr is usually more interesting mainly for air conditioning applications, due to his slightly higher COP. The cycle exploits the variation of the vapor pressure of the solute that is fixed for a given pressure and temperature. Basically the solute is absorbed at low temperature and pressure while it is released at a higher pressure due to vapor pressure increase as a result of a temperature increase.

2.9 Absorption cycle working fluids

Heating and cooling devices are widely adopted in industrial and resident applications. Besides, here is huge low grade heat in many industries, which could be reused to increase the energy efficiency. Among heat driven devices, absorption cycles (absorption heat pump, absorption chiller and absorption transformer) can use low grade heat in various industrial processes. Besides, absorption cycles can benefit the atmosphere by reducing the emission of carbon dioxide and adopting environment friendly working pair. Absorption cycle has been developed in 1700s. And it is well known that ice could be made by the evaporation of pure H2O from a vessel contained within an evacuated container in the presence of sulphuric acid [2] . Ferdinand Carre presented a novel machine using NH_3 + H_2O as working fluids in 1859, which took out a US patent in 1860. This is the original design of absorption cycles. An absorption cycle using H_2O + LiBr was created in 1950s.

The working fluid of an absorption cycle is combined by the refrigerant and absorbent. The strong solution into the absorber will absorb refrigerant vapor due to its pressure difference with evaporator. The strong solution comes into weak solution after absorbing refrigerant, which is pumped into the generator to ensure this cycle continuously. Refrigerant vapor is gained by heating the weak solution, then, it is condensed in the condenser to ensure a constant pressure in both generator and condenser. Performance of an absorption cycle is critically dependent on the thermodynamic properties of working fluids [3]. The mixture of absorbentrefrigerant should be chemically stable, non-toxic, and non-explosive. The requirements of working fluids of absorption cycles are listed [4].

- The elevation of boiling (the difference in boiling point between the pure refrigerant and the mixture at the same pressure) should be as large as possible;
- Refrigerant should have high heat of vaporization and high concentration within the absorbent in order to maintain low circulation rate between the generator and

the absorber per unit of cooling capacity;

- Transport properties that influence heat and mass transfer, e.g.,viscosity, thermal conductivity, and diffusion coefficient should be favourable;
- Both refrigerant and absorbent should be non-corrosive, environmental friendly, and low-cost.

A critical review of absorption technologies was given, in which contained a short introduction of working fluids reported before 2001 [5]. Although lots of working fluids are given in the literature, there is not a complete review with comparison. In order to present different working fluids clearly, they could be divided into five series generally according to the choice of refrigerant: NH_3 series, H_2O series, alcohol series, halogenated hydrocarbon series and other refrigerants.

2.10 Modified absorption cycles and their classification

The absorption cycle seen so far is the simplest version of the cycle. It is important for basic understanding and for modelling purposes. Many variations of the basic cycle have been developed in past. It is important to describe some typical features that are needed for a further comprehension of the matter. Following are briefly described [6].

Number of Effects The number of Effect is defined as the number of times the high temperature heat is exploited internally the cycle, directly or indirectly. Usually machines with more than one stage have internal heat recovery and this lead sometimes to merge two heat exchangers. This occur if the temperature of the flow outgoing from one heat exchanger is high enough to feed another one.

Number of Stages The stage can be ideally associated to a simple absorption machine referred as a single stage one. This characteristic is related with the structure of the cycle. In the case of multiple stage machine the number of stages indicate how many times the base absorption cycle is reproduced. Every single stage can be assumed that is composed of at least 4 heat exchangers that operate as evaporator, absorber, generator and condenser, and by a solution pump. Each stage has the same optional heat exchangers as the simple absorption cycle, so it can include also a sub-cooler and a solution heat exchanger.

Number of Pressure levels The absorption cycle can be classified also based on pressure levels that are included in the cycle. The number of pressure levels can be easily identified as the number of expansions that occur inside the cycle. Generally the number

of pressure levels is proportional to the number of stages in the machine. It is not a rule because there are some cycles that have many stages and effects but operate with only one pressure level.

2.10.1 Double effect absorption cycle

In order to increase the efficiency of the absorption cycle, double-effect cycle is a natural evolution. The main characteristic of this type if cycle is that it can be considered as composed of two single effect absorption cycles, one bottoming the other. The output heat from the condenser of the topping cycle has a temperature of the flow sufficiently high to power the generator of bottoming cycle. This cycles allows to take advantage of the higher availability of higher temperature heat sources to achieve higher performance(COP).

Due to low COP, in the range of 0.6-0.7, associated with single effect technology, it is difficult to compete economically with conventional vapor compression except in low temperature waste heat applications where the input energy is free. Th double effect absorption technology with COP in range of 1.0-1.2, is much more competitive. Usually the heat source temperature at the generator is around 140-160 °C. The double-effect cycle can have several possible configurations available, this affect the number of pressure levels and consequently the number of expansion stages and condensers.

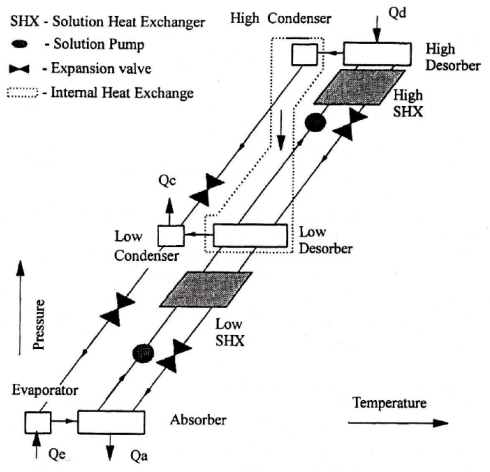

Figure 2.6: Schematic representation of a NH_3/H_2O absorption refrigeration heat pump cycle

2.10.2 Triple effect absorption cycle

As for the double-effect cycle, even in this case there are many internal heat exchanges in order to better exploit the availability of a source at higher temperature. This type of machine is in developing phase and there are some experimental plants around the world. It is not commercially available and so there is not a big practical knowledge of this technology. The internal build of the machine can have many configurations. The main issues related to this kind of machines, that need still to be solve, are internal piping corrosion, construction materials, and proper balance of internal flows.

Usually triple effect absorption machines are direct flame type and, generator inlet temperatures are in the range of 180-200 °C. The performance increases and the COP reaches values of 1.4-1.5, making this a very attractive technology.

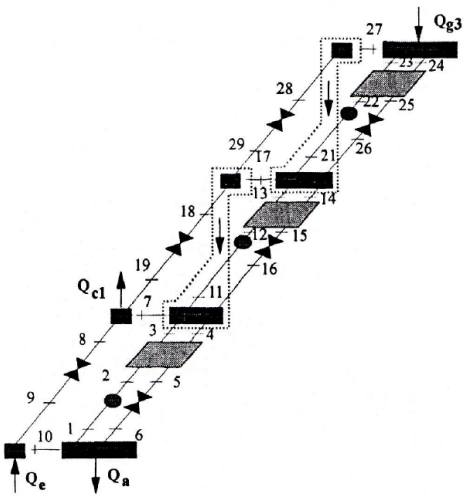

Figure 2.7: Schematic representation of a NH_3/H_2O absorption refrigeration heat pump cycle

2.10.3 GAX (Generator-Absorber heat eXchange absorption) cycle

The Generator-Absorber heat eXchanger absorption (GAX) cycle is a way to achieve a higher COP maintaining the configuration of a single stage cycle. However, it provides a higher coefficient of performance (COP) than any other single effect cycle due to the temperature overlap between the generator and the absorber. As the absorber

pressure increases, the corresponding absorption temperature increases, so the absorber and the generator temperature ranges partially overlap as the absorber exit temperature increases. Furthermore the heat can be internally transferred from the absorber to the generator leading to a higher COP. This overlapped heat is an attractive characteristic of the GAX cycle using NH_3/H_2O, which can not be realized in $LiBr/H_2O$ absorption systems. Recently, the GAX cycle is adopted in many applications such as space heating, space cooling and refrigeration. From economical and constructive perspective GAX cycle can be considered as single effect cycle while the performance can be compared to a double effect cycle. The COP of the GAX cycle is around 1.0 and the input heat temperature range is 140-150 °C.

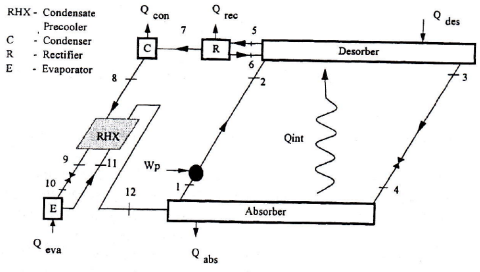

Figure 2.8: Schematic representation of a NH_3/H_2O absorption refrigeration heat pump cycle

2.11 Comparison between absorption and vapor compression refrigeration systems

The absorption refrigeration has many advantages over vapor compression technology. They are listed in the following table:

Ammonia Absorption Refrigeration	Vapor Compression Refrigeration
Low running cost on cheap fuels like agro fuels, furnace oil, waste heat, geothermal heat.	High running cost due to electricity as energy input
High Plant availability due to no reciprocating parts (only moving part is a centrifugal pump, installed with a standby pump)	Frequent outage due to maintenance of equipment; on big plants swing compressor is required
No loss of efficiency at part load; Efficiency improves at part load. motor electrical losses	Loss of efficiency due to fixed mechanical losses at part load
No fouling of evaporator surfaces due to lubricating oil.	Possibility of fouling due to lube oil on evaporator surfaces.
Very low maintenance costs due to no reciprocating parts or high wear and tear parts	High maintenance costs

Comparison between absorption and vapor compression refrigeration

2.12 Comparison between NH_3-H_2O and Libr-H_2O absorption refrigeration systems

H_2O -LiBr an NH_3-H_2O are the most widely used absorption working fluids, with the former being more popular due to its slightly higher coefficient of performance. However, several critical limitations exist for H_2O -LiBr machines:

- The freezing point of water is 0,1°C, and therefore, an H_2O -LiBr AHP that uses water as a refrigerant cannot operate at an evaporation temperature below 0°C, making it unusable for sub-freezing refrigeration or heating/domestic hot water (DHW) supplementation in cold regions.

- Crystallization of the H_2O -LiBr solution is quite common, especially when the absorption temperature is high or the evaporation temperature is relatively low, which presents a barrier for air-cooled absorption.

- High vacuum conditions should be maintained in the system for efficient operation of the H_2O -LiBr system; otherwise, the performance of the absorption cycle would be greatly degraded.

These factors make ammonia-based solutions more suitable for adoption as AHP working fluids in certain situations, especially for applications involving sub-freezing refrigeration, air-cooled ammonia heat pumps, heating ammonia heat pump, among others. In other applications (i.e., renewable energy utilization, waste heat recovery and thermal energy storage), ammonia-based working pairs have also attracted great attention due to the absence of crystallization and vacuum issues.

2.13 General observations on absorption machines

Absorption machines can be classified on mixture they use or the type of cycle they are based on. Beside this they can be also listed on the type of technology is used to feed the generator. Generally there are two main categories: direct fired and steam/hot water types. The direct fire type usually incorporate a gas burner that provide the heat to the desorber. The steam powered machines commonly use process steam that is already available in the plant. Hot water type can be powered with a hot secondary fluid flow. It can be furnished in many ways as heat from waste flue recovery and geothermal source. Sometimes it is easier to use the already available structures, such as boilers or solar collectors.

The latter is very useful if it is applied to waste heat recovery from cogeneration systems. This kind of plant configuration is also cold trigeneration because it can provide heating and cooling at the same time. Absorption chillers coupling to cogeneration systems is nowadays a very common set-up. The waste heat from the exhaust gases or from the oil cooling system are used to power the absorption machine. Typical applications of trigeneration are:

- Air conditioning (HVAC)
- Pre-cooling of inlet air in gas turbines (increase in power and efficiency)
- Refrigeration processes in food preservation and ice production
- Cooling in industrial processes (plastics industry)

Heat recovery from industrial processes is another sector where absorption technology has always an advantage over vapor compression machines. The use of absorption systems is economically advantageous for many industrial plants having large amounts of waste heat and high demands of cooling load. Examples of heat sources are:

- Fumes from dessicant processes, i.e. in pulp and paper industry

- Hot water from treatment processes in waste water plants
- Steam produced in the oil refining processes
- Low-pressure steam from steam turbines
- Incinerators flue gases in waste treatment processes

Benefits of waste heat recovery powered absorption refrigeration machines can be summarized as follows:

- Electric power installed much lower than the corresponding vapor compression machines
- Very silent and vibration free machines
- Energy savings compared to separate production of heat and cooling
- CO2 emissions reduction
- Use of natural refrigerants mixture having no impact on ozone depletion
- No emissions of polluting substances (refrigerant and oil)
- Exploitation of waste heat reducing electric power consumption
- Reduced operating costs during life cycle of absorption machine
- Low consumption of more expensive electric energy
- Low maintenance costs
- High availability and Reliability due to low outage
- Longer life cycle due to absence of moving components; mainly made of static components as heat exchangers and valves

3

STATE OF THE ART

In this chapter is reported an overview of the main research topics in ammonia-water absorption cycle covered by literature.

3.1 A critical component: the Absorber

A brief review of the literature on absorption heat and mass transfer is provided in this section. In absorption cycles there are different mechanisms for transferring the ammonia exiting from the evaporator to the water mixture, where the vapor is absorbed and then transported to high pressure side without compression process. In the literature three main mechanism to increase the ammonia absorption in the water solution are distinguished: mechanical, chemical and by nano-particles. Among the mechanical mechanism are indicated two main types of absorption. The first is the falling film type and the second is the bubble type absorber, operating through insufflation of ammonia in the liquid mixture. The bubble type is reported as more efficient than falling film type. In fact for equal geometrical dimensions of a plate heat exchanger, the same quantity of ammonia is absorbed in a shorter distance for equal cross-sectional area. The bubble type absorber allows a reduction of the volume of the absorber of the order of 48.7% if compared with a falling film type absorber that has the same absorption rate.

3.1.1 Bubble-type absorber

Lee et al. [7] analyze experimentally the ammonia-water absorption process for falling film and bubble modes in a plate heat exchanger absorber; they conclude that in the plate type absorber, the mass transfer rate is better in the bubble than in the falling film type. However more heat was generated in the bubble type, the transfer heat rate in the bubble mode is lower than in the falling film mode at low ammonia gas flow

rate. Merrill and Perez-Blanco [8] investigated increasing the interfacial area per unit volume of vapor and liquid mixing at the vapor-liquid interface by breaking the vapor up into small bubbles and injecting them into the liquid. Terasaka et al. [9] investigate the mechanism of gas absorption from a bubble containing soluble and insoluble components, a gaseous mixture of ammonia and nitrogen was bubbled into water and describes the mass transfer by separating it into three mass transfer resistances for the gas phase, interface and liquid phase. For the beginning of bubble formation, the resistance at the interface was important rather than the other resistances. They conclude that, by applying the mass transfer mechanism to the non-spherical bubble formation model, the bubble growth curves, the bubble shapes, the bubble volume at its detachment and the mass transfer rate from growing bubbles at an orifice were accurately estimated. For the case of ammonia absorption into water, 8090% of the ammonia in the feed gas was dissolved during the bubble formation. Kang et al. [11] evaluated the heat and mass transfer resistances in both the liquid and vapor regions in a counter current ammonia-water bubble absorber composed of a plate heat exchanger with offset strip fin inserts. They concluded that the heat transfer resistance was dominant in the vapor phase, while the mass transfer resistance dominated in the liquid phase. In addition, the interfacial mass transfer area and vapor hold up were found to be significant in determining the size of the absorber. A vertical-tube bubble absorber with co-current solution and vapor flow in an inner tube, and countercurrent coolant flow in the annulus, was modeled by Perez-Blanco [12]. Several simplified assumptions were made including: the absorption process was at steady state, the process occurred at a constant pressure, all bubbles had the same diameter and velocity at a given location along the absorber length, bubble breakup and coalescence were negligible, resistance to mass transfer in the bubble was negligible, and no direct heat transfer took place between the vapor and the coolant. They found that as the ammonia concentration within the bubble decreased to that at equilibrium, water transfer was in the opposite direction of ammonia transfer; however, when the ammonia concentration dropped below that at equilibrium, water and ammonia transfer were in the same direction.

3.1.2 Falling-Film absorption

Among the ammonia-water investigations there is an experimental study of a coiled-tube absorber Jeong [13] in which dilute solution flowed over the outside of the tubes with the ammonia vapor flowing upward in the shell and coolant flowing within the tube. They conducted experiments with and without absorption and found that film heat transfer coefficients were lower for experiments with absorption than those without absorption, perhaps due to insufficient wetting caused by vapor shear. For laminar, steady flow at low

Reynolds numbers with uniform wetting, Perez-Blanco [12] presented a simple 1-D model for the absorption process in a horizontal-tube, falling-film absorber, while accounting for water transport both into and out of the solution film. To avoid unrealistic excessively high mass transfer rates at the interface, he used a two-film model to decouple the interface concentrations of ammonia in the liquid and vapor. Potnis et al. [14] developed a computer program that simulated the GAX process with liquid-film absorption over a coiled fluted tube with counter current vapor flow, and convective desorption inside the fluted tube. Takuma et al. [15] analysed condensation of ammonia-water mixtures on horizontal tube bundles using a heat and mass transfer analogy and confirmed the predictions using measurements on a full-scale shell-and-tube condenser as well as a test apparatus using the Coherent Anti-Stokes Raman Spectroscopy technique for ammonia concentration measurement. They concluded that the accumulation of ammonia at the interface presents an important resistance to condensation. Attempts at obtaining compact ammonia-water absorber geometries include counter-current fluted-tube absorbers, Kang and Christensen [16]. A generalized design tool capable of modelling several components within an absorption system was presented by Kang et al. [17]. Goel and Goswami [18] proposed a new design of a falling film absorber that could considerably reduce the absorber size. The concept forms a liquid film between the horizontal tubes by a flow guidance system formed by wrapping a mesh alternatively between the left and right sides of the adjacent tubes. The mesh can be made of a compatible material, such as aluminum, steel, glass fiber, or nylon. In addition to increasing the liquid-vapor interfacial area, the concept also enhances the film stability by preventing coalescence of droplets on the horizontal tubes.

3.1.3 Other studies on ammonia absorption

Ferrario et al. [19] simulated ammonia mass diffusivity and estimated the diffusion coefficient values within the range 2 510-9 m2/s at a temperature of 20 °C. Takuma et al. [15] analysed condensation of ammonia-water mixtures on horizontal tube bundles using a heat and mass transfer analogy and confirmed the predictions using measurements on a full-scale shell-and-tube condenser as well as a test apparatus using the Coherent Anti-Stokes Raman Spectroscopy technique for ammonia concentration measurement. They concluded that the accumulation of ammonia at the interface presents a significant resistance to condensation. Data for boiling of the non-azeotropic binary mixture, water/ammonia, on a horizontal surface are presented by Hirofumi et al. [20]. Issa et al. [21] studied absorption of ammonia vapor into ammonia water solutions at several ammonia mass fractions, Ci, with a constant pressure difference of Δ P$_i$ = 50 kPa. Issa et al. applied three different methods to measure the rate of mass absorption, the first

one was based on vapor pressure drop, and the second one was estimated by converting the interface heat flux, and the third one involved an optical procedure to observe density change during heat and mass diffusions. They found that the estimation by the vapor pressure drop does not agree with that by interface heat flux, but agrees with the third procedure. Therefore, they recommended that the first method is more reliable.

3.2 Use of microchannels: the application in the absorber and the generator

Microchannel heat exchangers are introduced in order to reduce the total size of heat exchangers in absorption machines by increasing heat exchange efficiency. The use of microchannels is proposed for both the absorber and the desorber [22].

The falling film type absorber is used; the heat exchange takes place between the gas mixture and a fluid. The geometry of the microchannels achieve a high contact surface of vapor with liquid which allows a reduction of the resistance to heat and mass transfer allowing a very compact size.

This type of heat exchanger can be applied to any component of an absorption system(absorber, generator, condenser, evaporator, rectifier). In this study we present different cases which demonstrate the efficiency of this type of application for any type of binary mixture, in particular for ammonia and water couple. In the study [23] is seen as the microchannels are well suited especially for applications with small loads in which is fundamental the requirement of compactness. This principle can be extended to any application with heat recovery or similar where the key feature is a high phase transition enthalpy. Another very interesting feature is the high wettability due to high ratios of surface area/volume that allows a good distribution of the liquid film.

In the configuration as a generator [23] it is proposed to use hot water as heat transport mean through the microchannels. The rich mixture is dropped from above, wetting more panels fostering heat transfer rate, so it release the contained ammonia. In addition to the experimental tests was a well presented a model that describes the behaviour of the system and is rejected in the measurements made.

It is reported that the factor that opposes increased resistance to mass transfer is not the vapor pressure as expected, but the wetted surface is the most limiting factor. Additionally it was found that the released vapor is cooled along the generator allowing to obtain a very concentrated ammonia vapor at the generator output. The tests were carried out on a prototype composed of bundles of microchannels placed transversely, of the dimensions of 178x178x508mm, and the heat transfer rate is approximately of

17.5 kW. Previous experimental and analytical research by the authors demonstrated the performance of this same microchannel geometry as an absorber. Together, these studies show that this compact geometry is suitable for all components in an absorption heat pump, which would enable the increased use of absorption technology in the small-capacity heat pump market

Military is suppoporting research in small portable heat powered cooling systems [24], in order to avoid need for electricity for operarting cooling systems. These systems could be powered by direct combustion of high energy density liquid fuels or by recovering waste heat from fuel cells or vhicle exhaust. A 250 W breadbord heat operated personal cooling system has been developed. Microchannels provide the characteristics required by a such a system, intensifying the transport process by reducing the characteristic length-scale to less than a millimeter. The the major technical difficulties are associated with the absorber and desorber, due to requirements for two-phase processing and for balancing heat and mass transfer. Some concepts have been tested like fractal structure for desorber and wicking materilas within microchannels in ammonia water heat pump cycles. There is further potential for weight and size reduction. A 150 W portable cooling system for the individual soldier is described, it weights less than 3kg and can be reduced to less tha 2kg.

3.3 Absorption performance enhancement by nano-particles and chemical surfactants

Chemical enhancing techniques consist in increasing the absorption performance of the absorber by chemical additives that reduce the surface tension of water favouring the phenomenon of ammonia absorption. The physical phenomenon that describes this is the Marangoni convection. This is a practical method employed in thermal absorption technology in the past decades in order to improve significantly absorption processes. The literature devoted to this effect is rich, including theoretical and experimental studies on various working fluid-absorbentsurfactant combinations. Isvoranu et al. [25] explained the basic mechanism of the Marangoni effect, using the two-point theory (TPT) of mass and heat transfer. They concluded high surface tension gradient plays the most important role in Marangoni convection. TPT is a powerful tool in the refined qualitative/quantitative binary two-phase local interaction analysis. Kang et al. [26] investigated the enhancement of mass transfer rate by adding different kinds of alcohol as a surfactant and visualized Marangoni convection that is induced by adding a heat transfer additive, n-Octanol. They concluded that the absorption performance could be improved by

increasing the heat transfer additive concentration. The absorption heat transfer was enhanced as high as 3.04.6 times by adding the heat transfer additive.

More recently there are other experimental studies reported [27] where the performance of different additives at different concentrations are compared, causing the increase in ammonia absorption. The experimental use of chemical additives is carried out for bubble type absorbers. The ammonia bubbles allow a greater contact surface with the solution, so the reduced surface tension by surfactants have a greater impact if compared with other type of absorbers. Higehr performance is obtained using 2-ethyl-1-hexanol (2E1H) at a concentration of 700 ppm. The amount of absorbed ammonia in surfactant added mixture is 4.8 times the amount of ammonia absorbed only in the pure water mixture.

A further method to increase the efficiency of the absorber is to employ nano-particles. They have a size between 50 and 100 microns and are composed by different metals and their compounds. They are mixed together and they are in suspension with ammonia water mixture. Unlike for chemical additives, in this case the nano-particles are employed in falling-film and bubble type absorbers. Different metals are employed in the two cases. Even the nano-particles are reported to have a positive effect, increasing of the amount absorbed ammonia.

For the bubble type absorber a certain amount of nanoparticles is added [28]. A mixture has been prepared in order to obtain a uniform suspension. In this study, copper(Cu) in a concentration of 0.1 %, has been found as the best material, leading to an increase of the maximum absorption of 3.21 times compared to the plain ammonia water mixture. Besides the addition of only nano-particles, the effects of chemical additives and nanoparticles is verified. The best performance is obtained with a mixture containing 0.1 % of copper (Cu) and 700 ppm of 2E1H, obtaining a maximum value of ammonia absorption 5:32 times higher.

Another experimental study [29] is focused on falling-film type absorber. In this case a mixture is prepared with 0.1 % SDBS as chemical additive and a combination of different metal oxides. It has been found that the addition of 0.8% of Fe_2O_3 lead to the best results. Also in this case an increase of ammonia absorption is found and the maximum value is equal to 1.7 times the case without nanoparticles and additives.

In all the reported studies the employed surfactants, metals and oxides are easily available. There is not reported the difficulty of particles preparation that have dimension of the order of 50-100 microns.

3.4 Absorption cycle in heat recovery applications

An important aspect of the absorption chiller is not only the operation of the machine in itself , but also how it interfaces with other systems. This is idea is clear especially in systems with waste heat recovery or where absorption machine are coupled with power systems. There are different studies [30] [31] [32] on this type of application and most of them try to identify what are the working parameters that have to be considered in order to achieve the optimal system operational set-up. It is very interesting the exploitation of heat recovery from the exhaust gas from internal combustion engines suitable for electric power production. The coupling of a refrigeration absorption machine allows to have either hot or cold secondary flow, obtaining a trigeneration system. Usually, in addition to internal combustion engine, absorption chillers can be coupled to gas turbines and micro gas turbines. The cold produced with heat recovered from exhaust gas is used to cool the incoming air and thus increase the performance of the turbines themselves.

The simultaneous production of electric power, heating and cooling is identified as trigeneration. Absorption chillers find a good purpose in heat recovery from electric power generation plants with gas turbines or gas internal combustion engines [33]. In these application usually steam or pressurized water is produced and employed in ammonia-water absorption chillers. An indirect coupling of heat recovery and its usage allows a higher exploitation of heat for other applications or processes, increasing the advantage of the construction of these plants. The systems considered are sized 10MW, evaporating at -10. These values are reported as those deemed most representative in many sectors such as pharmaceuticals, food or ice production. Gas turbine has not the optimal match between the temperature glide of waste gas flow and the operating temperature glide of the absorption unit. Internal combustion engine is reported as a better solution compared to gas turbine trigeneration system. It has a better cooling performance in comparison to vapor compression chillers. Impact of heat exchanger surfaces on initial investment is considered. Gas turbine configuration is reported as most favourable due to higher temperatures that imply smaller surfaces. The trigeneration systems have the same payback period of normal cogeneration systems even if the initial investment is higher.

Integration of a microturbine and of an absorption chiller with a refrigeration unit is analysed [34]. The cooling produced by absorption chiller powered by recovered heat from microturbine can be employed in several ways. It can be used directly to cool down at -20, to sub-cool the refrigerant coming from the condenser of the refrigeration unit, to cool down the inlet air of the microturbine or to cool down the air-cooled condenser of refrigeration unit. The study compares the different configurations. It reports a

performance increase of the refrigeration machine in the order of 25%, for liquid subcooling setup and an increase of 5% for microturbine inlet air pre-cooling. The increase of performance of the cycle refrigerator also allows to use a smaller size of the microturbine. The use of both refrigerant liquid subcooling and air pre-cooling if the turbine is the best configuration reducing the payback periods of the system to 3 years.

In another study [35] it is reported the application of the heat recovery only for cooling of gas turbine air inlet to increase total power output. It is a industrial gas turbine with a rated power of 16 MW. The air inlet cooling increases the air density, therefore the generated power increases of 11%.The performance increase allows to reduce the payback period to only 4 years. This system has also the advantage of a higher power output especially during the hottest hours during the day, that correspond to peak production hours.

Internal combustion engines are also studied as topping cycles for an absorption chiller[36]. Total energy recovery is not the only parameter that is evaluated. The system is analysed in order achieve a reduction of emissions due to modifications of the system required to couple the two machines. The system has an internal combustion engine with 4 cylinders and a cubic capacity of 1600, and an ammonia-water absorption, derived from a commercial domestic refrigerator. The study shows the feasibility to exploit exhaust gas as a heat source for the absorption refrigerator. The refrigerator has a low COP figure and has an insufficient thermal load for automotive applications. The inclusion of the heat recovery system does not lead to significant pressure and power losses in the engine, demonstrating the feasability to use internal combustion engines for this purpose.

A further study [37] reports a variety of low-temperature heat sources, that are exploited to power an absorption chiller. Several case studies conducted in Germany are presented. The generated heat by a composting plant, is available at 40-50°C. It aids a double-stage direct fired chiller. Heat available from thermal water and heat generated with solar panel used to power an absorption chiller, are other two examples. All the cases brought as examples refer to mixed installations where the available heat is upgraded by the combustion heat of fossil fuels.

3.5 Solar cooling

The solar cooling application deserve to be examined by itself. It has a increasing diffusion especially in small and medium size civil buildings like offices or flats. In literature there are several studies that investigate the application of absorption chillers coupled with solar panels for cooling purposes. Generally, studies are focused on optimal

matching of absorption machines, generally commercial models, type of employed panels and the inlet temperature of the hot water produced by solar heat. Moreover in some cases are also investigated the effects of temperature on the heat transfer rate inside of the heat exchangers and the optimal size of the accumulation tanks. Usually, machines are employed, but there are also some studies on NH_3-H_2O absorption machines.

In a first study [38], the influence of hot water temperature,exiting the solar panels, on the coefficient of performance(COP) is analysed. The machine ha used a commercial 10.5 kW H_2O-LiBr absorption chiller and has been used in a civil application. It is presented a model that describe the system made up of the solar panels and the chiller. The values reported in the paper are obtained for an evaporation temperature of 7 °C and a condensing temperature of 33 °C and for solar collection surface area of 50 m2. The system also has a an electrical heater that keep constant the water temperature entering into the generator. The operating temperature affects the size of the storage tank; consequently supply of additional heat is needed to maintain this temperature. The best COP is obtained for an operating temperature of the absorption machine equal to 80 °C using the selective surface type collectors that provide consistently throughout the day a temperature superior to 82 °C, thus allowing to minimize the external auxiliary heat supply, and with a storage tank of 3750 kg.

In another study [39] the irreversibility in the absorption machine system and in the solar panels are considered. It has been analysed how they affect the performance of the machine. An ammonia water machine is used as testing absorption chiller. The second principle exergetic losses of the system and the pressure losses affect the energy transfer and therefore the performance of the system itself. In the study a model is presented to describe the exergetic losses of the system. The values so obtained are then compared with experimental data. The best performance, i.e. the higher the COP, is obtained for a pair of evaporator-generator temperatures respectively of 10 °C and 75 °C. On the other hand the lowest COP value is obtained with a couple of values of -10 °C and 28 °C. The exergetic analysis provide an advantage in the analysis of the performance of absorption chillers. It permit to assess losses that would not otherwise be taken into account in first principle heat balances. The maximum COP can be reached in any temperature set of condenser, generator and evaporator. This has been demonstrated experimentally. In the evaporator and the absorber present the higher exergetic losses, so to increase the machine performance it is suggested to consider some changes in these components.

Also a prototype of an aquaammonia absorption heat pump system (AHP) using solar energy is investigated [40]. The performance tests of the system were performed for the climate condition of Ankara in Turkey. The system has been designed operating with a parabolic slot type collector to obtain the required temperatures. In the experiments,

high temperature water is obtained from the collector used as heat source needed for the generator. The system design configuration was analysed by using the experimental data. Thermodynamic analysis shows that both losses and irreversibility have an impact on absorption system performance. The study indicates which components in the system need to be improved thermally. This study demonstrate the feasibility of solar-powered food cooling and commercial air conditioning.

3.6 Compression-absorption cycles

There are cycles where a compression cycle is coupled to an absorption. There are mainly two types of cycles that have been taken into consideration. The first configurations has the two cycles in cascade, namely the compression cycle is producing cold at the lower temperature, while the absorption cycle cools at an intermediate temperature. The other configuration of compression - absorption cycles is realized by placing the two cycles in parallel.

In the case of a refrigerator cascade configuration [41], both the use of ammonia and the use of CO2 for the compression cycle have been evaluated, while an ammonia-water chiller is used as absorption cycle. In the study, a model assess the feasibility of such a system. A thermal load of 1 kW is considered, with an evaporation temperature of -45 °C and condensation equal to 30 °C. It is seen that the intermediate temperature is an important parameter that affects the value of the COP. This influence is stronger when an ammonia is used in vapor compression cycle and must be carefully evaluated during design process. The developed model in the study can be a useful tool to do so. It has been also taken in account the possibility to employ a cogeneration unit to supply both electricity and heat. The loads difference between the two groups is such that make not exploitable this solution. Specifically, the heat demand is much higher than the amount of electricity needed to power the vapor compression chiller. The only recommended option is to install a cogeneration plant where the electricity in excess can be sold to the national grid.

In the other configuration typology, the compressor operate in parallel, between the absorber and desorber, and it transfers part of the gas to the high temperature side [42]. The heat generated during compression is recovered by a heat exchanger and it is used in the absorption cycle. In the studies emerges that the surfaces of the internal exchangers affect the performance of this type of cycles. The overall improvement of performance in comparison to a traditional vapor compression cycles is modest and it is never greater than 10%.

A detailed simulation of a 400 kW ammonia/water compression-absorption refriger-

ation system is presented for air conditioning water chilling application [43]. Simulation has been performed for three different configurations of system having 17%, 23%, and 30% relative solution heat exchanger areas. The effect of relative solution heat exchanger area and mass flow rate of weak solution on the COP, cooling capacity and absorber heat load has been studied. The results show that the COP of the system can be increased by maintaining low mass flow rate of weak solution and large relative solution heat exchanger area. Increase in the relative solution heat exchanger area from 10 to 30% resulted in an increase in COP by about 16%. Further increase in relative SHX area revealed that there exists an optimum area that maximize COP.

Studies on this topic are all based on numerical models and there are few experimental researches. The industrial applicability of this kind of cycles is low due an increased complexity of system and costs, without a substantial increase of performance.

3.7 Advanced absorption cycles

In the literature can be found several articles on advanced absorption cycles. All of these studies are focused on the analysis of the irreversibility that occur in the heat exchangers or in heat and mass transfer phenomena. They mostly present analysis according to the second principle, taking into account the energy balances in the advanced cycles [44]. It is a theoretical study, and it reports many considerations on how to increase the total efficiency of the single cycle considered. It take in account many types of pairs of fluids in order to evaluate the suitability of the taken cycle. All the studies considered assess the influence of temperature in the heat exchanges between the different stages.

Among the advanced cycles the GAX cycle, the double effect cycle and triple effect cycle that are the most commonly cited and studied. All of them shows good performance figures, and much higher tan the simple absorption refrigeration cycle. In all of these cycles, the common feature is a higher temperature of the heat supplied in the high-pressure generator, and the regeneration of the heat inside the machine realized with many temperature and pressure levels.

In general these cycles can achieved theoretical values of the COP greater than one, and in the case of triple effect machines [45] [46], COP can reach values as high as 1.5. The realization of these advanced cycles also entails an increase of complexity of the machine both from the point of view of construction / building both from the point of view of the flows regulation. This complexity is increasing from GAX cycles, to dual effect cycles to triple-effect cycles.

4

ABSORPTION CHILLER THERMODYNAMIC MODEL

This chapter describes theoretical analysis of the absorption chiller, the numerical models are defined and the simulation results discussed. The first section of the chapter shows the equations used and the assumption made in order to develop the different models. There have been modelled the single effect absorption cycle and the GAX cycle. Particularly, two different models have been realized, one to simulate the single effect absorption cycle and a second one to simulate the GAX cycle.

A comparison between these two is necessary in order to select the more appropriate to employ in the later prototype design and realization. The single effect cycle prove to be the most suitable choice for two main reasons: firstly this is providing the higher COP value with low hot water temperature (around 100 °C) and secondly a single effect chiller is simpler and less expensive to build than GAX cycle based one. The latter is mostly due to lower number of components required to employ.

The simple effect cycle has been simulated considering two different configurations, one with the distillation siever tower and without. The second one, again, presents a simpler design and lower costs. The only negative point is a lower performance, but the difference is in order of 5%.

The purpose of this research is to achieve the minimum complexity to acquire the experience needed to handle properly the absorption technology.

A second objective is to develop some charts that can be used to define if an absorption cycle is feasible for a given temperature set. This would allow to have an immediate feedback of the possibility to realize the cycle and it can be used for pre-sizing the chiller.

4.1 Model Design

The computer simulation model is based on fundamental physical laws such as energy and mass balances and heat transfer relations. In order to study the thermodynamic performance of the heat pump and simplify the model the following assumptions were made:

- Pressure drops due to friction in the system are negligible.
- The solution and the heat sink and heat source fluid flow counter-currently in the absorber and desorber. At the solution side the vapour and liquid are assumed to be in equilibrium.
- Heat losses to the surroundings are negligible.
- The strong solution leaving the absorber is saturated.
- The mixing of the weak solution and vapour at the absorber inlet is adiabatic.
- The vapour at the compressor inlet is assumed to be in thermodynamic equilibrium with the liquid in the liquid/vapour separator.
- The solution pump efficiency is 50%.

4.2 Thermodynamic Properties of Absorption Working Fluid

Typically, diagrams charts are used to determine the properties of working fluids. In the present study the properties have been obtained through the data available in the EES software. When designing an absorption system the most important thermodynamic properties are: pressure, temperature, mass fraction, enthalpy, specific volume and entropy. The values of these properties can be displayed only on a multidimensional diagram, but this is not a practical solution. Usually bidimensional diagrams are employed especially where some variables are shown as constant value curves.

The most used diagrams for calculations of pure fluid cycles are $T - s$, $ln(p) - h$ or $h - s$.

The following explanation is referring to a two-component (binary) mixture, as it is ammonia-water solution. In absorption processes an additional variable has to be considered; a mixture has an additional degree of freedom, if compared to a pure fluid, the mass fraction. Historically, enthalpy-mass fraction diagrams ($h - x$ diagrams) were

preferred with temperature and pressure as parameters [6]. The mass fraction is usually defined as:

$$x = \frac{mass\ of\ one\ component\ [kg]}{total\ mass\ of\ both\ components\ [kg]} \tag{4.1}$$

In the following sections the main typologies of diagrams used to evaluate the thermodynamical properties of absorption working fluids are described.

4.2.1 Temperature-Mass fraction Diagram

When a liquid and vapor phases of a mixture coexist in equilibrium, the saturation temperature change in function of the mass fraction even if the pressure is constant. This is a completely opposite phenomena compared to a pure fluid. The below figure shows a schematic of a Temperature - Mass fraction ($T - x$) diagram for a two component mixture, A and B, at constant pressure.

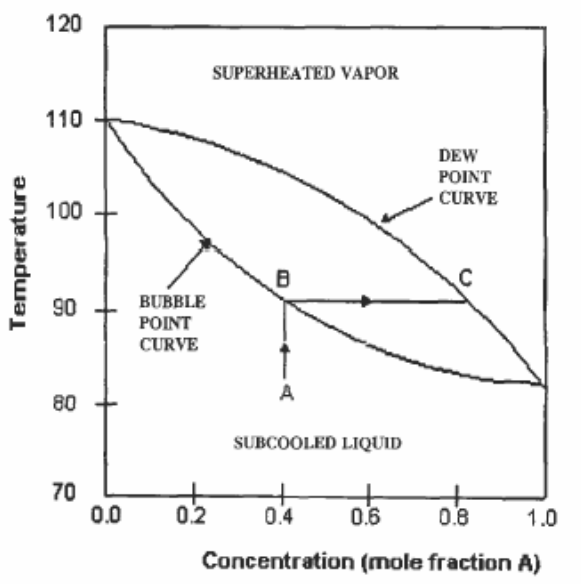

Figure 4.1: Temperature-mass fraction diagram

The mass fraction ranges from 0 (only component B is present) to 1.0 (only component A is present). The area below the boiling line represents sub-cooled liquid, while the are above the dew line represents superheated vapor. The area enclosed between the boiling and dew lines is the two phase region. The boiling point for a mixture of mass fraction

x is located on the boiling line at that mass fraction. The boiling point line indicates the temperature at which the first vapor bubble is formed for a specific pressure and mass fraction. The boiling points of the pure components T_A and T_B are found on the respective ordinates. In the example figure the boiling point of component A is higher than that of component B. The dew line indicates the temperature at which the first liquid droplet is formed when a gas mixture of a given mass fraction is cooled.

The mixtures reported in first figure are usually referred as non azeotropic mixture. In this mixtures the mass fraction of vapor and liquid phases are always different. For an azeotrpic mixture instead,the mass fractions of liquid and vapor phase is identical at certain pressure and temperature as shown in following figure. This state is called the azeotropic point; the temperature glide is zero. At all the other mass fractions the mixture exhibit zeotropic behavior.

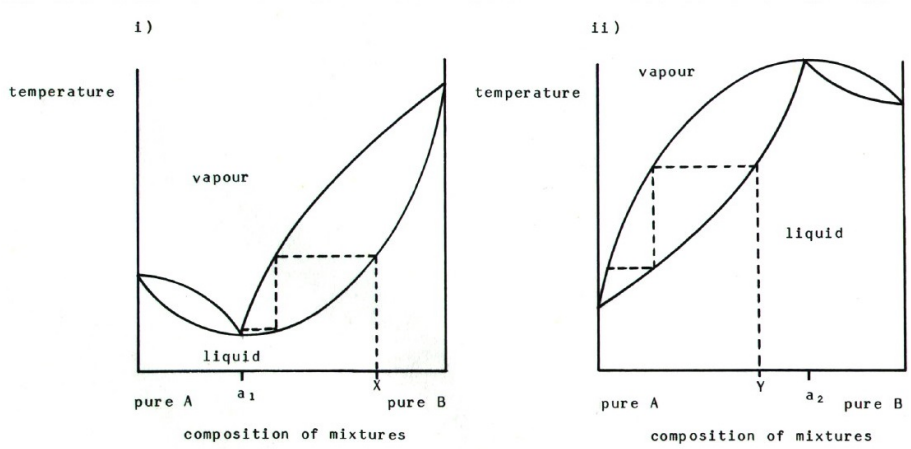

Figure 4.2: Temperature-mass fraction diagram

There are two types of azeotropes. They can be distinguished by the location of the boiling point at the azeotropic mass fraction relative to the boiling points of the pure fluids. Th boiling point can be either higher or lower than the boiling point of either of the two constituents as illustrated in previous figure.

4.2.2 Pressure-Temperature Diagram

Often absorption cycles are represented on $ln(p) - (1/T)$ diagram, called Dühring diagram. The main advantage of this representation is that fluid mixture saturation points are plotted as constant mass fraction straight lines. Constant concentration mixture

curves can be obtained, tracing the saturated liquid phase vapor pressures, in a similar manner to the constant lines obtained of saturated vapor pressure for a pure fluid. The two lines plotted on the extreme left and extreme right are the vapor saturated liquid phase lines corresponding to the pure elements constituting the mixture. The area of the diagram in between the two external lines is called the field of the mixture.

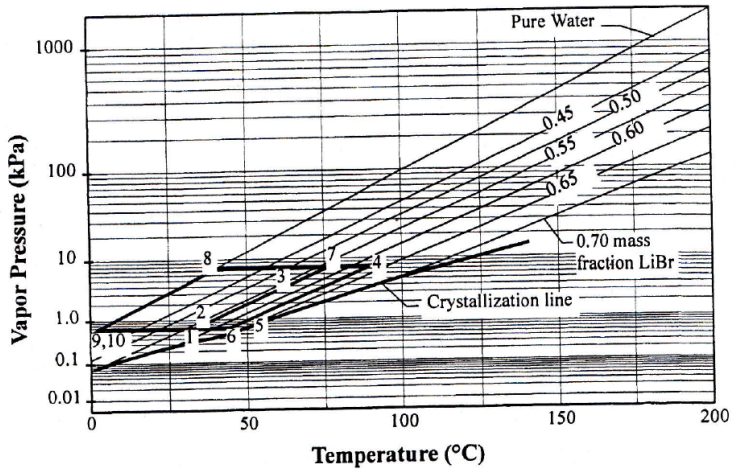

Figure 4.3: Dühring diagram for H_2O - BrLi mixture [6]

4.2.3 Pressure-Entalpy Diagram

In figure is shown the pressure-enthalpy $(ln(P) - h)$ diagram for ammonia. This diagram is traditionally used for the evaluation of vapor compression cycles. It becomes very useful whenever data for pure superheated ammonia are required for cycle calculations. None of the other diagrams employed in absorption refrigeration show data for superheated vapor, since the additional variable complicates the representation, making it incomprehensible on a two dimensional plot.

The two phase range is found under the vapor dome, the area where the isotherms are horizontal. On the left of the two-phase area there is the sub-cooled liquid region while on the right there is the vapor superheated domain. The lines of saturated liquid and saturated gas converge in the critical point.

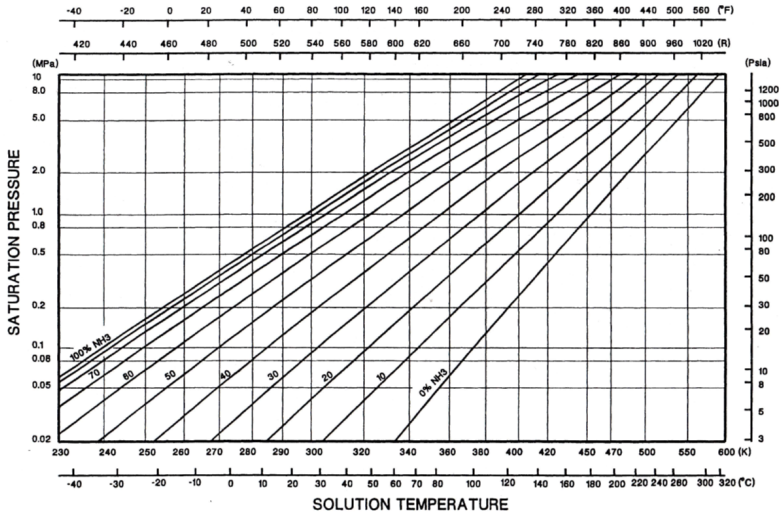

Figure 4.4: Dühring diagram for NH_3 - H_2O mixture [6]

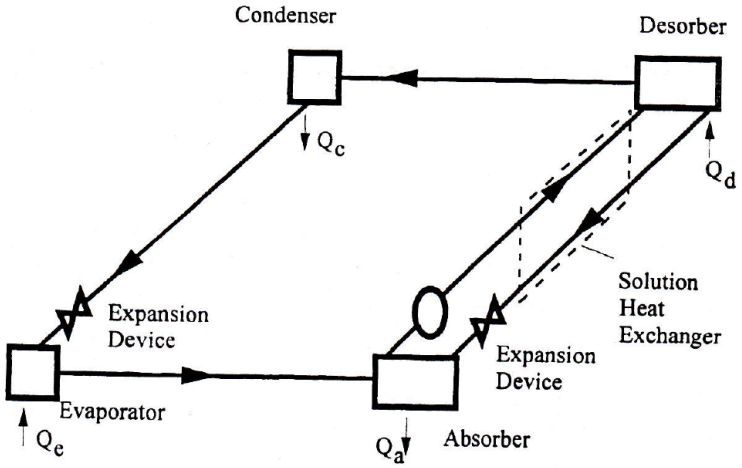

Figure 4.5: Representation of NH_3 - H_2O cycle on Dühring diagram [6]

4.3 Numerical model

In this work a model for water-ammonia absorption cycle is described for both the simple cycle and GAX cycle. The heat source of the desorber is a hot mixture of water and

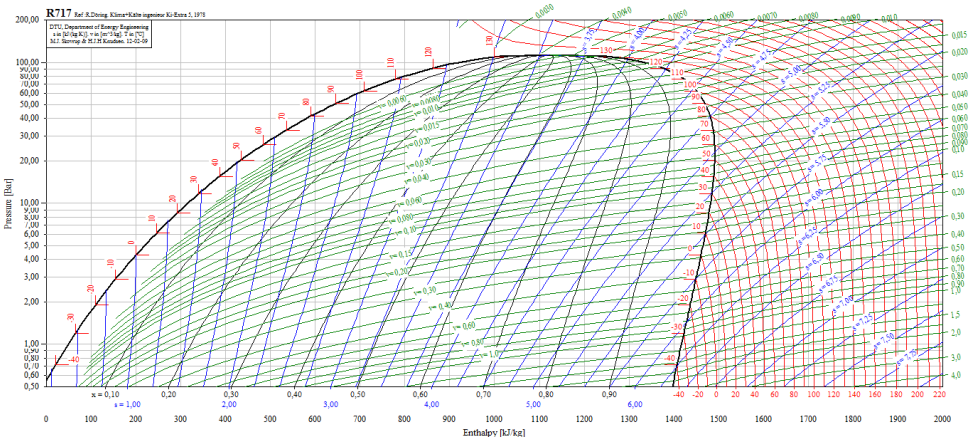

Figure 4.6: Temperature-mass fraction diagram

ethylen glycol from the exhausted gas heat recovery system of an industrial application.

For sake of clarity a short explanation of the basic processes occurring in an absorption cycle is provided. A simple effect absorption cycle is taken as example ans it is shown in Figure 4.7.

The heat is supplied to the generator where it is used to separate ammonia from a rich ammonia-water solution. Thereafter the vapor passes through the rectifier where it is partially condensed and thus the water present in the vapor stream is separated. After the rectifier the vapor stream flows in the condenser. Both components supply the condensation heat to an external heat sink, such as air or water, at a lower temperature.

Liquid ammonia from the condenser is expanded iso-entropically through a lamination valve and subsequently it evaporates removing heat from the cooled medium, obtaining the useful effect of the cycle. Afterwards the evaporated ammonia is drawn in the absorber where it is absorbed in the poor solution, the mixture concentration of ammonia is increased; the absorption process occurs only if mixing heat is removed from the solution and exchanged with a colder heat source.

The enriched solution is pumped into the desorber, the pressure increased and the ammonia released. The poor solution is throttled through an expansion valve and it flows back to the absorber where it is mixed with the incoming ammonia vapor.

In order to increase the overall performances of the cycle a heat exchanger is installed between the two currents of rich and poor solution. It preheats the rich solution before entering the generator and pre-cools the poor solution entering the absorber. In some cases an additional heat exchanger is installed between the ammonia liquid and vapor

phases. It is a liquid sub-cooler that increase the capacity of the evaporator and thus increases the performance of the cycle. Contrary to vapor compression, superheated vapor is not effecting negatively the COP of the cycle. For low evaporating temperatures a sub-cooler has a beneficial effect. The mass transfer occurring in the absorber is enhanced increasing the ammonia vapor temperature.

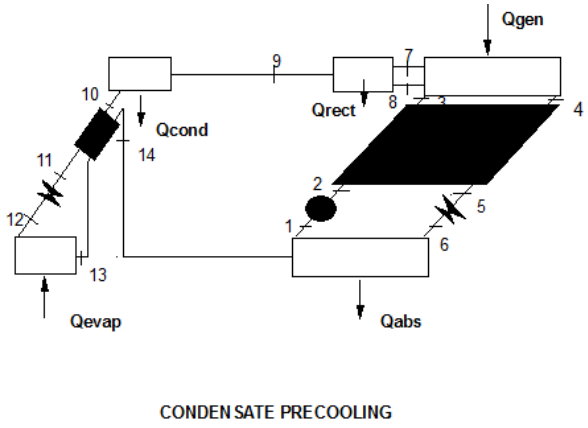

Figure 4.7: Single effect absorption cycle

The tow pressures levels(high and low pressure) in the cycle are determined by evaporation and condensation temperatures.

In the GAX absorption cycle the main processes occurring are the same as in the simple cycle. The main difference is that a part of mixing heat load of the absorber is partially recovered in generator, increasing the overall efficiency. In Figure 4.8 GAX schematic is shown.

From the numerical model point of view, previous considerations valid for simple cycle also apply to the GAX cycle except the solution heat exchangers. To describe the operation of the GAX heat exchanger, two further sets of equations are added in addition.

4.3.1 General assumptions

As previously stated, some simplifications are made in order to allow first principle energy balance of the cycle.

The model in EES (Engineering Equaition Solver) is mainly made of mass and energy balances. The thermodynamic properties of ammonia-water mixture are derived using the function CALL NH3H2O already implemented in EES software. The CALL NH3H2O

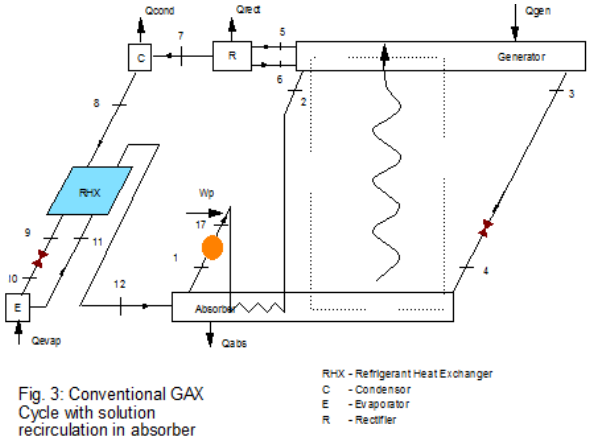

Figure 4.8: GAX absorption cycle

is a procedure which provides the thermodynamic properties of the mixture in the sub-cooling, superheat and saturation sates. Providing three parameters, the function will provide 8 parameters: T = [K], P = [bar], x = [mass fraction of ammonia], h = [kJ/kg], s = [kJ/kg · K], u = [kJ/kg], v = [m3/kg], q = [mass fraction of steam]. Saturated states are indicated with q comprised between 0 and 1. The sub-cooled states are indicated with q=-0.01, while superheated states have q=1.01. The correlations in CALL NH3H2O are taken from NIST REFPROP 9 program, including correlations developed by Reiner Tillner Roth, j. Phys. Rev. Lett. Chem. Ref. Date, Vol. 27 No. 1 (1998) [47].

In the cycle model the cycle, pressure drops inside the pipes and heat exchanger plates are not taken in count. The heat exchanges in the various components of the cycle such as condenser, evaporator, absorber and generator are theoretical values. No heat transfer model has been employed. In the case of regenerative heat exchangers on mixture and pure ammonia loops, a global efficiency value is given to consider the temperature difference that occur in any heat transfer process.

In order to to obtain more realistic results, a fixed temperature delta for each component has been used. The temperature delta is the temperature difference between inside process streams and the secondary fluids on the external side. This figure is set equal to 4 °C, the value can be found commonly when sizing a heat exchangers. Thus the absorption and condensation temperatures were increased by this value, while generating temperatures and evaporation were diminished compared to actual temperature values. In order to clarify the concept the condensation is taken as an example. In the case of air cooled condenser, condensing temperature internal to the cycle must be increased of δ T in order to set a proper value of condensation temperature.

4.4 Energy and Mass balances

The following balance equations can be written for each of the units in the system. Equations refers to total mass balances, single species balances (ammonia), global energy balances.

The balances for the heat exchangers are:

4.4.1 Absorber

$$m[14] + m[6] = m[1] \tag{4.2}$$

$$m[14] \cdot x[14] + m[6] \cdot x[6] = m[1] \cdot x[1] \tag{4.3}$$

$$m[14] \cdot h[14] + m[6] \cdot h[6] = m[1] \cdot h[1] + Qabs \tag{4.4}$$

4.4.2 Desorber

$$m[8] + m[3] = m[7] + m[4] \tag{4.5}$$

$$m[8] \cdot x[8] + m[3] \cdot x[3] = m[7] \cdot x[7] + m[4] \cdot x[4] \tag{4.6}$$

$$m[3] \cdot h[3] + m[8] \cdot h[8] + Qgen = m[7] \cdot h[7] + m[4] \cdot h[4] \tag{4.7}$$

The temperatures for points 7 and 3 are imposed equal.

$$T[7] = T[3] \tag{4.8}$$

4.4.3 Rectifier

$$m[7] = m[9] + m[8] \tag{4.9}$$

$$m[7] \cdot x[7] = m[9] \cdot x[9] + m[8] \cdot x[8] \tag{4.10}$$

$$m[7] \cdot h[7] = m[9] \cdot h[9] + m[8] \cdot h[8] + Qrect \tag{4.11}$$

Other two equations are setted to solve all the variables:

$$h[8] = h[3] \tag{4.12}$$

$$x[8] = x[3] \tag{4.13}$$

4.4.4 Condenser

$$Qcond = m[9] \cdot (h[9] - h[10]) \tag{4.14}$$

4.4.5 Evaporator

$$Qevap = m[13] \cdot (h[13] - h[12]) \tag{4.15}$$

4.4.6 Solution Heat Exchanger

To represent the regenerative heat exchanger it is defined a procedure that calculates the amount of heat that is exchanged in the solution heat exchanger. It evaluates the heat available on both streams and takes the minor of two, then it calculates the enthalpies of the exiting flows.

Amount of heat on rich solution side:

$$Qrs = m[2] \cdot (h3e - h[2]) \tag{4.16}$$

Amount of heat on poor solution side:

$$Qps = m[4] \cdot (h[4] - h5e) \tag{4.17}$$

Evaluation of the minimum between two amounts:

$$Qmin = MIN(Qrs, Qps) \tag{4.18}$$

The heat exchanged in the SHX is calculated introducing the solution heat exchanger effectiveness $eshx$:

$$Qshx = eshx \cdot Qmin \tag{4.19}$$

Entalpies $h[3e]$,$h[5e]$ are evaluated for $T[3] = T[4]$ and $T[5] = T[2]$. The outlet enthalpies are calculated:

$$h[5] = h[4] - eshx \cdot qmin/m[4] \tag{4.20}$$

$$h[3] = h[2] + eshx \cdot qmin/m[2] \tag{4.21}$$

4.4.7 Subcooler Heat Exchanger

As for SHX heat exchanger, a procedure that calculates the amount of heat exchanged is defined to evaluate the sub-cooling heat exchanger transfer rate. It evaluates the heat available on both streams and takes the minor of two, then it calculates the enthalpies of the exiting flows.

The amount of heat on vapor side:

$$Qrs = m[13] \cdot (h14e - h[13]) \tag{4.22}$$

The amount of heat on liquid side

$$Qps = m[10] \cdot (h[10] - h11e) \tag{4.23}$$

Evaluation of the minimum between two amounts

$$Qmin = MIN(Qrs, Qps) \tag{4.24}$$

The heat exchanged in the subcooler is calculated introducing the heat exchanger effectiveness $eshx$:

$$Qshx = eshx \cdot Qmin \tag{4.25}$$

Entalpies $h[11e]$,$h[14e]$ are evaluated for $T[11] = T[13]$ and $T[14] = T[10]$. The outlet enthalpies are calculated:

$$h[11] = h[11] - eshx \cdot qmin/m[11] \tag{4.26}$$

$$h[14] = h[14] + eshx \cdot qmin/m[14] \tag{4.27}$$

The other balances for the components are:

4.4.8 Pump

$$swp = v[1] \cdot (p[2] - p[1])/etap \tag{4.28}$$

$$h[2] = h[1] + swp \tag{4.29}$$

$$Wp = m[1] \cdot (h[2] - h[1]) \tag{4.30}$$

4.4.9 Solution expansion valve

Isoentalpic lamination valve:

$$h[5] = h[6] \tag{4.31}$$

4.4.10 Liquid refrigerant expansion valve

Isoentalpic lamination valve:

$$h[11] = h[12] \tag{4.32}$$

4.4.11 Overall parameters

There are defined further overall parameters that are needed to define the characteristics of the cycle. Moreover a global energy balance of heat transfer rates is required to check the convergence of calculations.

$$COP = \frac{Qevap}{(Wp + Wp1 + Qgen)} \tag{4.33}$$

$$checkQ = Qgen + Qevap + Wp + Wp1 - (Qrect + Qcond + Qabs) \tag{4.34}$$

$$pratio = \frac{phigh}{plow} \tag{4.35}$$

4.4.12 Initial conditions

Given that the study is aimed at developing a working prototype, following there are the working conditions that have been imposed, trying to take account of the conditions under which it will operate.

The limiting factors in this case are available heat, the condensing temperature and cooling the evaporator, and the evaporating temperature. The heat transfer rate at the generator was determined as a function of the size of the prototype, taking into account the amount of heat that you have in the future site of installation. In addition to the above values you need to set other operating conditions which are decided at the loop "design"/absorption machine. These parameters are linked to the thermodynamic conditions that will ensure the proper functioning of the cycle. For example, you must ensure that the vapor of ammonia into the condenser has a certain purity to the water vapor present not excessively penalise capacitor performance. In addition to the thermodynamic conditions assume the efficiency values of the pump and the regenerative heat

exchangers. In order to ensure the correct calculation of the parameters of the cycle we introduce mass budgets and mixture of ammonia, or only the equations of these budgets are not necessary to the resolution of the cancellation system ensures the correct calculation of the system. Below are listed the values assigned to the parameters listed above:

Efficiencies:

- isentropic efficency of the pump $etap$=0.50
- solution heat exchanger efectiveness $eshx$=0.8
- effectiveness of condensate precooler esc=0.0, if subcooler is not used esc=0,"

Temperatures [°C]:

- evaporation temperature t[13]=-3.5
- condensation temperature t_amb=35
- condensation temperature t[10]=t_amb
- absorber temperature t[1]=t_amb
- generator temperature t[4]=100

Mass fractions [kg $\backslash kg$] :

- NH3 purity, entering condenser x[9]=0,9996

Available heat [kW]:

- Heat transfer rate at the desorber Qgen=100

Vapor quality (mass fraction) [kg $\backslash kg$] :

- evaporator exit Q[13]=0,998
- condenser exit (liquid phase) Q[10]=0,00
- rectifier exit Q[9]=1
- desorber exit to rectifier Q[7]=1
- absorber exit Q[1]=0
- desorber exit to absorber Q[4]=0

4.4.13 Model settings

Model has many other settings to provide all the necessary equations and to check the mass and energy balances. There are trivial mixture and single species mass balances. The model provides also a complete table with the properties of all the state points. These settings are not reported and can be found in the models.

4.5 GAX cycle

In the GAX cycle model, the same equations used for simple cycle model are used. There are in addition two sets of equations that are used to describe the heat exchanger between the generator and the absorber. These can be be seen as two additional heat exchangers where the heat transfer rates are evaluated and the minor of two is used as available ampunt of heat.

In the case of GAX cycle the desorber heat supply temperature is the most important. It affects the performance as for the simple cycle but it is binding for its operation. The temperature must be higher than 120 °C in order to have available enough heat to transfer to the desorber. It has been also performed a parametric study to find out how δ T between the two sides of the GAX Analyser affect the overall performance.

Calculation conditions are the same as the input parameters reported previously. They differ for the maximum temperature of the desorber because a higher temperature is needed to operate properly.

4.5.1 GAX Analyzer

To simulate the GAX cycle it is necessary to introduce a supplementary heat exchanger that transfer heat from absorber to desorber, if the temperature in the absorber is high enough. The GAX heat exchanger is reported as Analszer and it is divided in two parts, one relative to tehe absorber and the other relative to the desorber.

The GAX Analysis Desorber is defined by the following equations:

$$m[2] + m[6] + m[16] + m14v = m[5] + m14l \tag{4.36}$$

$$m[2] \cdot x[2] + m[6] \cdot x[6] + m[16] \cdot x[16] + m14v \cdot x14v = m[5] \cdot x[5] + m14l \cdot x14l \tag{4.37}$$

$$m[2] \cdot h[2] + m[6] \cdot h[6] + m[16] \cdot h[16] + m14v \cdot h14v + Qrequired = m[5] \cdot h[5] + m14l \cdot h14l \tag{4.38}$$

$$T[14] = T[4] - deltat \tag{4.39}$$

The GAX Analysis Absorber is defined by the following equations:

$$m[4] + m13v = m13l + m[15] \tag{4.40}$$

$$m[4] \cdot x[4] + m13v \cdot x13v = m13l \cdot x13l + m[15] \cdot x[15] \tag{4.41}$$

$$m[4] \cdot h[4] + m13v \cdot h13v = m13l \cdot h13l + m[15] \cdot h[15] + Qavailable \tag{4.42}$$

$$T[13] = T2f + deltat \tag{4.43}$$

In order to evaluate the amount of heat available it is used a procedure that determines whether or not the heat required by the desorber exceeds that available from the absorber and limits the heat exchange accordingly.

```
PROCEDURE(Qavailable,Qrequired,Qgentot,Qabstot:Qabs,Qgen,Diff)
Diff=ABS(Qavailable-Qrequired)
If (Qavailable>=Qrequired)
then
Qabs= Qabstot-Qrequired
Qgen=Qgentot-Qrequired
else
Qabs=Qabstot-Qavailable
Qgen=Qgentot-Qavailable
endif
END
```

4.5.2 Influence of delta T on GAX performance

It is assumed a value of temperature of 150°C in order to appreciate significantly the performance increase of this cycle configuration. In Figure 4.9, the COP trend is a function of the temperature delta between the two currents in the GAX heat exchanger. The maximum value of COP that can be obtained with delta [T] = 0. It is a condition

that is physically impossible, since no heat exchange can occur without temperature gradient. It can be seen that for a value of δ T of 4°C, which is realistic figure, there is already a strong performance penalty.

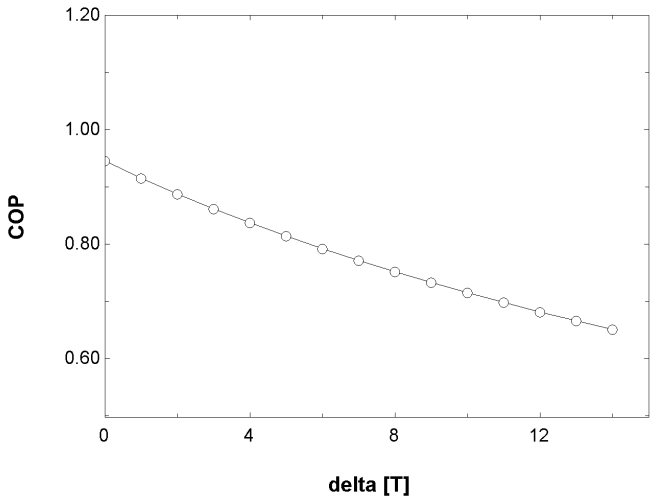

Figure 4.9: copmarison of COP curves between ammonia water GAX and single effect absorption chiller)

4.6 A comparison between simple absorption cycle and GAX cycle

Before proceeding further with model analysis, a comparison between the simple effect and the GAX cycles has been made in order to find the most suitable cycle to operate with the available installation parameters.

In Figure 4.10 it is shown the COP curve for both cycle for given range of generator temperatures. It is easy to spot how the GAX has higher COP values compared to the simple cycle only for high temperatures. For temperatures lower than 120 °C, the simple absorption cycle is most suitable.

The prototype will be operated with a mixture of ethylen-glycol and water with a temperature in the range of 95-105 °C. So it results clear that the most suitable cycle that has a higher performance in the chosen range is the single effect cycle. For this reason the following analysis has been performed only on the simple cycle to investigate

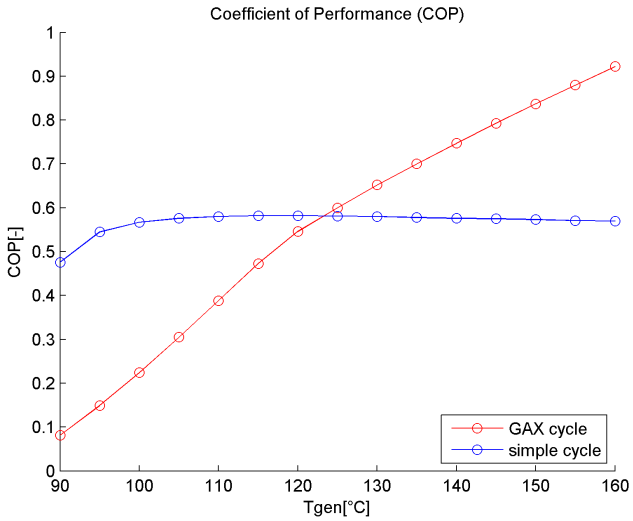

Figure 4.10: copmarison of COP curves between ammonia water GAX and single effect absorption chiller)

the prototype characteristics.

4.7 Simulation results

Several simulations were carried out by varying the generator temperature T_{gen} between 90°C and 180°C. The temperature at the condenser and absorber T_{cond} has been varied between 30 and 50°C (corresponding to a variation of the ambient temperature between 26°C and 46°C). The evaporation temperature T_{evap} has been kept constant to -3.5°C. The Figures 4.11-13 show the trends of the main performance parameters at the operating ambient temperature of 31°C (corresponding to $T_{cond} = 35$°C).

The heat transfer rates of heat exchangers are shown in Figure 4.12 as specific rates and they are normalized to the heat transfer rate of the generator. The curves show a substantial independence of performance parameters (COP, specific heat transfer rates of heat exchangers, flow rate and pump power) for a wide temperature range, between 100°C and 180°c. At lower temperatures, however, the performance declines. This is shown by the decrease of the COP, the increase in specific heat transfer rate of the regenerator, the solution flow and the power absorbed by the pump. At the same time the specific heat transfer rate of the evaporator decrease. The performance decline has a very high gradient; the ammonia concentration difference Δx, between the rich and the poor

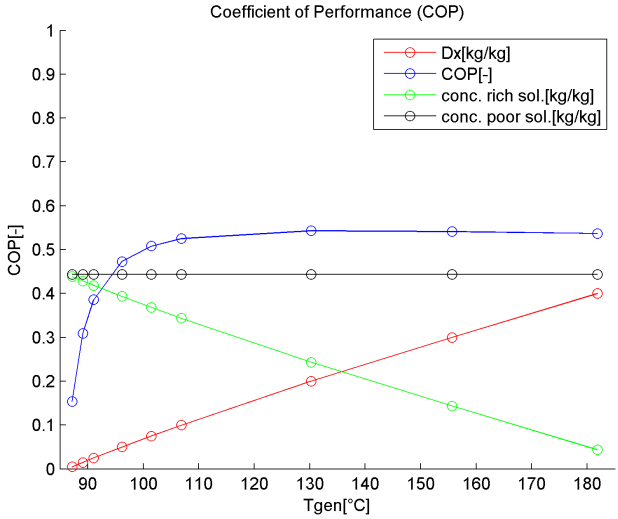

Figure 4.11: COP, concentration of NH3 in poor and rich and solution concentration difference Δx as a function of T_{gen} (T_{cond} = 35°C, T_{evap} =-3.5°C)

solution, generation tends to zero. The Δx is almost a linear function of temperature. The concentration of the rich solution out of the absorber is in saturation conditions. Since the pressure is fixed, related to the evaporation temperature, this is the maximum possible concentration of ammonia in the solution for a given ambient temperature. If the ambient temperature is fixed, then this concentration is constant.

The Figures 14 and 15 instead show the variation of COP at fixed evaporation temperature of -3.5°C. The COP is ploted as a function of the ambient temperature, thus the temperatures of the condenser and the absorber, as a function generation temperature and of concentration difference a x. In Figure 14 can be observed that the COP decreases with increasing temperature at condenser. It can be also seen that the value of T_{gen} for which there is a COP degradation, increases.

The figure 4.15 shows instead that the decay of the COP occurs for the same values of concentration difference Δ x, at all the condensing temperatures. This parameter is useful to assess whether the project operating conditions (evaporating, generating and ambient temperature) are feasible to operate a cycle that can work with acceptable values of the coefficient of performance. There is, in fact, a range of values of Δx of 0.1 0.15, above which the increase in COP related to increase in generation temperature is minimal. So waste heat can be effectively used. Below these values, the performance of the absorption cycle is insufficient. If the values of functional parameters reach the working point that

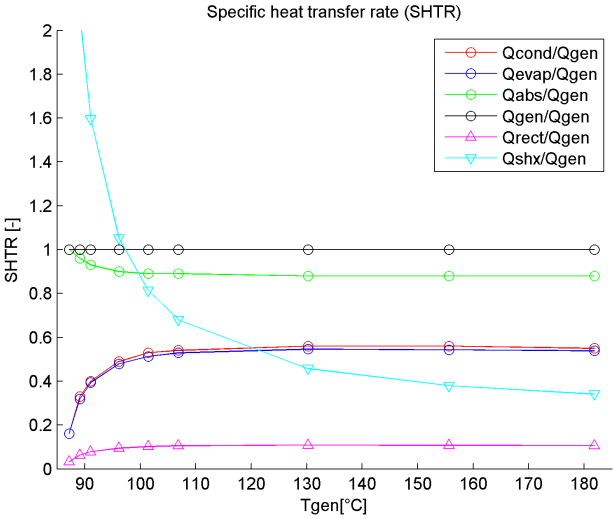

Figure 4.12: Specific heat transfer rate SHTR: Q_{gen} absorber heat transfer rate, generator, Rectifier Qrect Q_{gen} and regenerative heat exchanger the solution Qshx, compared to Qevap, according to T_{gen} (T_{cond} = 35°C, T_{evap} =-3.5°C).

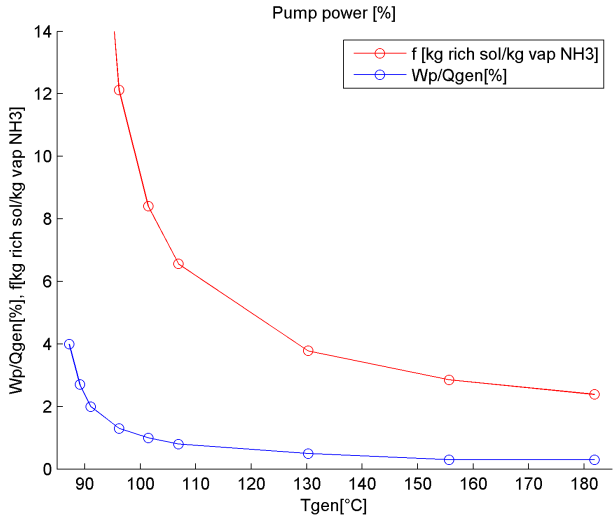

Figure 4.13: power absorbed by the pump Wp/Q_{gen} and circulating factor f as a function of T_{gen} (T_{cond} = 35°C, T_{evap} =-3.5°C).

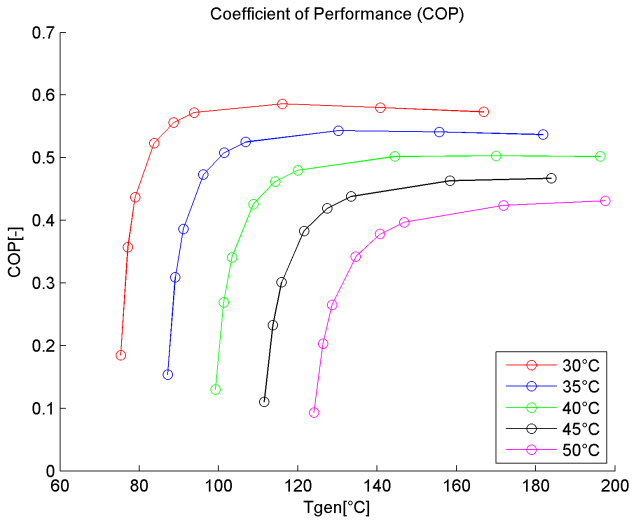

Figure 4.14: COP as a function of desorber temperature for different T_{cond} (T_{evap} =-3.5°C).

has concentration difference near the limit, it is sufficient a small fluctuation to lead to failure of operation.

Under these considerations, further simulations have been carried varing the evaporating temperature in the range of -24°C to 21°C, for a range of values of Δ x . The condensing temperature is fixed to 35°C, since, as shown in the qualitative trend curves, the COP is more affected by concentration difference Δx, thus the generation temperature.

The results were collected in synthetic way in the diagrams of figures 4.16-19, which contain respectively the isolines of COP and specific heat transfer rates for the evaporator, absorber and regenerator on T_{evap} plan-T_{gen}. There are also plotted on the same diagrams some Δ x constant curves with values between 0.005 and 0.400. As already noted in figure 4.15, for low values of concentration difference (less than 0.050) there is a drop of the COP. In figure 4.16 this trend is stronger with the decrease of the evaporation temperature. In figure 4.17 under the same conditions, the evaporator specific heat transfer rate decreases. The absorber and regenerator specific heat transfer rates increase, as shown in figures 4.18 and 4.19: there is an increase in the size of heat exchangers and therefore an increase of costs of the absorption machine.

As expected, the decrease of the difference between generation and evaporation temperature lead to an increase in the COP. The minimum generation temperature value, for

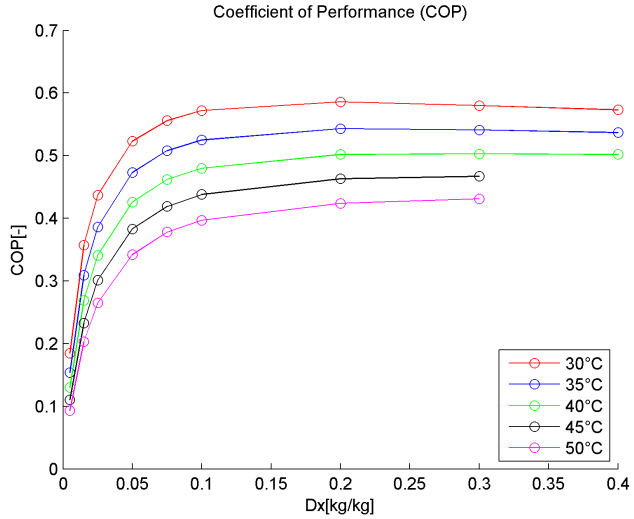

Figure 4.15: COP as a function of concentration difference Δ x for different temperatures of condensation (T_{evap} =-3.5).

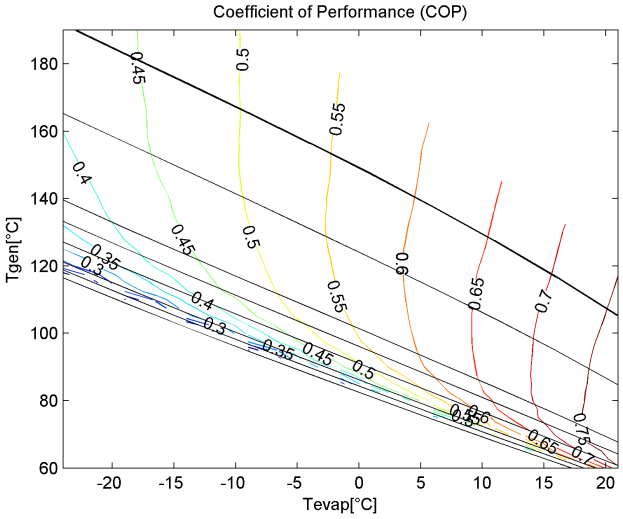

Figure 4.16: COP iso-lines and iso-Δx related to evaporation and generation temperatures (T_{cond} = 35°C).

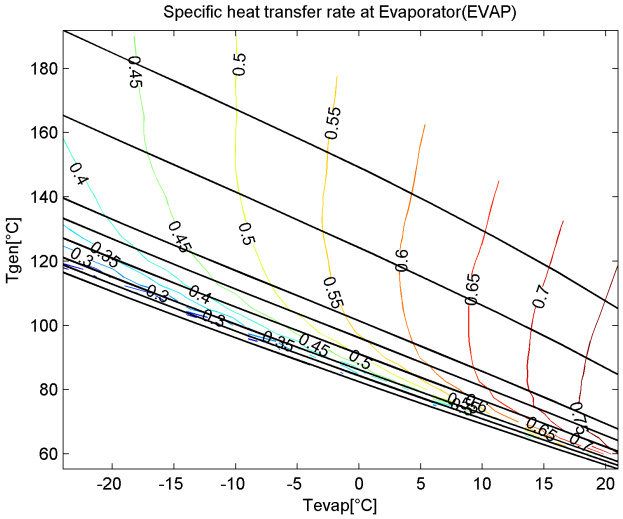

Figure 4.17: Heat transfer rate iso-lines of the evaporator and iso-Δx as a function of T_{evap} and T_{gen} ($T_{cond} = 35$).

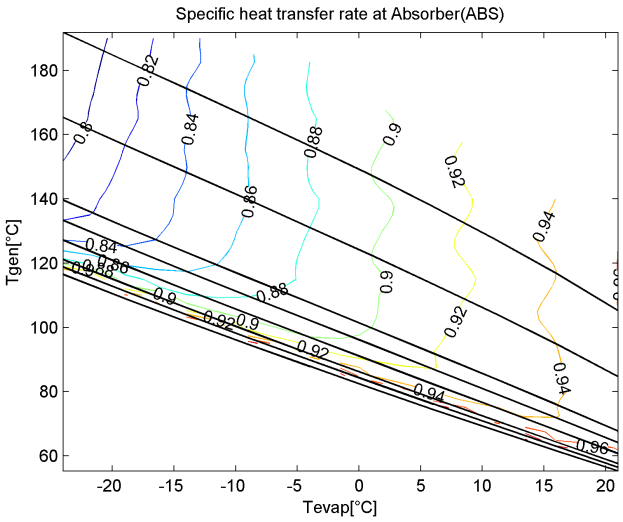

Figure 4.18: Iso-specific heat transfer rate for the absorber and iso-Δx as a function of T_{evap} and T_{gen} ($T_{cond} = 35$).

which Δx value is higher than those which penalise the COP, increases with decreasing of the evaporation temperature. It varies from 80°C for evaporating temperatures of 15-20°C and it rise to 130°C for evaporating temperatures of -20°C.

For higher values of Δ, the COP is poorly influenced by corresponding increase in generation temperature, in particular for the values of the evaporating temperature around -10°c. For values of Δx greater than the penalty limit, specific heat transfer rates of evaporator and absorber heat exchangers are again poorly affected by generation temperature. This does not apply to the regenerative heat exchanger, for which the specific heat transfer rate always decreases with increasing temperature of generation. In General, with the decrease of the difference between evaporation and generation temperatures, there is a slight decrease of the heat transfer rates of the heat exchangers.

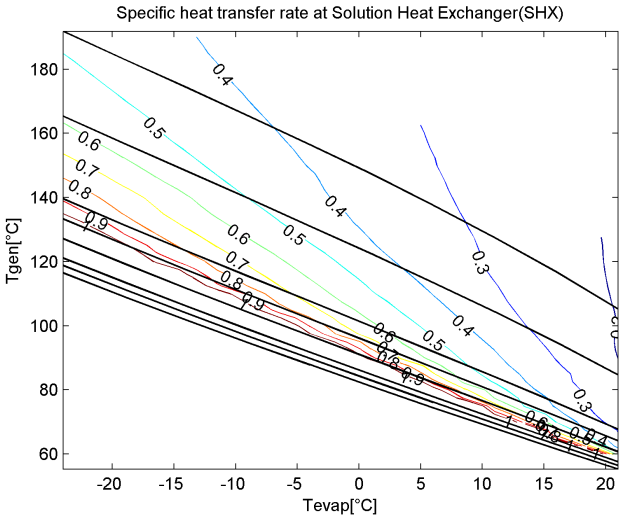

Figure 4.19: Iso-thermal heat transfer rate for regenerator and iso-Δ x as a function of T_{evap} and T_{gen} (T_{cond} = 35°C).

For cold generation applications from waste heat recovery, it is important to maximize the exploitation of available recovery heat. The best compromise between different needs has to be achieved:

- Maximum COP, or maximum performance of the thermodynamic cycle.
- Minimum generation temperature, in order to maximize the heat transfer rate from a finite capacity source.
- Stable operating conditions, i.e. not susceptible to temperature variations.

- Acceptable size of major components, i.e., heat exchangers and solution pump.

Figure 4.18 gives useful tips to identify those solutions, and it permits to evaluate the margin of corresponding concentration difference referred to permissible minimum values. In particular, it can be determined an optimal value of concentration difference for a certain evaporating temperature (and for a given ambient temperature: the computational model presented extends the analysis to different values of ambient temperature, and then of condensation and absorption temperatures). In addition, over this optimal value, there is a reduction of the heat transfer rates of the heat exchangers, but the value of COP is slightly lowering and the generation temperature is higher. Economic optimizing considerations must therefore take account of the relative weight of a decrease in heat recovery efficiency against a reduction of the exchange surfaces.

4.7.1 Final remarks

A thermodynamic calculation procedure, based on main working parameters, has been developed for first sizing of an ammonia water absorption cycle fed by recovery heat. It requires only the temperature of the secondary fluid operating the generator, the required process fluid temperature and outer ambient temperature. It is thus possible to proceed to determine a working point that allows absorption chiller to operate chillers in optimal conditions.

The concentration difference between rich and poor solution is a significant parameter for determining the working point. In particular it allows to determine the figure for which there is no appreciable increases of COP. In fact working point lays in range were there is no exploitable increase of generation temperature and it is above the value of generation temperature for which there is a marked drop of performance. Furthermore heat exchangers loads vary accordingly: the choice of the project must take into account the economic factors related to their size. Moreover the minimum required temperature of the secondary fluid operating the generator has to be limited.

In this regard, the absorption chiller operating at maximum COP working conditions do not guarantee to maximize the useful effect at the evaporator. Indeed lowering the temperature of recovered heat out-coming heat secondary system allows to increase the thermal heat transfer rate available at the generator. It is therefore necessary to investigate the correlation between the outlet temperature of the secondary fluid recovery circuit. This has to be related to the cooling capacity achieved so. The maximum global COP of the whole system, both absorption chiller and recovery system, is thus the goal.

The model developed can be employed to size both the absorber and the recovery facility. The heat exchangers loads and pump power allow to proceed for the economical

evaluation of the system.

5

ABSORPTION PROTOTYPE DESIGN

The numerical model described in the previous chapter is now used to define the single effect ammonia water absorption cycle that is used to design and build the prototype. The aim of this section is to determine the operating conditions of the prototype. There are defined all the state points that define the single components of the cycle. The data obtained so are used for selection of the components. The design process is divided in these phases:

- Identification of working conditions and determination of state points of the cycle
- Finalization of cycle with the heat exchanger supplier
- Definition of Process and Instrumentation Diagram
- Sizing and selection of the components
- 3D model design and drawings for construction
- Workshop construction of the prototype

5.1 Prototype cycle definition

As seen previously the first parameters to be defined are the evaporation generation, absorption and condensation temperatures. The absorption and condensation temperature are related to the available cooling heat sink and it is the same for both.

The prototype cycle has T_{gen} = 100°C, T_{evap} = -3.5°C (a glycol solution at 0.5°C. It has been considered an approach temperature of 4°C for all heat exchangers. The thermal

heat transfer rate of the evaporator Q_{evap} is 75 kW. The condenser and absorber cooling technology is evaluated, and then it is fixed to T_{cond}, T_{abs} = 35 °C.

The objective of this section is to determine the operating conditions of the prototype and use these data to select the key components that will be used to build it. The heat transfer rates, flow and input and output temperatures of the heat exchangers will be defined. Flow and head of solution pump and regulation valves will be determined.

5.1.1 Initial parameters

Project data are below listed:

- Evaporator cooling load = 75 kW
- Output temperature of refrigerated fluid = 0.5 °C (Glycol-Ethylen mixture side)
- Evaporation temperature = -3.5 °C (ammonia side)
- Input temperature of the generator solution = approx. 100°C (Glycol-Ethylen mixture side)

Air has been proposed as cooling sink for absorber and condenser. It can be added as further condition to the project:

- Condensing/Absorption Temperature = temperature of the outlet solution from the absorber = 40 °C

Feasibility of the above described conditions is proposed. Using the model developed in the previous chapter, a comparative study of influence of the condensation/absorption temperature on performance is reported for some cooling technologies.

5.1.2 Condensation/absorption cooling: air cooled heat exchanger

- Condensing temperature T_{cond} = 40 °C

A condensing temperature of 40 °C is considered. This value is obtained considering an ambient temperature of 35 °C and a approach temperature of 5 °C.

The below graphics show the performance chart and the thermal loads of components for a fixed condensation and absorption temperature. There is shown also the influence on the solution flow and on the absorbed power of the pump.

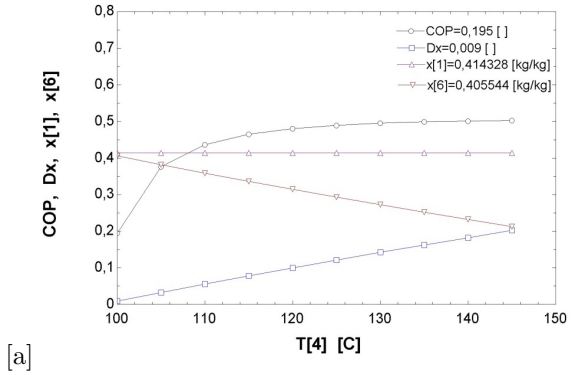

[a]

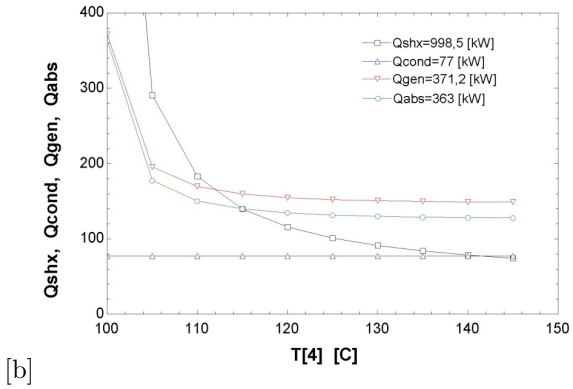

[b]

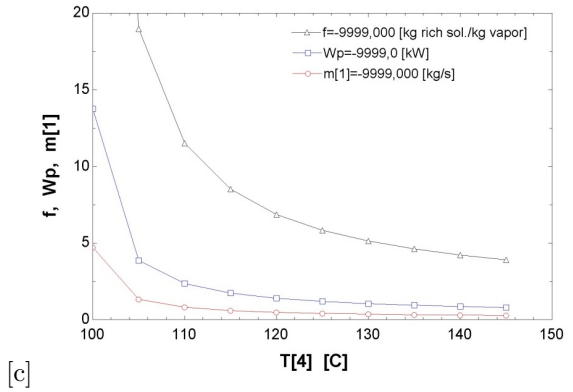

[c]

Figure 5.1: Charts for fixed temperatures T_{gen} at T_{amb} = 40 °C: a) Performance parameters: COP, δ x, x_1, x_6; b) Heat transfer rates; c) Flow and absorbed power of the pump and solution recirculating ratio

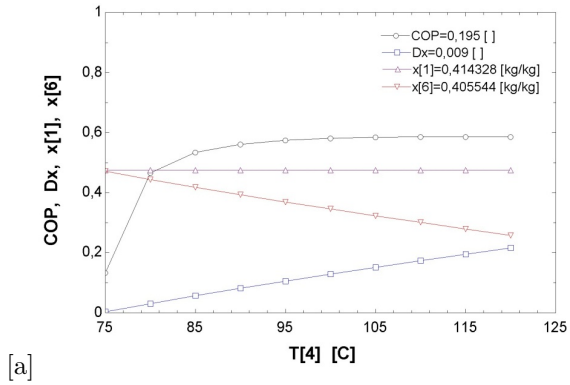

[a]

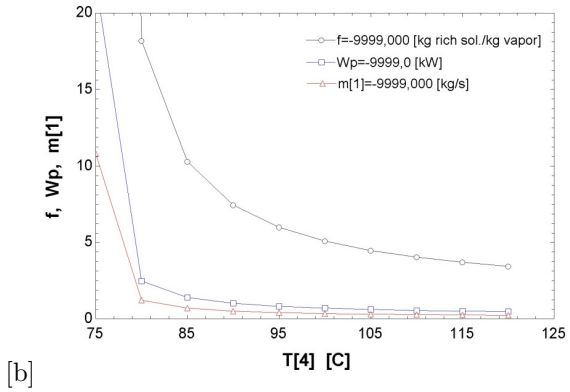

[b]

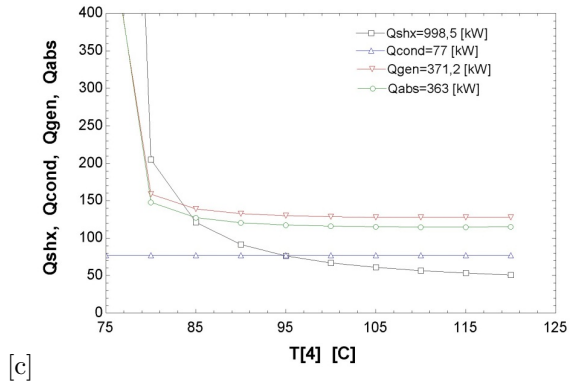

[c]

Figure 5.2: Charts for fixed temperatures T_{gen} at $T_{amb} = 30$ °C: a) Performance parameters: COP, δ x, x_1, x_6; b) Heat trensfer rates; c) Flow and and absorbed power of the pump and solution recirculating ratio

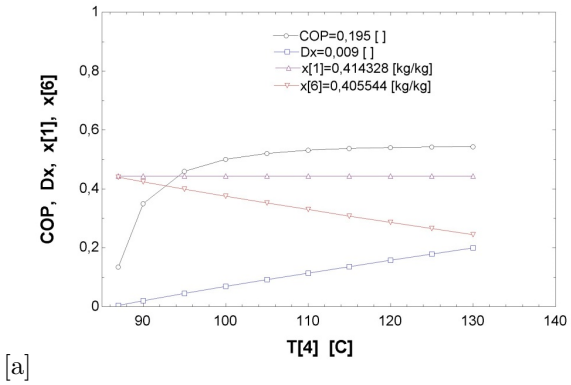

[a]

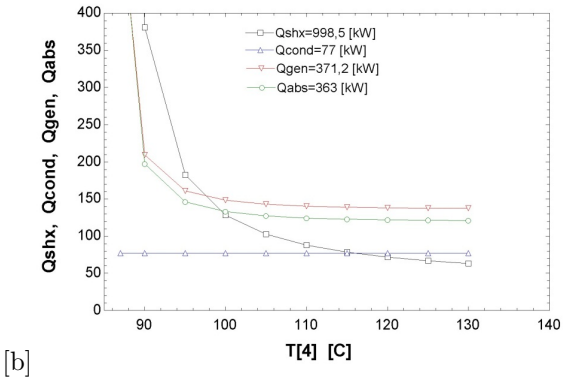

[b]

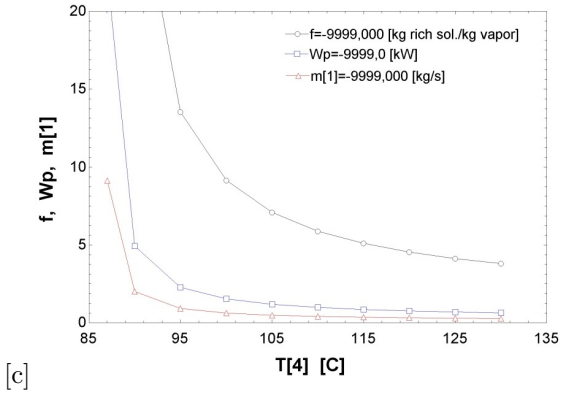

[c]

Figure 5.3: Charts for fixed temperatures T_{gen} at T_{amb} = 35 °C: a) Performance parameters: COP, δ x, x_1, x_6; b) Heat transfer rates; c) Flow and and absorbed power of the pump and solution recirculating ratio

5.1.3 Condensation/absorption cooling: evaporative condenser

- Condensing temperature T_{cond} = 30 °C

A condensing temperature of 30 °C is considered. This value is used to select an evaporative condenser in the zone of Trieste (T_{cond} = 30 °C and wet bulb temperature of 26 °C).

The below graphics show the performance chart and the thermal loads of components for a a fixed condensation and absorption temperature. There is shown also the influence on the solution flow and on the absorbed power of the pump.

5.1.4 Condensation/absorption cooling: wet cooling tower

- Condensing temperature T_{cond} = 35 °C

A condensing temperature of 35 °C is considered, it is an intermediate temperature between the two previous cases. This value is used to select a wet cooling tower condenser in the zone of Trieste.

This temperature is the most realistic condition between the two previously hypothesized, always keeping in mind the climatic conditions of Trieste area. The diagrams are shown to compare the values with those of previous cases.

5.1.5 Selection data

Parametric studies have been carried out in order to find the best working conditions to operate the prototype.

The influence of cooling temperature of the condenser and absorber has been investigated, keeping constant evaporation and generation temperatures equal to -3.5°C and 100°C respectively. It has been seen that the performance of the cycle vary and that the maximum temperature of condensation is 40°C. This occurs because the concentration difference between rich and poor solution decreases down to zero for a too high condensation temperature. This leads to an increase of the solution flow for same heat transfer rate of the evaporator. It is proportional to ammonia mass flowing in the absorber. Therefore there are required higher pump power and bigger heat exchangers.

In the second step have been taken into account three operating conditions with constant condensing temperature: air cooled heat exchanger, evaporative condenser and wet tower cooling, intermediate between the first two (then employed for dimensioning of the components of the prototype). For all the cases examined, an analysis of the influence of generation temperature has been reported, in order to understand what is the lowest hot water temperature at which operate the prototype.

Lowering the temperature of the condenser it is possible to lower the temperature of generation. In addition to this an increase in performance of the cycle can be also observed. Beside to of the minimum generator temperature it must be paid attention to the solution flow that negatively impacts on heat transfer rate of heat exchangers and on the required pump power. Therefore, during the absorption machine dimensioning, working conditions must be a compromise between the minimum generation temperature required to operate the cycle and the solution flow value. A working condition set must be selected in a way to ensure that the off design conditions permit a stable operation of the machine and reduced components sizes.

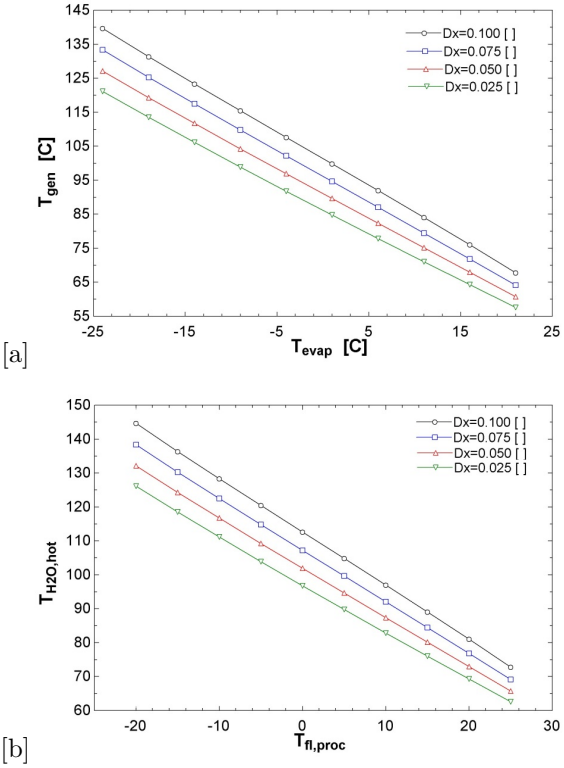

Figure 5.4: (a)Constant differential concentrations between rich and poor solution for given generation and evaporation temperatures. (b)Constant differential concentrations between rich and poor solution for given hot water feed and process fluid temperatures.

After the previously described analysis it is necessary a simple way to assess the operation conditions. It is possible to evaluate the operating temperatures, without running a simulation in EES. It has been observed that an absorption machine operates

in sufficiently stable conditions if there is a sufficient ammonia concentration difference between rich and poor solutions. A good trade-off between performance and components sizes can be obtained if the concentration difference value is greater than 0.05.

The charts in Figure 5.4 have been created keeping the condensation temperature of 35°C. The outlet temperature of the absorption is equal to that of condensation which is the minimum available in the cycle for cooling. A parametric study for various values of evaporation temperature for fixed concentration differences are run (0.100 0.075 0.050 0.025). The graph with generator outlet vs evaporation temperature is reported in Figure 5.4 a). In a second chart, shown in Figure 5.4 b), for easier reading, the process and the available hot water temperatures are employed. In order to calculate these temperatures a fixed approach of 4°C between the evaporation and the process temperatures and an approach of 5°C between the hot water and generation temperatures are used.

	h [kJ/kg]	m [kg/s]	p [kPa]	Q	s [kJ/kg K]	T [C]	v [m3/kg]	x [kgNH3/kg]
[1]	-80.191	0.622	319.053	0.000	0.375	35.00	0.001	0.443566
[2]	-77.735	0.622	1350.714	-0.001	0.379	35.35	0.001	0.443566
[3]	153.791	0.622	1350.714	0.001	1.073	86.31	0.001	0.443566
[4]	225.017	0.554	1350.714	0.000	1.253	100.00	0.001	0.375236
[5]	-34.958	0.554	1350.714	-0.001	0.497	41.96	0.001	0.375236
[6]	-34.958	0.554	319.053	-0.001	0.5	42.16	0.001	0.375236
[7]	1462.71	0.071	1350.714	1.000	4.732	86.20	0.120	0.977579
[8]	151.887	0.003	1350.714	0.000	1.068	86.20	0.001	0.443566
[9]	1297.122	0.068	1350.714	1.000	4.238	39.94	0.097	0.999634
[10]	165.994	0.068	1350.714	0.000	0.579	35.00	0.002	0.999634
[11]	165.994	0.068	1350.714	0.000	0.579	35.00	0.002	0.999634
[12]	165.994	0.068	319.053	0.156	0.637	-7.68	0.061	0.999634
[13]	1267.661	0.068	319.053	0.998	4.776	-3.50	0.397	0.999634
[14]	1267.661	0.068	319.053	0.998	4.767	-3.33	0.390	0.999634

Figure 5.5: Table of thermodynamic parameters of the prototype cycle

Component selection data based on previous analysis are reported below. The condensing temperature and the absorption temperature are fixed to 35 °C, while the temperature of the generator is fixed to 100 °C. It is used an approach of 5 °C between the temperature of the generator outlet of poor solution and the generator inlet of the water and glycol mixture. For wet cooling tower is used an approach of 4 °C between condensing temperature and the temperature of the process fluid (water).

Thermodynamic parameters of the cycle for dimensioning the prototype are reported in Figure 5.5.

The main parameters of the cycle are:

- COP=0.494
- f=9.138 [kg rich sol./kg vapor]
- pratio=4.234
- Qabs= 117.3[kW]
- Qcond= 79.4[kW]
- Qevap=75.0 [kW]
- Qgen=151.8 [kW]
- Qrect=18.0 [kW]
- Qshx=144.2 [kW]
- Wp=1.5 [kW]

SOLUTION PUMP

The solution pump must ensure the required flow and head to operate correctly and must work with a solution of water and ammonia with a concentration of ammonia by weight of 44.5 %. Data for the selection are:

- Flow = 0.622 kg/s
- Suction Pressure = 319 kPa = 3.19 bar
- Discharge Pressure = 1350 kPa = 13.5 bar
- Head = 1013 kPa = 10.31 bar
- Pressure Ratio = 4.234

HEAT EXCHANGERS

The heat exchangers are reported in the table in Figure 5.6. There are listed the main characteristics

	Fluid 1		Fluid 2	$T_{in,1}$ [°C]	$T_{out,1}$ [°C]	$T_{in,2}$ [°C]	$T_{out,2}$ [°C]	$Q_{1,in}$ [kg/s]	$Q_{1,out}$ [kg/s]	p_1 [kPa]	p_2 [kPa]	HTR [kW]
HX	Inlet	Outlet										
1 (ABS)	NH3-H2O (99,9634%) vapor + NH3-H2O (37,5236%) liquid	NH3-H2O (44,3566%) liquid	Water	-3.4 42.2	35	30	32	0.068 0.554	0.622	319	-	117
2 (SHX)	NH3-H2O (44,3566%)		NH3-H2O (37,5236%)	35.4	86.4	100	42.2	0.622	0.622	1350		144
3 (GEN)	NH3-H2O (44,3566%) liquid + NH3-H2O (44,3566%) liquid	NH3-H2O (99,7579%) vapor + NH3-H2O (37,5236%) liquid	Ethylen Glycol-Water mixture (25%)	86.4 86.4	86.4 100	105	95	0.622 0.003	0.071 0.554	1350	-	151
4 (RECT)	NH3-H2O (99,7579%)	NH3-H2O (99,9634%) vapor + NH3-H2O (44,3566%) liquid	Water	86.4	39.9 86.2	35	45	0.071	0.068 0.003	1350	-	18
5 (CON)	NH3-H2O (99,9634%) vapor	NH3-H2O (99,9634%) liquid	Water	39.9	35	30	35	0.068	0.068	1350	-	91
6 (EVAP)	NH3-H2O (99,9634%) liquid	NH3-H2O (99,9634%) vapor	Ethylen Glycol-Water mixture (25%)	-3.5	-3.5	5	0.5	0.068	0.068	319	-	75

Figure 5.6: Schematic representation of heat pump cycle

5.2 Prototype absorption cycle finalization

The above selection table for heat exchangers has been sent to many plate heat exchangers producers. Only Alfa Laval is able to provide the quote for them. Before that a Alfa Laval consultant has provided a table sheet with the main parameters of the cycle used to verify the selection table sent. There are minor differences on overall performance and parameters values. The thermodynamical properties are based on RefProp software. The properties provided in this way are far more accurate and updated if compared with EES values.

The properties refer to NIST Reference Fluid Thermodynamic and Transport Properties Database. [refprop] The program uses the most accurate equations of state and models currently available for many fluids and their mixtures, including ammonia-water solution. It can be used as a plugin in Microsoft Excell to evaluate the properties in each point.

The cycle has been modified according to the new values proposed in the cycle in Figure 5.7. There are reported the temperatures, enthalpies, concentrations and mass flow values for all the main points in the cycle. There is a slight difference in all the values evaluated with a different property database. The heat transfer rates for each heat exchanger are almost the same as the one evaluated in EES. This confirm the validity of the proposed model in EES.

Based on the values so evaluated Alfa Laval has made the selection of the heat exchangers for each component. The selected heat exchangers are reported in Components Description section.

5.3 Process and Instrumentation Diagram

Once the cycle has been finalized, the Process and Instrumentation Diagram (PID) has been defined. In the PID are reported the main values of thermodynamic properties, the interconnecting piping and the instrumentation of the prototype. Furthermore there are reported the vessels that are inserted lately in the 3D model.

5.3.1 Absorption Cycle

Referring to the absorption cycle, there are some aspects that must be defined. The absorber and the evaporator types. For cycle calculation the properties are evaluated in saturation conditions. It is not possible to consider the effects of these solutions with the model in EES and in Excell.

The absorber has been selected by Alfa Laval with specific request to be operated

as Falling film type. This solution is proposed by Alfa Laval itself in their technical manuals for absorption applications. it has been also requested the possibility to operate the same component also in bubble type mode. This has been kept in count during selection process and to different distributors were designed. In Figure 5.10 it is shown the technical solution adopted for the prototype. A Plate Heat Exchanger (PHE) can make an excellent absorber, due to its ability to mix fluids while simultaneously cooling them.An absorber is composed of two sections, injection of the absorbing liquid into the ammonia vapour and the subsequent absorption and cooling of the mixture.

The evaporator can be considered as a pure fluid evaporator in a refrigeration plant. It operates as a normal pure ammonia evaporator. However, in some cases, especially if a thermosiphon evaporator is used, the water content of the evaporated vapour is less than in the incoming condensate. Water then concentrates in the evaporator separator and the evaporation temperature increases. A special additional evaporator is then necessary. A direct expansion (DX) evaporator is then a better choice, especially if it can be arranged so that all liquid droplets leaving the evaporator move directly to the absorber, without encountering any pockets, where they can collect. For this Prototype has been adopted the latter solution for its higher simplicity.

5.3.2 Process Description

Observing the PID it is possible to notice some vessels. Their main purpose is to collect liquid solution or liquid refrigerant out of the PHE and separate it from the vapor that is present in the same point. This is very important especially for rectifier and generator vessels where the vapor and liquid flow in different circuits. In the case of the absorber the vessel has also the function to assure a sufficient liquid head in order to avoid cavitation of the following solution pump. In fact the vessel is provided with a level gauge that is used to maintain the minimum liquid level.

Every vessel is provided with sight glass to help charging operations. The sight glass permit to control the levels during the operation helping to obtain a better understanding of transients during prototype operations.

In the prototype are installed some valves that are requested for service purpose. Some of them are requested to void the system through a void pump. Other are used to fill the absorption chiller with refrigerant.

There have been installed regulation valves on the secondary fluid side. They are requested to regulate the water or Glycol-water flows incoming in each single PHE. On the internal side it has been installed a barostatic valve to control the poor solution flow from solution heat exchanger to the absorber.

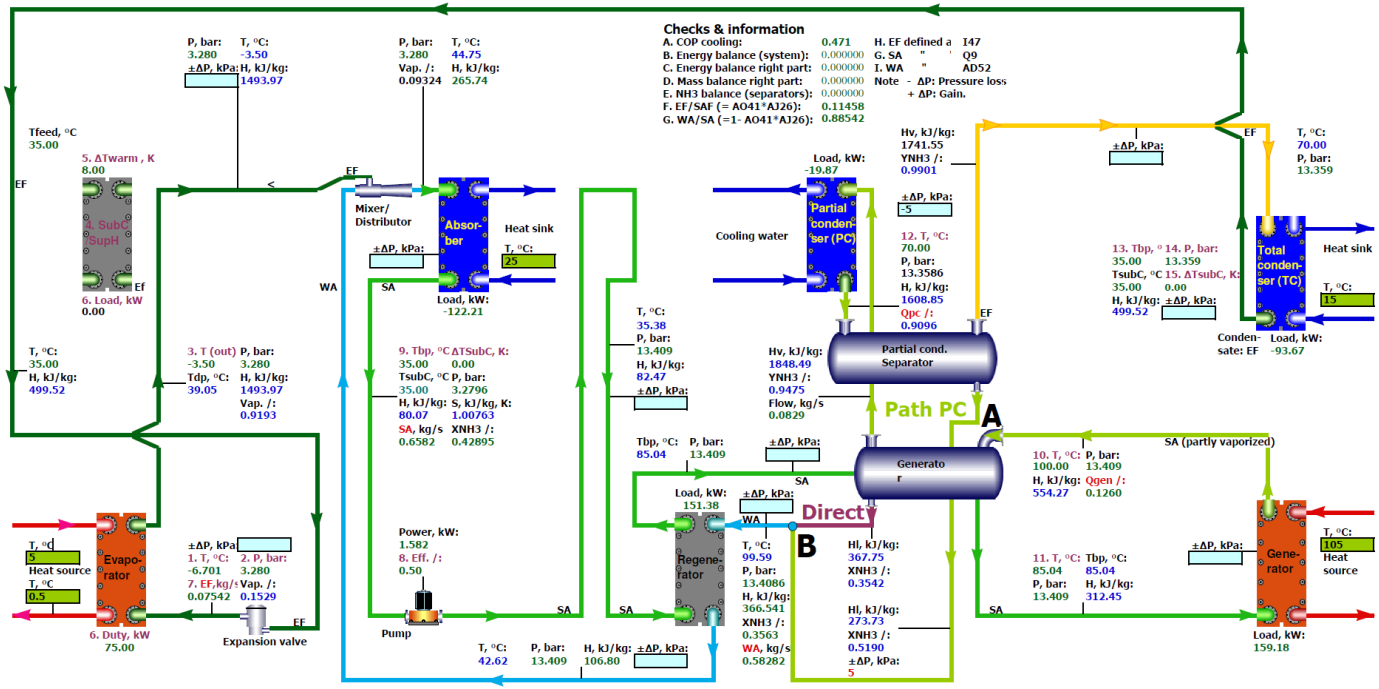

Figure 5.7: Schematic representation of heat pump cycle

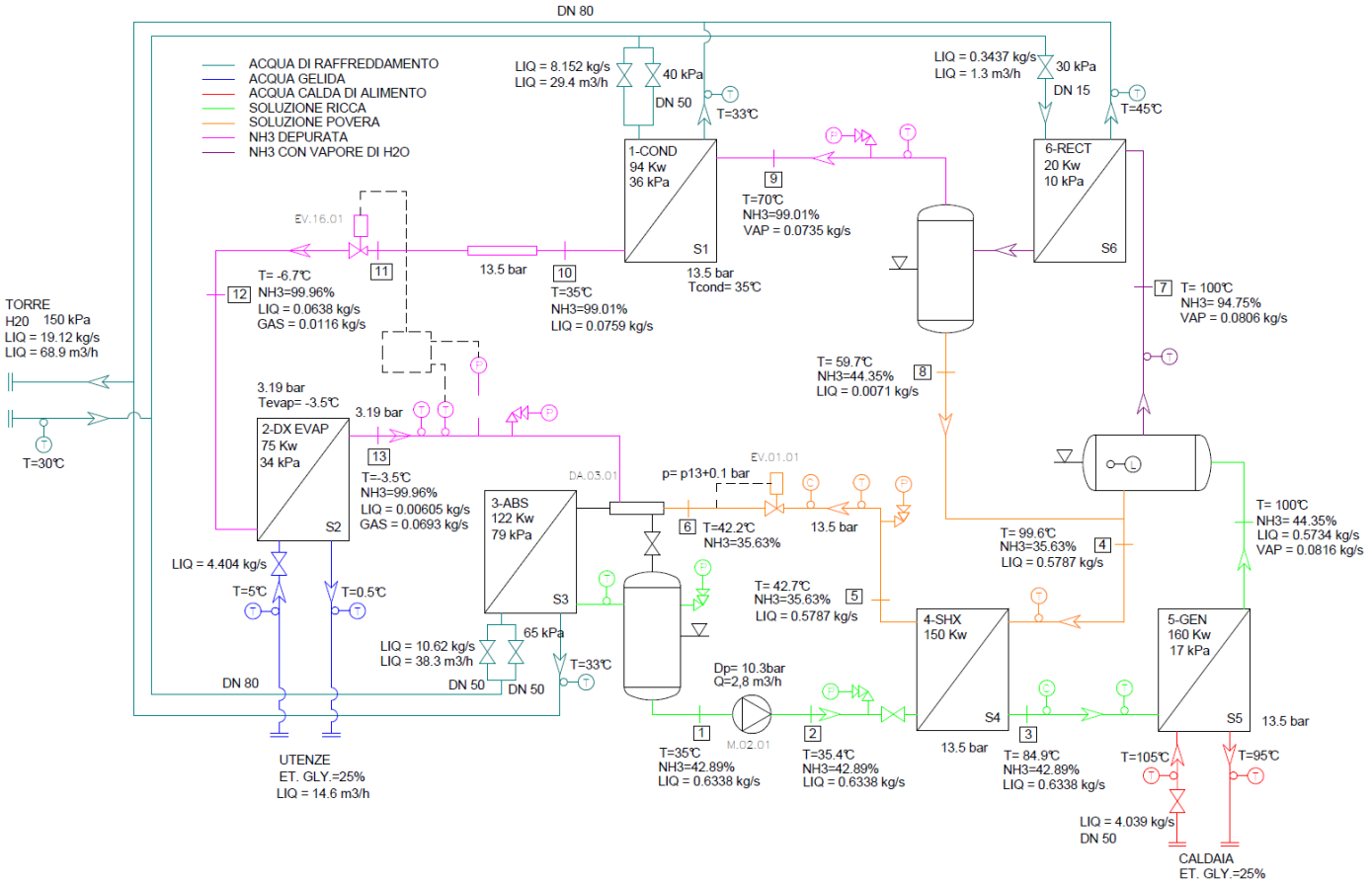

Figure 5.8: Schematic representation of heat pump cycle

5.4 Components Description

In this section is reported a brief description of each component. For further details, data sheets of components are reported in Annex section.

5.4.1 Heat Exchangers

Plate heat exchangers have been selected for their superior characteristic compared to standard shell and tube heat exchangers. There are several advantages of this typology and they can be listed as follow:

- Higher heat transfer performance.
- 40 % m3/kW space saving due to the compact design of plate heat exchangers compared to Shell and Tube heat exchangers.
- Rapid response to changes in temperature due to small hold-up volume and lower refrigerant charge

All heat exchangers of the absorption prototype are AlfaNova plate heat exchangers manufactured by Alfa Laval. They are made of 100% stainless steel. They are based on welding stainless steel components together, bestowing high resistance to corrosion. AlfaNova heat exchangers are well suited in applications which put high demand on cleanliness, applications where ammonia is used or applications where copper or nickel contamination is not accepted. They are extremely compact compared to their capacity to withstand great strains in demanding heat transfer applications.

Figure 5.9: Plate heat exchangers in DX expansion and condenser configurations [**?**]

The heating surface consists of thin corrugated metal plates stacked on top of each other. Channels are formed between the plates and corner ports are arranged so that the two media flow through alternate channels, always in counter current flow. The media are kept in the unit by a bonded seal around the edge of the plates. The contact points of the plates are also bonded to withstand the pressure of the media handled. All the units are tested to withstand high pressures.

A plate heat exchanger has very complicated flow geometry with sudden contractions and changes in flow direction. This may keep the two phases of the working fluid mixture well mixed.Due to this characteristics they have been applied to all the absorption chiller components.

In Figure 5.8 are shown two plate heat exchangers in direct expansion evaporator and condenser configurations.

5.4.2 Distributors

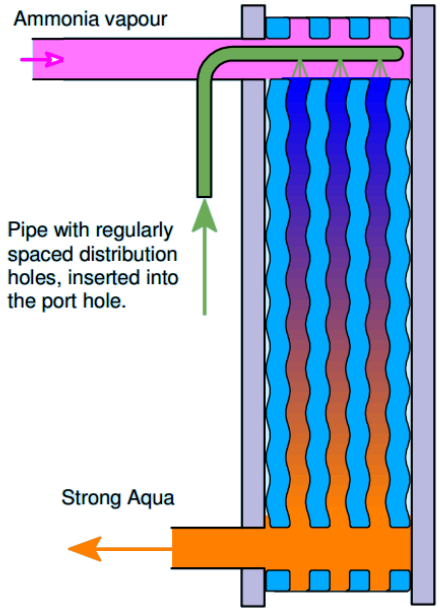

Figure 5.10: Distributor configuration for falling film type absorber [**?**]

Distributors are a very important and critical component, especially for the absorber. The problem lies in the distribution of the mixture to the channels. Each channel should be fed with its share of vapour and liquid. Unfortunately, it can happen that the vapour

and liquid separate after the injection and the liquid then normally enters predominantly the first channels, while the vapour enters the last channels. Various methods have been proposed to obtain good distribution, most of them proprietary.

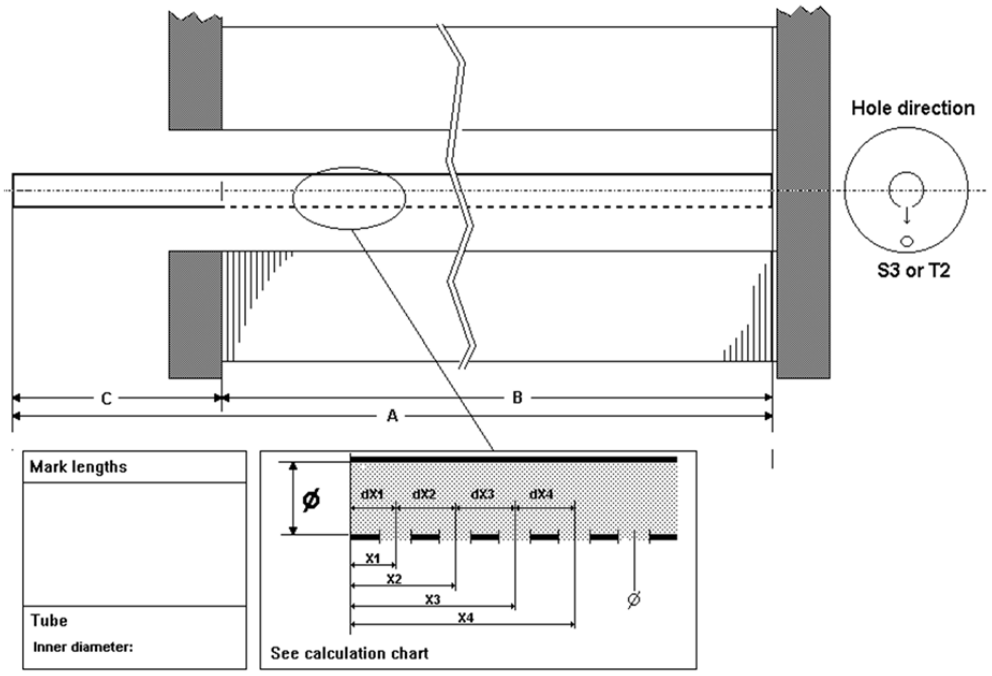

Figure 5.11: Distributor construction drawing. The quotes are calculated based on PHE and plates dimensions.

Some general rules can be given [**?**]:

- There are no entirely reliable design methods, but a PHE can be designed as a condenser, with a portion already condensed at the inlet. The ammonia-water system is a refrigerant with a very large glide. The heat release when the two vapours condense is due not only to the latent heat but also to a high mixing heat.
- Avoid bends (i.e. centrifugal forces) and large distances between the injection point and the entrance to the PHE. The liquid then settles and separates.
- The weak aqua should be injected into the ammonia vapour pipe. Multiple injection points along the inlet pipe have been tried with good result as shown in figure 5.10.

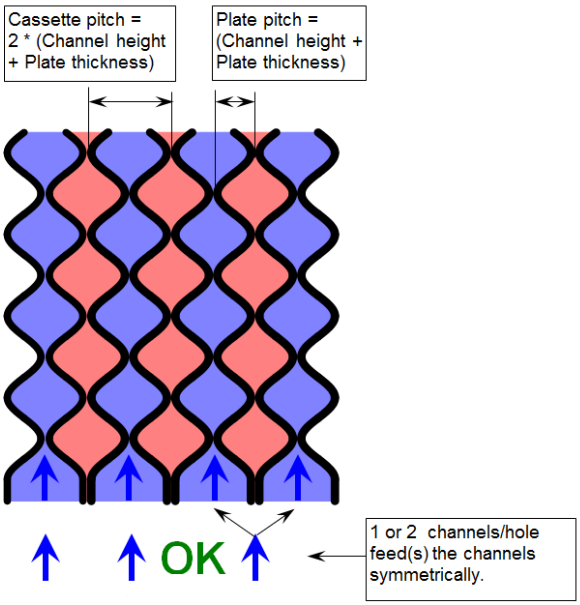

Figure 5.12: Distribution of the liquid over the single plate channels

- Injection, type ejector pump, is untried but might be a good idea. The high velocity in the nozzle breaks down the liquid in fine droplets.

- It is an unsolved question whether the inlet should be mounted from the top or from the bottom. Most installations are from the top. It is however easier to ensure a good distribution, especially of the liquid, from below, but the flow may be unstable at least at low capacities.

5.4.3 Pump

The ammonia/water mixture in the liquid/vapour separator is saturated. The pump selection has been one of the most critical design assumptions. An extensive market research for a suitable pump has been carried. Many technical solutions have been screened: membrane pumps, gear pumps and water pumps. The first two resulted many times more expensive than the water pump. Beside that the membrane pumps require higher maintenance and have lower operative life.

Low capacity ammonia water absorption chillers usually employ membrane pumps to manage a two phase flow. In this case, a common multi-stage centrifugal water pump

has been selected and tested. A normal water pump employs materials that are perfectly compatible with ammonia water solution. In order to avoid the cavitation conditions some precautions have been put in place. As previously described a liquid separation vessel is installed out of the absorber to provide a sufficient liquid head. Furthermore a low NPSH pump has been selected. It is a special pump version with a specifically designed first stage and a bigger impeller and suction section. The pump is controlled with a variable speed driver (inverter).

In the following table there are listed main pump characteristics:

Manufacturer	Loware (Xylem group)	Technical
Type	Multistage vertical pump (low NPSH)	
Flow	0.75 l/s	
Pressure (nominal)	1350 kPa	
Temperatures	-30°C +90°C	
Absorbed power	1.5 kW	

data of the solution pump

In Figure 5.12 the pump curve with the working point is reported.

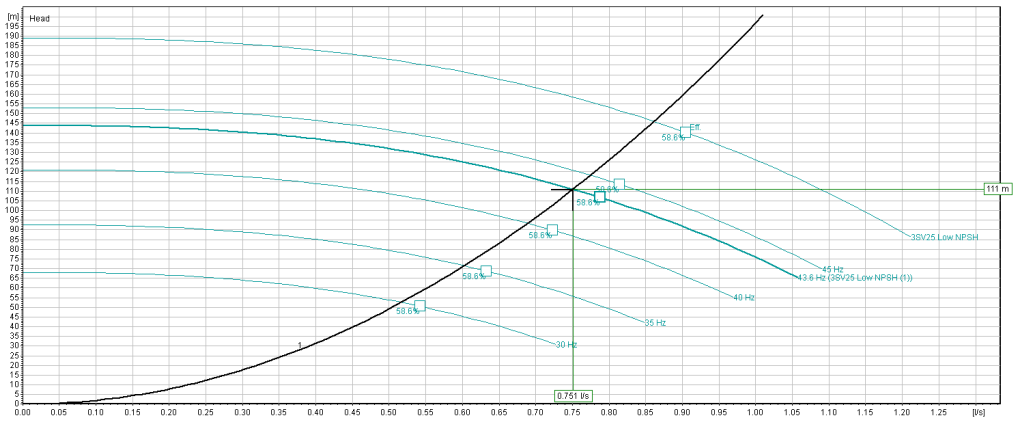

Figure 5.13: Pump curve from the producer selection software [**?**]

5.4.4 Valves

Expansion valve An electromechanical expansion valve of type Siemens MVS661.25-0.40N with a linear characteristic is used. It is hermetically sealed and butt welded to the interconnecting piping. It has a high resolution and control accuracy, precise positioning control and position feedback signal and short positioning time (¡ 1 second). It has a kvs values 0.4 m/h. The valve is supplied with his own electronic board that controls the super-heating temperature of the vapor from evaporator. It has been setted a 5 K superheat value.

Barostatic valve

ICM valves are designed to regulate an expansion process in liquid lines with or without phase change or control pressure or temperature in dry and wet suction lines and hot gas lines. The ICM valves are designed so that the opening and closing forces are balanced, therefore, only three sizes of ICAD actuators are needed for the complete range of ICM from DN 20 to DN 150. The ICM motorised valve and ICAD actuator assembly offers a very compact unit with small dimensions.

The installed ICM valve has a kv value of 2,4 m/h.

Regulation valves

In order to regulate precisely the cooling flow to the heat exchangers, regulating valves have been installed on secondary circuits. The correct balance of hydraulic systems is essential to ensure the functioning of the system under the design conditions. In Caleffi 131 series threaded valves, the flow measurement is made with a Venturi, housed inside the body valve. This device ensures accuracy, high ease of use as well as during the calibration.

There have been installed on the returns of absorber, condenser and rectifier heat exchangers.

5.5 Instrumentation and Measurements

All primary reference instrumentations are certified by accredited calibration laboratory (LAT). Their certificates are issued according to the Decree No. 273/1991 establishing the National Calibration System (Sistem Nazionale di Taratura - SNT). Calibration certificates are associated to each sample probe for comparison.

5.5.1 Data Acquisition

A data acquisition system is installed to enable on-line measurement and control of the absorption chiller prototype. The measurements have been acquired and recorded

by management system present on the system (PLC Siemens S7 300) installed inside the control panel.

All measurements are measured every second for the whole operating period and stored on line on the on-line server. The measurement system acquires data and processes it on-line. After acquiring data, the performance of prototype and its components are downloaded and used to evaluate the main functioning parameters.

All the measured displays are visualized on a touch screen on the front door of the control panel. Some of them are used to run properly the system and avoid any dangerous situation, like over temperatures and over pressures. There are many safety blocks that control maximum temperatures and pressures. There are also controls on the minimum temperatures that put in stand by the system, like low outgoing evaporator process fluid temperature. In this case the prototype stops to work to avoid an excessive cooling of the process fluid.

5.5.2 Temperature Measurement

All temperature measurements were carried out by resistance thermometers (RTD), Pt100 type temperature sensors with an accuracy of 0.05°C. The temperatures probes are inserted into steel thermowells. These probes are equipped with a transducer that convert the signal from resistance thermometer (Pt100) into a current signal 4-20 mA, sent to the management and data acquisition system. The measurement chain from Siemens PLC to the temperature sensors was calibrated on-site against a Endress+Hauser TST310-B5A1C4A2B1A Pt100 temperature sensor provided with digital display. The calibrated probe was tested in 5 points from -15°C to 150°C.

5.5.3 Pressure measurement

The pressures were measured with Endress+Hauser PMP51 and PMP131 pressure transmitters. The measurement points were installed vertically on the pipe surface. The accuracy of the pressure transmitters is 0.015% of the measured value. The measurement chain from logger to the pressure transmitters were calibrated in laboratory by a certified body against a Endress+Hauser PMP131 model with range from 0 to 16 bar and an accuracy of 0.05% of full scale. The measurement chain was calibrated at 5 pressures. The sensors provide a current signal 4-20 mA that is read by the data acquisition system.

5.5.4 Flow measurement

Electromagnetic flow measuring system from Endress+Hauser (type PROMAG 50P1H DN100) is installed in the chilled water circuit and it is used to evaluate the evaporator

heat transfer rate on the secondary fluid side. The certified accuracy of the electromagnetic flow meter is 3.5 % for volume flow.

The water and water/glycol volume flows on the secondary fluid of heat source and heat sink side were measured with ULTRASOUND CONTROLOTRON 1010 System flow meter. The accuracy of the flow meters is 3.0 % of the measured value. Rich and poor ammonia solution circuits are measured with ULTRASOUND CONTROLOTRON 1010 System flow meter.

5.6 Design and construction

The last step of prototype design process is 3D model phase. This stage is very important because it is necessary for the correct assembly of each component and the check of the allowances between components. It is necessary to evaluate if it is feasible the construction and assembly of the machine. In this phase there are further considerations that cannot be made in the previous steps. The height of each heat exchanger has been taken in count in way to have the correct internal flows.

For example, the rectifier has a precise relation with the generator and its vessel. The vapor must flow from generator to the rectifier where it is purified and separated from liquid that flows back to the common line back to solution heat exchanger. The outlet of rectifier must be above the minimum height of head equal to pressure loss in the rectifier. It is necessary to avoid to flood the rectifier.

The same for absorber and its vessel. They must guarantee that there is a sufficient head at pump suction and that the absorber is not flooded by the rich solution liquid at outlet.

To finalize the prototype design a 3D modeller has been employed. Solid Edge is a Siemens software that is very useful for assembly design, like a chiller. It has a handy process to handle the single 3D parts like valves. It is also easy to manage a the parts bill that has to be produced for purchase and later for workshop. It is a fundamental phase of the design because there are evaluated all the interferences and the relative spaces between components necessary to easily access for service.

Below is shown a snapshot of the 3D model.

The prototype has been constructed in the workshop of Zudek srl. The components were collected at the warehouse and they were prepared using bill of materials produced with Solid Edge from the 3D model. The components and the piping were welded and selected complying with PED code, with a nominal pressure of 16 bar.

Both carbon steel and stainless steel are seamless pipings .The materials used for construction are:

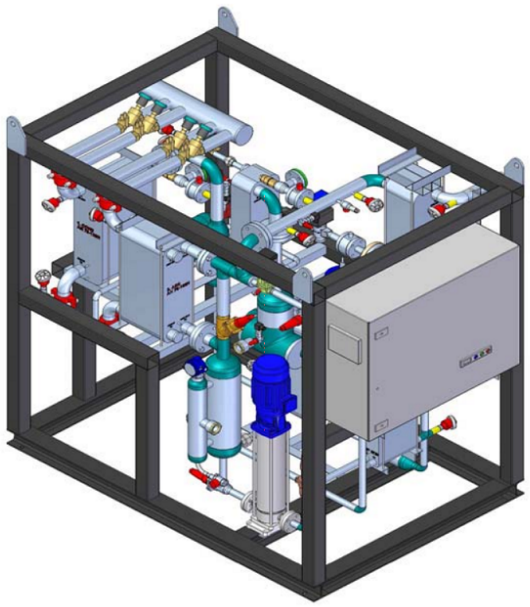

Figure 5.14: Schematic representation of heat pump cycle

	Material	Design code
		Piping
ASTM A333 GR.6	ANSI B36.10	
Fittings	ASTM A420 WPL6	ASME B31.3
Flanges	ASTM A350 LF2	EN1092-1

Material and code specifications

The prototype as installed in the facility is shown in Figure 5.15.

5.7 Final remarks

The prototype was deigned to operate first in the test facility of Zudek srl, but after the prototype was build it has been decided to test the prototype directly in the Illy caffè facility. Due to this change the test of the prototype was delayed of several months reducing the available time for tests.

Figure 5.15: Two views of the absorption chiller prototype as installed

6

EXPERIMENTAL TEST

This section illustrate the experimental work carried out as part of this project. The test facility and procedure are described. The collected data are presented, elaborated, discussed and compared with calculated numerical data.

A series of tests were carried out to investigate the operational range of the prototype in the industrial facility of Illy caffè. The aim of the tests was to establish the working parameters of the absorption chiller prototype.

Initially the prototype was supposed to be tested in a controlled environment. Zudek srl has a test facility that is used for in house chiller tests. This test rig is designed for standard chillers and has only two circuits: cooling and cooled glycol water circuits. They are required to simulate the thermal loads on the condenser and on the evaporator. These two circuits alone are not sufficient to complete the test on the prototype. In fact a third circuit to simulate the thermal load on the generator is required. It has been proposed to exploit the already installed 200 kW electric resistance to simulate the load, but it would require a small modification on the test plant.

Due to a Zudek management decision it has been decided to not modify and use the test facility. Therefore the only feasible solution to test the prototype has been to install it directly in the industrial facility. The chiller was supposed to be installed in this facility, but only in a second time to monitor his operating capabilities in a industrial environment.

The hot glycol-water circuit is very difficult to set and a stable output temperature has not been possible to be maintained. This has effected the testing conditions and the final measures. Due to plant conditions, the input chilled water temperature was not settable and very limited in range.

6.1 Test facility

The absorption chiller has been used to cool down the chilled water circuit of the Illy caffè production plant. Part of the water flow, on the line returning to the existing chillers has been diverted and pumped back in the same circuit. The absorption machine duty has been to pre cool chilled water in order to reduce the workload of the existing vapor compression chillers.

The heat input required to operate the prototype, has been provided by the existing waste heat recovery plant. This plant has been installed with the purpose to reduce the load of the heating plant composed by two 1 MW condensing boilers. A water and glycol solution with a 20% concentration of Ethylen Glycol has been used as thermal fluid.

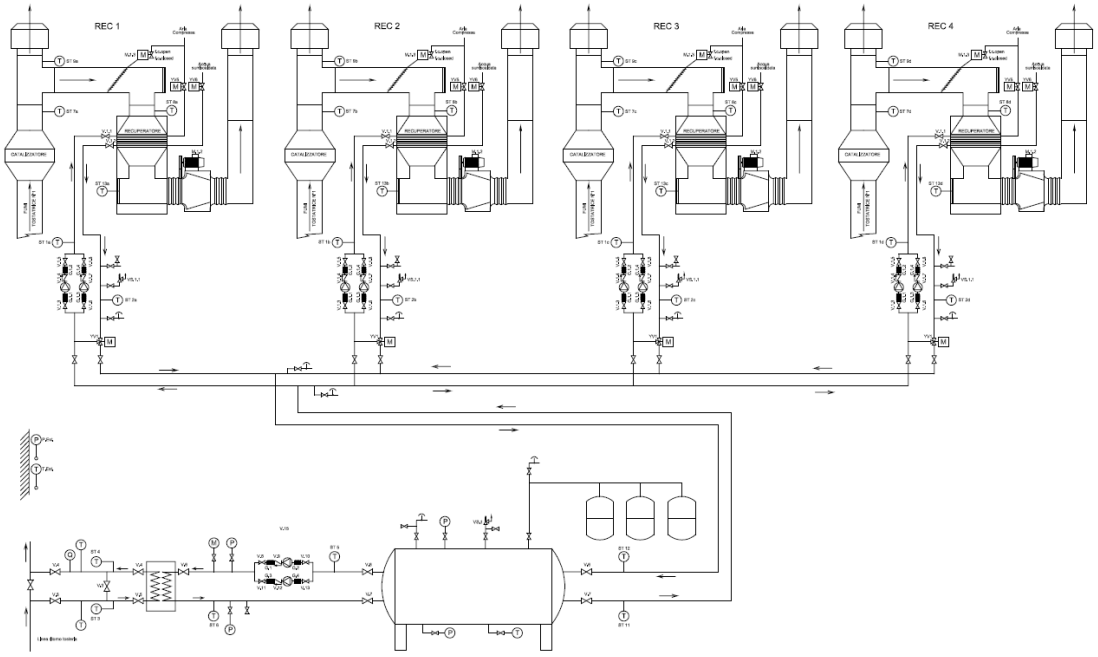

Figure 6.1: Heat recovery plant pID

The PID of waste heat recovery plant is shown in Figure 6.1. The heat is recovered from the chimneys of the toasting plant. The waste gases are diverted using a fan and they flow through the recovery heat exchangers installed in flue gases chimneys. The heat from the natural gas flue is recovered and transferred to the heating circuit. A buffer tank is used to equalise heat load from chimneys and heat load of the heating circuit. All the system is automated and controlled with a Siemens S7 series PLC.

Figure 6.2: Heat recovery plant

In order to evaluate the performances of the absorption chiller prototype, the temperatures, flows and pressures have been acquired and recorded on the PLC system. Refer to Table 6.1 for the complete list of the recorded parameters. Beside the thermodynamical parameters of the cycle, pump rotational speed,

As can be seen on the test facility PID reported in Figure 6.3, the absorption chiller is placed in an system that is composed of the following components:

- a wet cooling tower: it cools the absorber, condenser and rectifier cooling water
- pump on the chilled water circuit: guarantees the project flow to the evaporator of the absorber
- pump on cooling circuit: ensures the flow required to cool the condenser, absorber and rectifier
- stop valves on hot glycol-water, chilled water and tower cooling circuits
- filter on tower cooling circuit
- safety valves on the hot water circuit, automatic vents valves, service valves and regulation valves
- threaded deadlifts for pressure probes

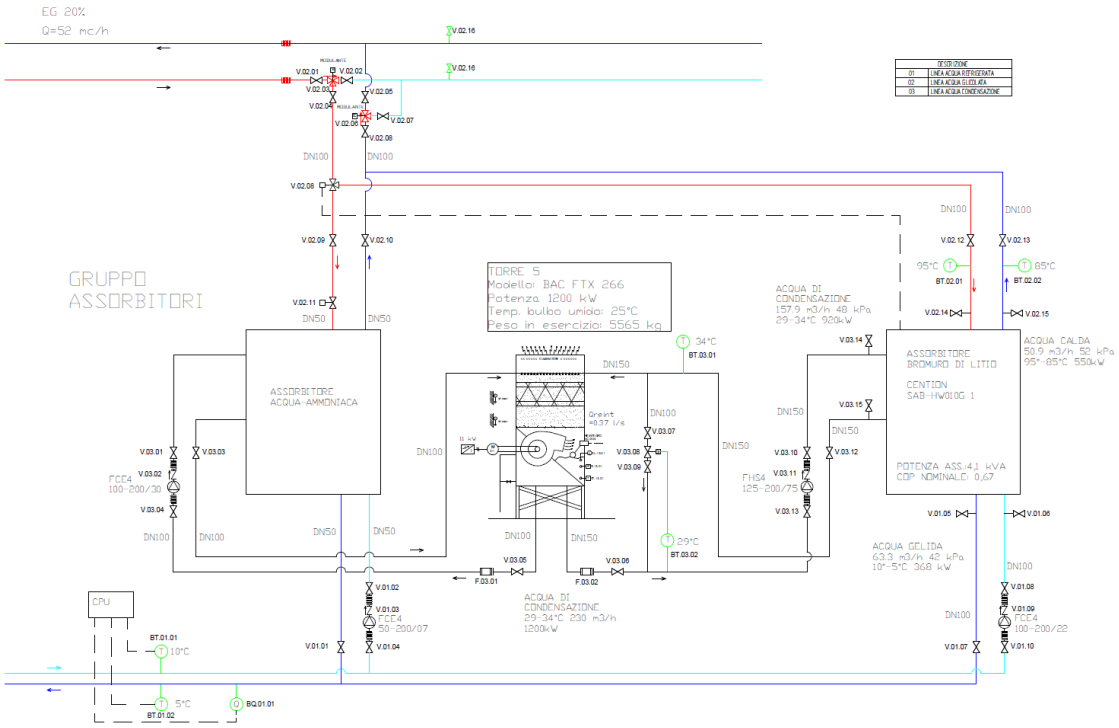

Figure 6.3: Test facility PID

- temperature sensors on flow and return sides of each circuits
- flow meter and temperature sensors connected to a control unit for energy metering
- H_2O/LiBr absorbtion chiller: installed in the same system and working independently. It is connected to the same cooling tower and to the same chilled water circuit.

6.2 Prototype commissioning

The design specification is for a 43/35 in weight-% of ammonia-water mixture on strong and waek solution sides. The total system charge concentration has been determined to be 41 in weight-% with a total system charge of 18.5 kg of ammonia.

Prior to charging, the system was evacuated to remove any unwanted gas that can effect the performance and the correct operation of the prototype.

Figure 6.4: Heat recovery plant view

Firstly, distilled water was inserted through the service valve close to the generator. After water has been charged the prototype has been put in service in order to verify internal flows and to clean the impurities inside the syste. Then the distilled water has been eliminated and repeated the operation.

Ammonia was added through the service valve on the suction line. To do this the water has been kept circulating in order to foster the absorption in water. The ammonia vapor has been added slowly to the system. The vapor has flown to the system due to pressure difference between gas cylinder and the system and due to high mixing affinity of ammonia with water.

First time the absorption chiller has been installed the pumps have been checked and tested. All the pumps were run singularly inspected and the correct direction have been controlled. The measurements sensors have been checked for correct position, measurement range and to work properly.

6.3 Test procedure

Before to start the test runs, the following preliminary operations has been put in place, to ensure the proper performance of the test:

- check the vacuum level required for the correct operation of the absorber (only first time)
- verification of correct installation of measuring instruments and their correct oper-

ation

- check on the plc the absorprtion chiller settings
- calibration of measuring instruments (pressure sensors and temperature) through the use of certificated sample instruments (only first time)
- on field setting of ultra sound flow meter
- measurement of all the flows at the beginning of each test run

During the test the following actions have been performed:

- The circulation pumps of the tower cooling water and chilled water circuits were switched on.
- The flow regulation valves in the the tower cooling water and chilled water circuits have been set fully open.
- The expansion valve was set to a fixed superheat temperature working point. The opening of the valve is controlled by the Siemens control unit with his specifically designed PID controller.
- The mass flows in the water and brine circuit were set to their specified values.
- The absorption chiller was operated until steady state conditions were obtained.
- All measuring point were logged.

The test rig is equipped with a control system connected to the PLC. The solution pump, and the mains water control valve are controlled from the computer. The circulation pumps in the secondary circuits have been manually set from the PLC. The circulation pumps have three flow rate settings. Manual valves installed in the circulation pump outlet lines are used to achieve additional flow rate adjustments.

6.3.1 Control philosophy

The absorption chiller prototype components are controlled through the Siemens PLC. During commissioning phase the components were manually operated in order to find the right setting parameters. Once the control program has been setted, the absorption chiller has been run automatically by the PLC. Anyway, all the test runs have been supervised.

The control program is :

- The solution pump is started at minimum speed.
- The barostatic pressure control valve is opened and setted to the regulation value.
- The solution pump start to regulate speed. The pump speed is controlled in order to maintain the liquid level in the absorber liquid receiver. It has a maximum speed and a minimum speed equivalent to the maximum and minimum liquid height in the vessel.
- When the suction pressure is stabilised the expansion valve is opened. The opening is controlled by dedicated control unit.
- If evaporation pressure falls under minimum setted value, the expansion valve is closed and the PLC runs the prototype in stand by mode.

The plant has been started in automatic mode according to the standard operation.

The system is brought to run automatically in order to reach the nominal operating conditions. Have been verified on flow three circuits: flow on chilled water circuit was acquired by already installed meter, while the other two circuits were measured using the Portable Ultrasonic Flowmeter. The internal solution flows were measured on the inlet and outlet piping of the solution heat exchanger.

6.4 Data acquisition

Prototype have been working for several days. The experimental campaign consisted in data acquisition during these periods. The data acquisition has lasted only during the working hours, due to the impossibility to runa safely in automatic mode. Unfortunately the prototype and the test facility in Illy caffè production plant have been available only for a short period, so the data are not too extensive.

The condensation temperatures have a limited range between 22°C and 32°C and are not exactly the design values. This has been effected by the limited activity period during the year.

The temperature of the hot circuit are in the range of 70°C to 96°C. It has never been reached a higher temperature range due to the maximum temperature setting of the heat recovery plant setted equal to 100°C.

The range of chilled water is in the range of 4°C to 9°C. The boundaries of the range are related to the working range of the vapor compression chillers.

In Figures 6.3 and 6.4 are reported temperature and pressures acquired during a single test day.

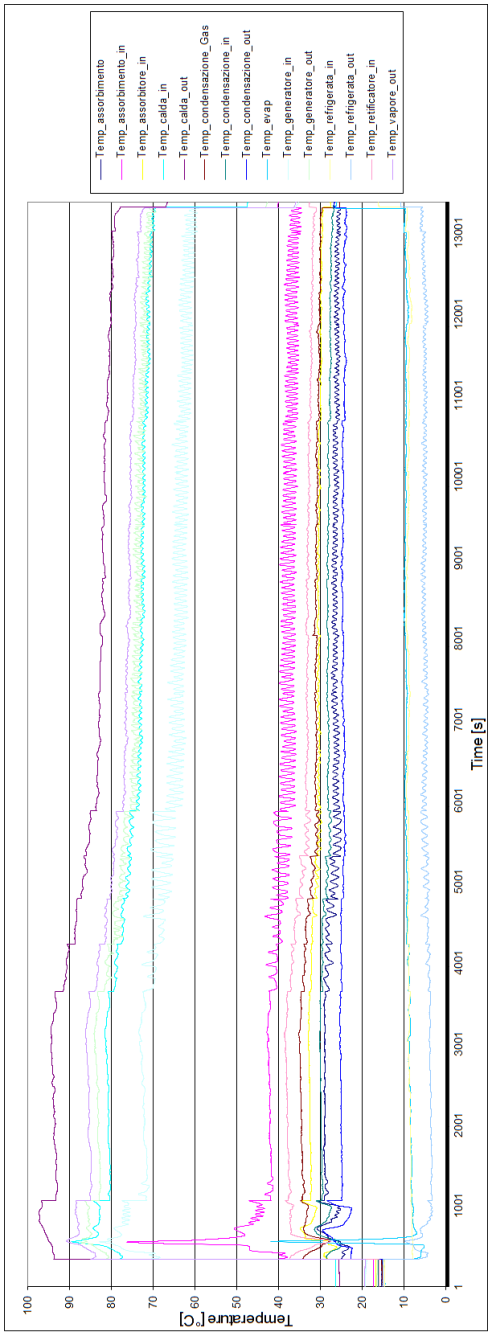

Figure 6.5: Temperatures acquired during a test run

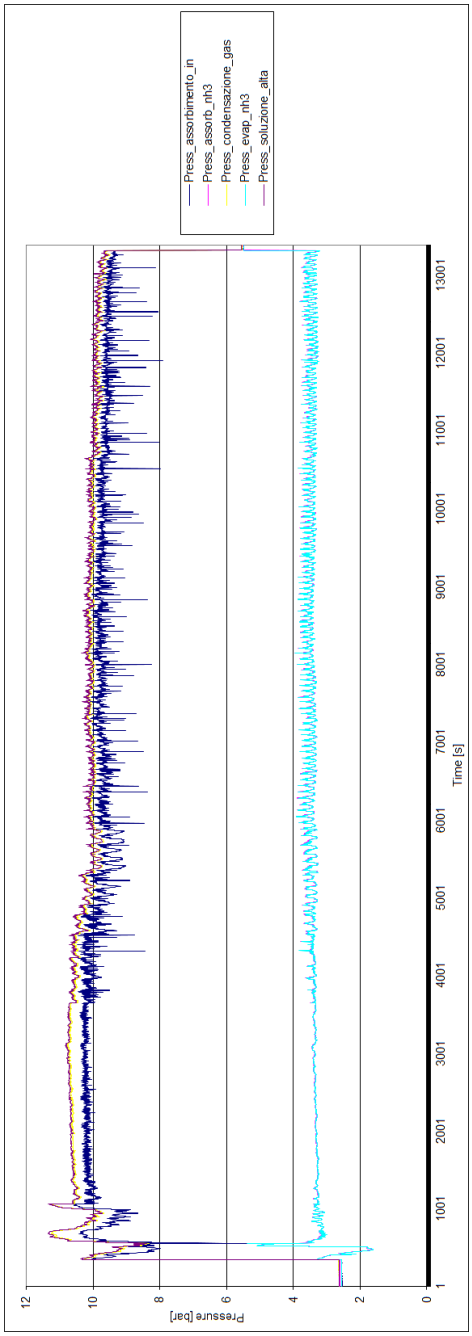

Figure 6.6: Pressures acquired during a test run

6.5 Data processing

Once the data have been acquired, they have been processed in order to find the main working parameters of the absorption chiller as the heat transfer rates for each heat exchanger. To do so have been used some data from literature and the flow values measured at the beginning of each test session.

6.5.1 Calculated parameters

The chiller working parameters are calculated such as indirect measures:
Mass flow rates:

$$\dot{m} = \dot{Q} \cdot \rho \tag{6.1}$$

where:

- $\dot{Q}$ is the volume flow rate of the fluid [m3/h]
- ρ is the fluid density under test [kg/m3]

Heat transfer rate:
The heat loads of the evaporator, condenser, solution heat exchanger, absorber, desorber and the desuperheater were determined with the following energy balances on the heat sink and heat source side.

$$Q = \frac{\dot{m} \cdot c_p \cdot \Delta T}{3600} \tag{6.2}$$

where:

- c_p is the specific heat. This value has been found in literature according to the composition and concentration of the non freezing fluid [kJ/kgK].
- $\dot{m}$ is the mass flow rate of the fluid in the circuit considered [kg/h]
- ΔT is the difference of fluid temperature between inlet and outlet

  The coefficient of performance COP:

  The coefficient of performance for heating is defined as the ratio between the useful heat transfer rate at the evaporator and the sum of heat transfer rate delivered at the desorber and the work of the solution pump. It is possible to define the cooling effectiveness, called cooling coefficient of performance COP_C by the relation:

$$COP_C = \frac{Q_{evap}}{Q_{gen} + W_p} \tag{6.3}$$

where:

- Q_{evap} cooling heat transfer rate, measured in [kW]
- Q_{gen} generator heating heat transfer rate, measured in [kW]

In Table 6.1 are reported the measured values of flows for each heat exchanger. The heat transfer rates have been obtained using these values.

Quantity	Flow
Qgen $[m^3/h]$	13.50
Qabs $[m^3/h]$	16.20
Qcond $[m^3/h]$	12.00
Qrect $[m^3/h]$	2.40
Qevap $[m^3/h]$	12.40

Table 6.1: Measured flow values used to evaluate the indirect measures.

Some parameters have been taken from literature as the ones reported in Table 6.2 The used values for the calculation have been obtained from Coolpack software version 1.46 (Technical University of Denmark - Department of Mechanical Engineering).

Quantity	Value
cp H2O [4 °C]	4.18
cp H2O [25 °C]	4.2122
cp H2O [38 °C]	4.2253
cp GlyEth 20% [94 °C]	3.985
cp GlyEth 20% [81 °C]	3.954
H2O [4 °C]	1000
H2O [25 °C]	1000
H2O [38 °C]	1000
GlyEth 20% [94 °C]	990
GlyEth 20% [81 °C]	999

Table 6.2: Values used to evaluate the indirect measures.

6.5.2 Processed data

Using the equations reported in section 6.5.1 the heat transfer rates are calculated and reported in Figure 6.7. They are plotted as function of time.

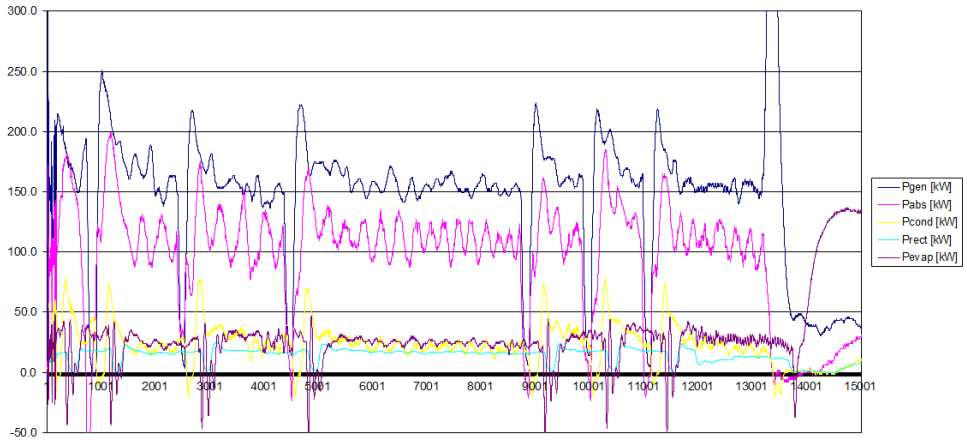

Figure 6.7: Heat transfer rates of prototype heat exchangers

Using the equation for coefficient of performance reported in section 6.5.1, the COP values are calculated and reported in Figure 6.8. They are plotted as function of T_{gen}.

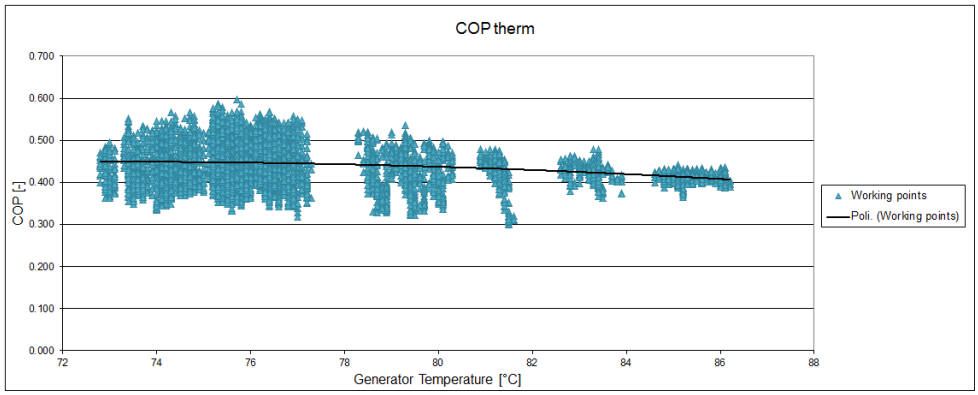

Figure 6.8: All the COP values are reported in function of T_{gen}

6.6 Uncertainty estimation in the experimental measurements

The relative uncertainty in the calculated values is estimated using the theory of propagation of errors as outlined in this section. In many cases, an important quantity is not directly measured by rather calculated as a function of one or more variables that are directly measured, i.e., Y = $f($ X_1, X_2, ...). The measured variables, X_1, X_2, etc. have with a random variability which is referred to as its uncertainty.

A result of a given measurement is only an estimate of the specific value of the quantity subject to the measurement. The result is therefore complete only when supplemented with a quantitative uncertainty. The uncertainties of the calculated value is predicted using the uncertainty calculation capability of the Engineering Equation Solver program [47]. The method for determining this uncertainty propagation is described in NIST Technical Note 1297 [48] . Assuming the individual measurements are uncorrelated and random, the uncertainty in the calculated quantity can be determined as per (6.4) where U represents the uncertainty of the variable. The relative uncertainty of a quantity is defined as the ratio of its absolute uncertainty to its value:

$$U_Y = \sqrt{\sum_i \left(\frac{\partial Y}{\partial X_i}\right)^2 \cdot {U_{X_i}}^2} \tag{6.4}$$

where U represents the uncertainty of the variable.

The relative uncertainty of a quantity is defined as the ratio of its absolute uncertainty to its value:

$$U\% = \frac{U_Y}{Y} \cdot 100 \tag{6.5}$$

Heat transfer rates The heat transfer rates were determined by the following energy balance:

$$\dot{Q} = \dot{m} \cdot c_p \cdot (T_{out} - T_{in}) \tag{6.6}$$

and the uncertainty becomes:

$$\Delta\dot{Q} = \sqrt{\left(\Delta\dot{m} \cdot c_p \cdot (T_{out} - T_{in})\right)^2 + \left(\dot{m} \cdot \Delta c_p \cdot (T_{out} - T_{in})\right)^2 + 2 \cdot \left(\dot{m} \cdot c_p \cdot \Delta T\right)^2} \tag{6.7}$$

where $\Delta\dot{m}$ is the uncertainty of the mass flow measurement, and ΔT is the uncertainty of the temperature measurements.

Coefficient of performance

The cooling coefficient of performance is defined as a ratio of the cooling capacity to the power input:

$$COP_C = \frac{Q_{evap}}{Q_{gen} + W_p} \tag{6.8}$$

The solution pump power was neglected for the uncertainty estimation purpose so it becames:

$$COP_C = \frac{Q_{evap}}{Q_{gen}} \tag{6.9}$$

The uncertainty becomes:

$$\Delta COP_C = \sqrt{\left(\frac{\Delta Q_{evap}}{Q_{gen}}\right)^2 + \left(-\frac{Q_{evap}}{{Q_{gen}}^2} \cdot \Delta Q_{gen}\right)^2} \tag{6.10}$$

Where the quantities ΔQ_{evap} and ΔQ_{gen} were calculated with the previous correlation.

The application of the equations described above through the built-in EES Uncertainty Propagation Table permitted to evaluate the relative uncertainty. It resulted to be practically constant, and equal to 6% of the calculated values, corresponding to a value of 0.02 when COP figure is equal to 0.413.

6.7 Results

The previously presented data in Figures 6.7 and 6.8 are filtered for a reduced range of condensation and evaporation temperatures, in order to compare with correspondent numerical curves.

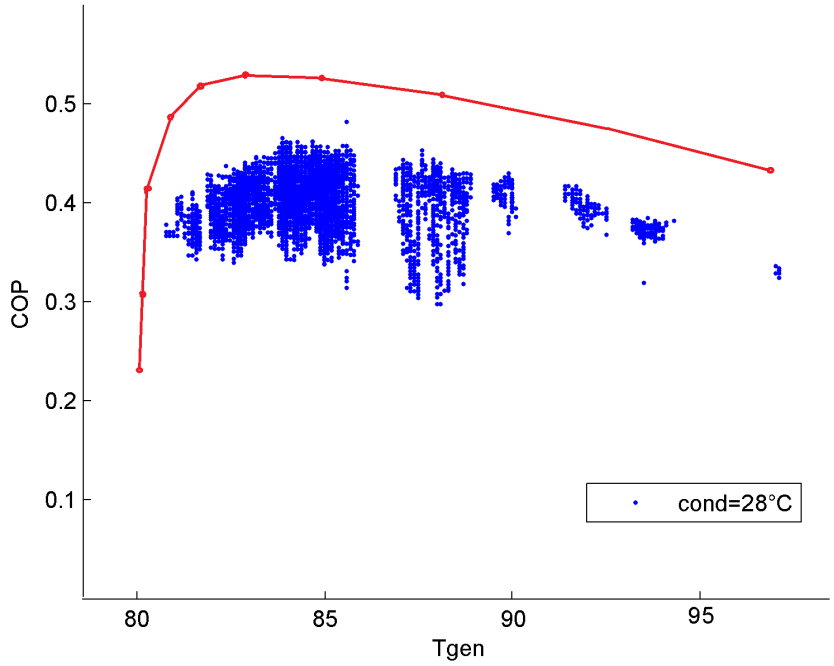

Figure 6.9: Test facility

In Figure 6.9, comparison between experimental and numerical numbers is shown. It is represents the values of COP for different values of T_{gen} for a fixed value of evaporation T_{evap} equal to 0°C. It can be noticed that the experimental values of the prototype present a similar trend to the numerical curve. The absolute values differ in their magnitude.

Referring to the data set reported in Figure 6.9 there is a more extensive comparison with numerical data and it is reported in Table 6.1. All the measured values are averaged on a interval of 5 minutes. The interval has been taken in a way that the oscillations are lower of 0,5°C. They can be considered almost constant on that period of time.

The maximum value of COP is obtained and it is equal to 0.413. This can be compared to the corresponding numerical value for the same working conditions, imposing the same working temperatures. The numerical value of COP is 0.521 and it can be considered as a comparable value. The difference is in the order of 20%.

Sensor tag	Reference	Experimental	Cycle corr.	Num. Value
BT.25.01	Temp_assorbimento	28.95	T1	29
BT.25.04	Temp_assorbimento_in	42.42	T5	46.52
BT.42.02	Temp_assorbitore_in	32.73	-	
BT.43.01	Temp_calda_in	81.1	-	
BT.43.02	Temp_calda_out	93.9	-	
BT.13.01	Temp_condensazione_Gas	34.72	T9	35
BT.42.03	Temp_condensazione_in	30	-	
BT.42.01	Temp_condensazione_out	25.28	-	
BT.22.01	Temp_evap	8.62	T13	0
BT.25.02	Temp_generatore_in	72.78	T3	69
BT.25.03	Temp_generatore_out	83.6	T4	86
BT.41.01	Temp_refrigerata_in	8.75	-	
BT.41.02	Temp_refrigerata_out	3.8	-	
BT.42.04	Temp_retificatore_in	38.09	-	
BT.26.01	Temp_vapore_out	85.74	T7	86
BP.25.02	Press_assorbimento_in	10.24	P5	10.99
BP.25.01	Press_assorb_nh3	3.35	P1	3.59
BP.13.01	Press_condensazione_gas	10.68	P9	10.99
BP.22.02	Press_evap_nh3	3.35	P13	3.59
BP.26.01	Press_soluzione_alta	10.73	P7	10.99
	Delta Tgen [C]	12.79		
	Delta Tabs [C]	7.46		
	Delta Tcond [C]	4.73		
	Delta Trect [C]	12.81		
	Delta Tevap [C]	4.95		
	Pabs [kW]	141.35	Qabs	155
	Pcond [kW]	66.36	Qcond	72
	Prect [kW]	36.1	Qrect	20
	Pevap [kW]	71.2	Qevap	75
	Pgen_1 [kW]	172.61	Qgen	172
	COP_1 therm	0.413	COP	0.521

Table 6.3: Comparison of experimental data with numerical

6.8 Design review

The design process can be considered satisfactory. In fact it has lead to a functioning prototype that has confirmed all the design assumptions. There are many aspects that need further investigation and improvements, but the it has showed a good overall performance as first generation prototype.

In figure 6.10 the performance values of a commercial ammonia-water absorption chiller are reported for comparison. It can be noticed that the COP values for same working range conditions are comparable to the COP values obtained during experimental activity in this research.

		Application	Air conditioning	Cold Storage	Refrigeration	Freezing
Refrigerant/Absorbent	R717/R718	Temperature	12 / 6 °C	4 / 0 °C	0 / -3 °C	-5 / -7 °C
Heat Input Temperature	95 / 85 °C	COP	0.50	0.42	0.36	0.32
Heat Output Temperature	25 / 30 °C	Capacity	kW	kW	kW	kW
		XS 30	40	30	25	20
		XL 30	120	90	75	60
		XS 40	200	150	125	100
		XL 40	280	210	175	140

Figure 6.10: COP values for a commercial NH_3-H_2O absorption chiller

It is clear that further investigation on inconsistencies between numerical model and experimental values are strongly recommended.

6.8.1 Plate heat exchangers

The prototype has been easily commissioned and started up. It presents all the characteristics that have been listed in Chapter 2, i.e. the oil free running. It has very short start up, and it reaches full load conditions in a couple of minutes. The short start up time is due to plate heat exchangers characteristics. This has also permitted to obtain a very compact design. It must be considered that in case of next generation absorption chiller, the overall dimensions can be drastically reduced. For this prototype the internal spaces have been kept intentionally very large in a way to permit a easy access to components during tests.

6.8.2 Solution pump

The centrifugal water pump has been running properly. It has never incurred cavitation during test runs. It has always provided the required flow. It has demonstrated as a valid choice for this kind of application, confirming the design assumptions.

6.8.3 Expansion Valve

The expansion valve has not shown any problem. The dedicated Siemens control unit has a well calibrated PID logic that run smoothly the opening of the valve. While the external parameters has been very stable the opening of the valve has been almost constant. An electronic valve is a fine solution for a direct expansion evaporator avoiding any problems that could be faced while regulating the opening of a fixed expansion valve, especially witha broad range of working conditions.

6.9 Final Remearks

The prototype is still installed and running in the industrial plant facility. It provides cooling for chilled process water during summer months while the required heating load is very low and the recovered heat is in excess. The prototype works out of design conditions, however it carries out the function it has been designed for. The heat recovery plant working conditions are very time variable, due to available heat and heating demand. In fact is a typical industrial application presenting variable loads.

7

CONCLUSIONS

7.1 Project results

This research project confirmed the validity of the selected design process. An ammonia-water absorption chiller has been designed, built and tested. The machine is now installed and working in an industrial facility.

A numerical model has been developed . The obtained results have been used to firstly design the thermodynamic cycle of the prototype and secondly to select the components used to manufacture the prototype.

The concept at the core of the design process is to obtain a simple and cost effective absorption chiller. The design has been kept as simple as possible and the following technical solutions have been adopted. All the tests carried out during this work confirmed the validity of the adopted technical solutions.

The main difference between the prototype and a standard absorption chiller is the type of heat exchangers employed. The commonly used shell and tube heat exchangers were replaced by plate heat exchangers (PHE), which have a higher transfer rate, a more compact design and a reduced cost.

I n order to reduce costs and machine complexity, a direct expansion evaporator was preferred to a flooded one and a falling film type absorber was used. The mixing of vapor and liquid is achieved with a spayed liquid injection system; the liquid weak solution is sprayed in a stream of vapor. This arrangement was preferred over the bubble type absorber for lower pressure losses and simpler construction.

A very critical component of the system is the solution pump. A membrane pump is usually used for medium-small size plants. This type of pump is very expensive

and subject to high wearing. Instead of a membrane pump, a low NPSH water pump with teflon seals has been installed. This material is perfectly suitable to operate with an ammonia and water solution. The tests on the absorption chiller confirmed the suitability of the selected pump for this application.

A partial condenser was selected to replace the distillation column. The impact on the overall performance was negligible, so in order to reduce costs it has been preferred a cycle with a partial condenser to eliminate the water contained in the ammonia refrigerant.

It has been also demonstrated the feasibility to operate the chiller with hot water obtained with a heat recovery plant. The prototype was installed and tested in an industrial facility of Illy Caff in the city of Trieste. The heat from the flue gases, result of the toasting process, is recovered to produce a stream of hot water used to power the absorption chiller.

The prototype is inserted in an absorption system where it is installed beside a LiBr-water chiller and the group is used to chill the process water to 5°C. The chilled water is employed to cool down some production processes like welding plant and air conditioning units.

The prototype was tested in many working conditions to verify the performances of the unit and it showed a stable working condition for all ranges of temperatures. The values of COP obtained during the tests are lower than the values obtained with numerical model. Overall performances were close to experimental values and differ of 14.6 %.

7.1.1 Economical evaluation

The final step of the project was the cost evaluation. The figure of Euro /kW is a typical parameter employed in economical estimation regarding the installation of a new chiller for industrial refrigeration application. Usually vapor compression chillers are adopted as basic solution for industrial refrigeration, and they can be used as basic value for an economical comparison in case of adoption of a different technology as absorption chiller. The figure for compression chiller is usually around 200-220 Euro /kW. If we switch to absorption chillers, the single effect LiBr type is the basic solution which presents a value similar to standard chillers that is around 260-280 Euro /kW. Going further, the ammonia absorption chillers are more costly, due to higher construction requirements, and have a typical range of 1200-1500 Euro /kW.

The prototype was developed with the idea of keeping it simple and reduce the cost related. The prototype as built, without considering the development costs and including the standard mark up, which is 850 Euro /kW. It is important to consider that a further development can easily reduce the cost of 20%, making its final price even more competitive, especially if compared with ammonia absorption chillers for below 0°C applications.

7.1.2 Improvements

This work have explored many topics regarding the state of the art of the absorption technology, with a particular interest for ammonia-water type machines. Some of these are very interesting and worth of further study. The following are suggested as possible future developments.

- Buble type absorber: the absorber heat exchanger selected and installed on the prototype can be used in both falling film and bubble conditions. The piping was build considering the possibility to switch to the other operating condition for further tests. Unfortunately, due to a lack of time it was not possible to investigate further this other topic.
- Rectifier cooling: it can be provided employing rich solution stream exiting the solution heat exchanger instead of using a separate circuit, as in the prototype.
- Subcooling heat exchanger: it can be installed on refrigerant side, to increase slightly the performance of the chiller and its evaporating capacity.

During the project some errors have been made and they are listed below in order to improve the design process and avoid the same mistakes in the future.

- Capacity control on hot fluid circuit is required to run the prototype completely in automatic mode. In order to do so, installation of a motorized valve is required on hot fluid circuit. The actual configuration must be supervised to guarantee safety of the plant.
- Some temperature gauges are missing: on condensed liquid receiver and on expanded liquid pipe injecting in the evaporator. These temperature were assumed as corresponding to saturated liquid condition.
- No measures of mixture concentration. There aren't concentration measures, so it has been supposed that the mixture were in saturated condition.
- To simulate o off design conditions it is necessary to introduce a heat exchanger model.

7.1.3 Further research proposal

I suggest as future investigation more advanced features like microchannel heat exchangers for absorber and generator and use of chemical surfactants solved in ammonia water mixture to increase absorption performance. Further investigations and research proposals might include

- Surfactants addition to evaluate the increase of performances.
- Microchannel heat exchangers and air cooled absorber configuration.
- Increase of detail of the numerical model adding a heat exchanger model .
- Development of heat exchanger sizing model. A consultant has been necessary to size the heat exchangers because the heat exchanger suppliers were not able to size and quote absorber and generator.
- More complex cycles implementation to increase overall performance of the chiller, i.e. GAX cycle.
- Investigation of an absorption chiller working in heat pump mode.

Bibliography

[1] L. Borel and D. Favrat. Thermodynamics and energy systems analysis: from energy to exergy. 1st edition. EPFL Press, Lausanne, 2010.

[2] W.B. Gosney. Principle of refrigeration. Cambridge University Press; 1982.

[3] B.H. Perez. Absorption heat pump performance for different types of solution. International Journal of Refrigeration 1984;7:11522.

[4] P. Holmberg, T. Berntsson. Alternative working fluids in heat transformers. ASHRAE Transactions 1990;96:15829.

[5] S. Pongsid, A. Satha, C. Supachart. A review of absorption refrigeration technologies. Renewable and Sustainable Energy Reviews 2001;5:34372.

[6] K.E. Herold, R. Radermacher, S.A. Klein. Absorption Chillers and Heat Pumps. CRC Press, 1996.

[7] B. Lee, B.H. Chun, J.C. Lee, J.C. Hyun and S. H. Kim. The Comparison of Heat Mass Transfer in Absorber between Falling Film and Bubble Column in Heat Pump System. Korean Journal of Chemical Engineering, January 2002, Volume 19, Issue 1, pp 87-92

[8] T.L. Merrill and H. Perez-Blanco. Combined heat and mass transfer during bubble absorption in binary solutions. International Journal of Heat and Mass Transfer, (1997), 40 (3): 589-603.

[9] K. Terasaka, J. Oka and H. Tsuge. Ammonia absorption from a bubble expanding at a submerged orifice into water. Chemical Engineering Science, (2002), 57: 3757 3765.

[10] G.S. Herbine and H. Perez-Blanco. Model of an ammonia-water bubble absorber. Proceedings of the 1995 ASHRAE Annual Meeting.

[11] Y. T. Kang, T. Kashiwagi and R.N. Christensen. Ammonia-water bubble absorber with a plate heat exchanger. Proceedings of the 1998 ASHRAE Winter Meeting, (1998), 2: 1565-1575.

[12] H. Perez-Blanco. A Model of an Ammonia-Water Falling Film Absorber. ASHRAE Transactions, (1988), 94, 1: 467-483

[13] S. Jeong, K.K. Koo and S.K. Lee. Heat transfer performance of a coiled tube absorber with working fluid of ammonia-water. Proceedings of the 1998 ASHRAE Meeting, (1998), 2:1577-1583.

[14] S.V. Potnis, G. Anand, A. Gomezplata, D.C. Erickson and R.A. Papar. GAX component simulation and validation. Proceedings of the 1997 ASHRAE Meeting, (1997), 454-459.

[15] M. Takuma, A. Yamada and T. Matsuo. Condensation Heat Transfer Characteristics of Ammonia-Water Vapor Mixture on Tube Bundles. Condensation and Condenser Design , ASME, (1993). 207-217.

[16] Y.T. Kang and R. N. Christensen. Development of a counter-current model for a vertical fluted tube GAX absorber. Proceedings of the International Absorption Heat Pump Conference, (1994), 7-16.

[17] Y. T. Kang, W. Chen and R. N. Christensen. A Generalized Component Design Model by Combined Heat and Ma ss Transfer Analysis in NH3-H2O Absorption Heat Pump Systems. ASHRAE Transactions: Symposia, (1997), 444-453.

[18] N. Goel, and D. Y. Goswami. A compact falling absorber. ASME Journal of Heat Transfer, (2005), 127, 957-965.

[19] M. Ferrario, M. Haughney, I.R. McDonald, M.L. Klein. Molecular-Dynamics Simulation of Aqueous Mixtures: Methanol, Acetone, and Ammonia. The Journal of Chemical Physics , (1990), 93-7:5156-5166.

[20] A. Hirofumi, M. Masanori and Y. Mitsutake. Heat transfer in pool boiling of ammonia/water mixture. Heat and Mass Transfer, (2003), 39:535543.

[21] M. Issa, K. Ishida and M. Monde. Analysis of ammonia vapor absorption into ammonia water mixture: mass diffusion flux. Heat and mass transfer, (2005), 41:875-889.

[22] M. D. Determan and S. Garimella. Ammonia-Water Desorption in Microchannel Heat and Mass Transfer Devices. International Journal of Refrigeration, Vol. 34, Issue 5, August 2011, pp. 1197-1208

[23] T. M. Bandhauer, A. Agarwal, and S. Garimella (2006). "Measurement and Modeling of Condensation Heat Transfer Coefficients in Circular Microchannels." ASME Journal of Heat Transfer, 128(10), 1050-1059.

[24] W. E. TeGrotenhuis, V. S. Stenkamp, B. Q. Roberts, J. M. Davis, and C. M. Fischer. Miniaturization of an Ammonia-Water Absorption Cycle Heat Pump using microchannels. International Sorption Heat Pump Conference - June 22-24, 2005 Denver, CO, USA

[25] D. Isvoranu and M.D. Staicovici. Marangoni convection basic mechanism explanation using the two-point theory (T PT) of mass and heat transfer and the ammonia/water medium. International Journal of Heat and Mass Transfer , (2004), 47:37693782.

[26] Y.T. Kang and T. Kashiwagi. Heat Transfer Enhancement by Marangoni Convection in the NH3-H2O Absorption Process. International Journal of Refrigeration, (2002), 25:780-788.

[27] J.K. Kim, J.Y. Jung, Y.T. Kang. Absorption performance enhancement by nano-particles and chemical surfactants in binary nanofluids. International Journal of Refrigeration Vol.30 (2007) 50-57

[28] J.K. Kim, J.Y. Jung and Y. T. Kang. The effect of nano -particles on the bubble absorption performance in a binary nanofluid. International Journal of Refrigeration Vol.29 (2006) 22-29

[29] L. Yang, K. Du, X. F. Niu, B. Cheng and Y. F. Jiang. Experimental study on enhancement of ammoniae water falling film absorption by adding nanoparticles. International Journal of Refrigeration vol.34 (2011) 640-647

[30] C. Mostofizadeh, D. Bohne, C. Mergardt. Use of district heating in summer for cold production with the aid of an absorption process. Applied Thermal Engineering 22 (2002) 577-586

[31] J.I. Yoon, K.H. Choi, C.G. Moon, Y.J. Kim, O.K. Kwon. A study on the advanced performance of an absorption heater / chiller with a solution preheater using waste gas. Applied Thermal Engineering 23 (2003) 757-767

[32] Y. Hwang. Potential energy benefits of integrated refrigeration system with microturbine and absorption chiller. International Journal of Refrigeration 27 (2004) 816-829

[33] P. Colonna, S. Gabrielli. Industrial trigeneration using ammonia-water absorption refrigeration systems (AAR). Applied Thermal Engineering 23 (2003) 381-396

[34] A.M. Bassily. Performance improvements of the intercooled reheat recuperated gas turbine cycle using absorption inlet-cooling and evaporative after-cooling. Applied Energy 77 (2004) 249-272

[35] M. Ameri, S.H. Hejazi. The study of capacity enhancement of the Chabahar gas turbine installation using an absorption chiller. Applied Thermal Engineering 24 (2004) 59-68

[36] A. A. Manzela, S.M. Hanriot, L. C. Gmez, J.R.Sodr. Using engine exhaust gas as energy source for an absorption refrigeration system. Applied Energy 87 (2010) 1141-1148

[37] C. Keil, S. Plura, M. Radspieler and C. Schweigler. Application of customized absorption heat pumps for utilization of low-grade heat sources. Applied Thermal Engineering 28 (2008) 2070-2076

[38] A. Sozen, A. Duran, H. Usta. Development and testing of a prototype of absorption heat pump system operated by solar energy. Applied Thermal Engineering 22 (2002) 1847-1859

[39] A. Lecuona, R. Ventas, M. Venegas, A. Zacarias, R. Salgado. Optimum hot water temperature for absorption solar cooling. Solar Energy 83 (2009) 1806-1814

[40] I. Atmaca, A. Yigit. Simulation of solar powered absorption cooling system. Renewable Energy 28 (2003) 1277-1293

[41] J.F. Seara, J. Sieres, M. Vazquez. Compression-absorption cascade refrigeration system Applied Thermal Engineering 26 (2006) 502-512

[42] M. Hulten, T. Berntsson. The compression/absorption heat pump cycle- conceptual design improvements and comparisons with the compression cycle. International Journal of Refrigeration 25 (2002) 487-497

[43] A.K. Pratihar , S.C. Kaushik, R.S. Agarwal. Simulation of an ammonia water absorption refrigeration compression system for water chilling application. International Journal of Refrigeration vol.33 (2010) 1386-1394

[44] M. Yari, A. Zarin, S.M.S. Mahmoudi. Energy and exergy analyzes of GAX and GAX hybrid absorption refrigeration cycles. Renewable Energy 36 (2011) 2011-2020

[45] M. Jelinek, A. Levy, I. Borde. Performance of a triple pressure level absorption-compression cycle. Applied Thermal Engineering (2011) 1-4

[46] Y. Kaita. Simulation results of triple effect absorption cycles. International Journal of Refrigeration 25 (2002) 999-1007

[47] Engineering Equation Solver (EES): http://www.fchart.com/ees/

[48] Taylor B.N. and Kuyatt, C.E., Guidelines for Evaluating and Expressing the Uncertainty of NIST Measurement Results, National Institute of Standards and Technology Technical Note 1297, 1994

A

Plate Heat Exchangers datasheets

Customer:
Project: Zudek/
Item: 1-COND

Alfa Laval Plate Heat Exchanger **Technical Specification**

1*AN76-STD Countercurrent PED 2 ALLOY 316 0.40 mm 118/120pl 11.8/12.0 m² FOIL ALLOY 316

p_{des}=16.0/3.0 bar **T_{des}**=75.0/35.0 °C **k**=1730/1162 W/(m²*K)
Marg.=50 % **Osurf**=49 % **Foul.**=0.0(2.8)*10^{-4} m²*K/W **Load**=93.67 kW **MTD**=6.8 K

Hot Side 1-COND			**Cold Side 25.0% Eth.glycol**		
Condensing			Liquid Heating		
1*59H Dp=0.0854< kPa			1*60H Dp=35.9< kPa		
Dp(ch) 0.104 Dp(p) -0.020/0.001			Dp(ch) 28.173 Dp(p) 1.131/6.418		
(c) 1/1 53.0/53.0 mm Dp(c)=0.000/0.000			(c)1/1 53.0/53.0 mm Dp(c)=0.000/0.000		
v(c/neck/ch)=3.56/0.897/0.299			v(c/neck/ch)=3.58/0.886/0.295		
v(ch/neck/c)=0.00487/0.0146/0.0581			v(ch/neck/c)=0.295/0.887/3.58		
T (v/l)	**P**	**Q**	**T (v/l)**	**P**	**Q**
In 70.0		0.997	30.0		Subcooled
Out 35.0/34.2		0.00	33.0		Subcooled
Twall min/max	32.8/36.2		Twall min/max	32.3/35.5	
1-COND = 0.07586 kg/s			**Eth.glycol = 8.152 kg/s**		
In v/l	0.07564/0.0002124			In v/l	0.000/8.152
Out v/l	0.000/0.07586		Out v/l	0.000/8.152	

	Hot side		**Cold side**
	Liquid	**Vapour**	**Liquid**
	In/Out	**In/Out**	**In/Out**
Dens	773.6/591.9	9.626/10.45	1033/1032
Sp.Heat	4.945/4.866	2.816/3.194	3.827/3.832
Visc	0.304/0.126	0.0118/0.0105	1.46/1.35
Th.Cond	0.460/0.466	0.0318/0.0276	0.509/0.510
Mol.W.			
Cr.pr.			
Cr.temp.			
Lat.heat		994.1/1123.8	

Figure A.1: Condenser PHE datasheet

Customer:
Project: Zudek/
Item: 2-DX EVAP

Alfa Laval Plate Heat Exchanger **Technical Specification**

1*AN76-STD Countercurrent PED 2 ALLOY 316 0.40 mm 62/64pl 6.2/6.4 m² FOIL ALLOY 316

p_{des}=16.0 bar T_{des}=-20.0/-20.0-50.0/50.0 ℃ k=3252/1357 W/(m²*K)
Osurf=140 % Foul.=0.0(4.3)*10^{-4} m²*K/W Load=75.00 kW MTD=8.9 K

Hot Side 25.0% Eth.glycol			**Cold Side 2-DX EVAP**		
Liquid Cooling			Vapourizing		
1*32H Dp=33.9< kPa			1*31H Dp=6.52< kPa		
Dp(ch) 31.832 Dp(p) 0.302/1.708			Dp(ch) 6.245 Dp(p) -0.012/0.266		
(c) 1/1 53.0/53.0 mm Dp(c)=0.003/0.035			(c)1/1 53.0/53.0 mm Dp(c)=0.003/0.035		
v(c/neck/ch)=1.92/0.890/0.296			v(c/neck/ch)=2.05/0.985/0.328		
v(ch/neck/c)=0.296/0.889/1.91			v(ch/neck/c)=1.95/5.86/12.2		
T (v/l)	**P**	**Q**	**T (v/l)**	**P**	**Q**
In 5.0		Subcooled	-6.7	3.28	0.153
Out 0.5		Subcooled	-3.5	3.28	0.920
Twall min/max	-3.1/4.1		Twall min/max	-3.8/4.0	
Eth.glycol = 4.404 kg/s			**2-DX EVAP = 0.07539 kg/s**		
In v/l	0.000/4.404		In v/l	0.01156/0.06383	
Out v/l	0.000/4.404		Out v/l	0.06933/0.006054	

	Hot side	**Cold side**	
	Liquid	**Liquid**	**Vapour**
	In/Out	**In/Out**	**In/Out**
Dens	1042/1043	651.1/696.9	2.606/2.572
Sp.Heat	3.788/3.781	4.577/4.765	2.474/2.514
Visc	3.02/3.54	0.200/0.301	0.0089/0.0090
Th.Cond	0.497/0.495	0.561/0.554	0.0228/0.0231
Dew p.			6.5
Mol.W.			17.03/17.03
Cr.pr.			113.33/113.33
Cr.temp.			132.4/132.4
Lat.heat			1288.0/1281.5

Note: Nucleate boiling multiplier = 0.
Result might be unreliable when using more than 2 ref. points for boiling fluids

Figure A.2: Evaporator PHE datasheet

Customer:
Project: Zudek/
Item: 3-ABS

Alfa Laval Plate Heat Exchanger **Technical Specification**

1*AN76-STD Countercurrent PED 2 ALLOY 316 0.40 mm 98/100pl 9.8/10.0 m² FOIL ALLOY 316

p_{dec}=16.0 bar T_{dec}=45.0/50.0 ℃ k=4084/1645 W/(m²*K)
Osurf=148 % **Foul.**=0.0(3.6)*10^{-4} m²*K/W **Load**=122.0 kW **MTD**=7.6 K

Hot Side 3-ABS			**Cold Side 25.0% Eth.glycol**		
Condensing			Liquid Heating		
1*49H Dp=1.11< kPa			1*50H Dp=78.5< kPa		
Dp(ch) 1.664 Dp(p) -0.622/0.063			Dp(ch) 65.843 Dp(p) 1.864/10.577		
(c) 1/1 53.0/53.0 mm Dp(c)=0.002/0.001			(c)1/1 53.0/53.0 mm Dp(c)=0.002/0.001		
v(c/neck/ch)=12.8/3.88/1.29			v(c/neck/ch)=4.66/1.38/0.461		
v(ch/neck/c)=0.0344/0.103/0.341			v(ch/neck/c)=0.461/1.39/4.66		
T (v/l)	**P**	**Q**	**T (v/l)**	**P**	**Q**
In 44.9	3.19	0.0923	30.0		Subcooled
Out 35.0/33.8	3.19	0.00	33.0		Subcooled
Twall min/max	31.7/38.7		Twall min/max	31.3/37.3	
3-ABS = 0.6338 kg/s			**Eth.glycol = 10.62 kg/s**		
In v/l	0.05850/0.5753		In v/l	0.000/10.62	
Out v/l	0.000/0.6338		Out v/l	0.000/10.62	

	Hot side		**Cold side**
	Liquid	**Vapour**	**Liquid**
	In/Out	**In/Out**	**In/Out**
Dens	854.9/843.0	2.122/2.336	1033/1032
Sp.Heat	4.173/4.136	2.302/2.319	3.827/3.832
Visc	0.644/0.722	0.0108/0.0105	1.46/1.35
Th.Cond	0.526/0.524	0.0286/0.0275	0.509/0.510
Mol.W.			
Cr.pr.			
Cr.temp.			
Lat.heat		1627.5/1557.9	

Note: Inlet port recovery unreasonably high! Try double inlet, more units in parallel or choose other unit type with bigger connections!

Figure A.3: Absorber PHE datasheet

Customer:
Project: Zudek/
Item: 4-SHX (Thermal)

Alfa Laval Plate Heat Exchanger **Technical Specification**

1*AN52-STD Countercurrent PED 2 ALLOY 316 0.40 mm 94/99pl 4.8/5.0 m² FOIL ALLOY 316

p_{dec}=16.0 bar T_{dec}=110.0/110.0 ℃ k=4153/3067 W/(m²*K)
Marg.=5 % **Osurf**=35 % **Foul.**=0.0(0.85)*10^{-4} m²*K/W **Load**=149.5 kW **MTD**=10.2 K

Hot Side 2-SHX warm			**Cold Side 2-SHX Cold**		
Liquid Cooling			Liquid Heating		
2*25H Dp=15.3< kPa			2*24H Dp=21.9< kPa		
Dp(ch) 14.776 Dp(p) 0.073/0.401			Dp(ch) 20.756 Dp(p) 0.092/0.538		
(c) 1/1 32.0/32.0 mm Dp(c)=0.008/0.025			(c)1/1 25.0/25.0 mm Dp(c)=0.008/0.025		
v(c/neck/ch)=0.889/0.372/0.143			v(c/neck/ch)=1.58/0.419/0.161		
v(ch/neck/c)=0.134/0.348/0.834			v(ch/neck/c)=0.171/0.445/1.67		
T (v/l)	**P**	**Q**	**T (v/l)**	**P**	**Q**
In 99.6		Subcooled	35.4		Subcooled
Out 42.7		Subcooled	84.9		Subcooled
Twall min/max	39.2/92.7		Twall min/max	38.5/91.1	
2-SHX warm = 0.5787 kg/s			**2-SHX Cold = 0.6532 kg/s**		
In v/l	0.000/0.5787		In v/l	0.000/0.6532	
Out v/l	0.000/0.5787		Out v/l	0.000/0.6532	

	Hot side Liquid In/Out	**Cold side Liquid In/Out**
Dens	809.2/863.0	843.0/795.5
Sp.Heat	4.809/3.989	4.145/4.870
Visc	0.262/0.690	0.716/0.292
Th.Cond	0.479/0.532	0.524/0.468
Mol.W.		
Cr.pr.		
Cr.temp.		
Lat.heat		

Figure A.4: Solution economiser PHE datasheet

Customer:
Project: Zudek/
Item: 5-GEN

Alfa Laval Plate Heat Exchanger **Technical Specification**

1*AN76-STD Countercurrent PED 2 ALLOY 316 0.40 mm 78/80pl 7.8/8.0 m² FOIL ALLOY 316

p_{des}=10.0/16.0 bar **T_{des}**=120.0/120.0 °C **k**=3792/2714 W/(m²*K)
Marg.=20 % **Osurf**=40 % **Foul.**=0.0(1.0)*10⁻⁴ m²*K/W **Load**=160.0 kW **MTD**=7.6 K

Hot Side 25.0% Eth.glycol			**Cold Side 5-GEN**		
Liquid Cooling			Vapourizing		
1*40H Dp=16.6< kPa			1*39H Dp=6.63< kPa		
Dp(ch) 14.803 Dp(p) 0.272/1.534			Dp(ch) 6.366 Dp(p) -0.019/0.237		
(c) 1/1 53.0/53.0 mm Dp(c)=0.002/0.031			(c)1/2 53.0/53.0 mm Dp(c)=0.002/0.031		
v(c/neck/ch)=1.84/0.683/0.227			v(c/neck/ch)=0.373/0.142/0.0473		
v(ch/neck/c)=0.226/0.679/1.83			v(ch/neck/c)=0.632/1.90/2.49		
T (v/l)	**P**	**Q**	**T (v/l)**	**P**	**Q**
In 105.0		Subcooled	84.9	13.5	0.00
Out 95.0		Subcooled	100.0	13.5	0.125
Twall min/max	92.4/103.3		Twall min/max	91.7/102.8	
Eth.glycol = 4.039 kg/s			**5-GEN = 0.6550 kg/s**		
In v/l	0.000/4.039		In v/l	0.000/0.6550	
Out v/l	0.000/4.039		Out v/l	0.08162/0.5734	

	Hot side	**Cold side**	
	Liquid	**Liquid**	**Vapour**
	In/Out	**In/Out**	**In/Out**
Dens	996.4/1002	795.5/809.0	8.276/7.939
Sp.Heat	3.972/3.951	4.870/4.808	2.712/2.694
Visc	0.403/0.454	0.292/0.261	0.0123/0.0128
Th.Cond	0.525/0.524	0.468/0.479	0.0335/0.0351
Bub. p.			84.9
Dew p.			110.0
Mol.W.			17.05/17.08
Cr.pr.			109.08/104.19
Cr.temp.			137.8/144.4
Lat.heat			1328.4/1458.4

Note: Nucleate boiling multiplier = 0.
Result might be unreliable when using more than 2 ref. points for boiling fluids

Figure A.5: Generator PHE datasheet

Customer:
Project: **Zudek/**
Item: **6-RECT**

Alfa Laval Plate Heat Exchanger **Technical Specification**

1*AN76-LSTD Countercurrent PED 2 ALLOY 316 0.40 mm 38/40pl 3.8/4.0 m² FOIL ALLOY 316

p_{dec}=16.0 bar **T_{dec}**=100.0/100.0 ℃ **k**=467.3/109.1 W/(m²*K)
Osurf=328 % **Foul.**=0.0(70)*10⁻⁴ m²*K/W **Load**=19.80 kW **MTD**=47.8 K

Hot Side 6-RECT			**Cold Side 25.0% Eth.glycol**		
Condensing			Liquid Heating		
1*19L Dp=0.458< kPa			1*20L Dp=0.186< kPa		
Dp(ch) 0.400 Dp(p) -0.030/0.087			Dp(ch) 0.174 Dp(p) 0.002/0.011		
(c) 1/1 53.0/53.0 mm Dp(c)=0.000/0.001			(c)1/1 53.0/53.0 mm Dp(c)=0.000/0.001		
v(c/neck/ch)=4.61/3.60/1.20			v(c/neck/ch)=0.151/0.112/0.0373		
v(ch/neck/c)=0.984/2.96/3.78			v(ch/neck/c)=0.0375/0.113/0.152		
T (v/l)	**P**	**Q**	**T (v/l)**	**P**	**Q**
In 100.0	13.5	1.00	30.0		Subcooled
Out 70.0/59.7	13.5	0.912	45.0		Subcooled
Twall min/max	42.4/66.6		Twall min/max	42.0/65.9	
6-RECT = 0.08063 kg/s			**Eth.glycol = 0.3437 kg/s**		
In v/l	0.08063/0.000		In v/l	0.000/0.3437	
Out v/l	0.07352/0.007111			Out v/l	0.000/0.3437

	Hot side Liquid In/Out	**Vapour In/Out**	**Cold side Liquid In/Out**
Dens	809.6/555.8	7.933/8.830	1033/1027
Sp.Heat	4.805/5.223	2.691/2.760	3.827/3.854
Visc	0.262/0.317	0.0128/0.0118	1.46/1.03
Th.Cond	0.479/0.465	0.0351/0.0318	0.509/0.514
Mol.W.			
Cr.pr.			
Cr.temp.			
Lat.heat		1894.7/1560.8	

Figure A.6: Rectifier PHE datasheet

B

Solution pump datasheet

LOWARA
a xylem brand

3SV25FL022T

1016LA31F

Operating data

Pump type	Single head pump		Fluid		Water
No. of pumps / Reserve		1 / 0	Operating temperature t A	K	277
Nominal flow	l/s	0.745	pH-value at t A		7
Nominal head	m	110	Density at t A	kg/m³	1000
Static head	m	0	Kin. viscosity at t A	mm²/s	1.569
Inlet pressure	kPa	0	Vapor pressure at t A	kPa	100
Environmental temperature	K	293	Solids		0
Available system NPSH	m	0	Altitude	m	1000

Pump data

Make	Lowara			Nominal	l/s	,7	(,7)
Speed	1/min	2900	Flow	Max-	l/s	1,1	
Number of stages		25		Min-	l/s		
Max. casing pressure	kPa			Nominal	m	110	
Max. working pressure	kPa	1393,4	Head	at Qmax	m	64.8	
Head H(Q=0)	m	140		at Qmin	m	142	
Weight	kg	35	Shaft power		kW	1.5	(1.5)
Max.	mm		Max. shaft power		kW	1,5	
Impeller R designed	mm		Efficiency		%	58.44	
Min.	mm		NPSH 3%		m	,5	

Pump Materials

Pump body	Stainless steel / AISI 304
impeller	Stainless steel / AISI 304
Diffuser	Stainless steel / AISI 304
Outer sleeve	Stainless steel / AISI 304
Shaft	Stainless steel / AISI 304
Adapter	Cast iron
Coupling	Aluminium
Seal casing	Stainless steel / AISI 304
Coupling protection	Stainless steel / AISI 304
Shaft sleeve and bushing	Tungsten carbide
Fill / drain plugs	Stainless steel / AISI 304
Tie rods	Stainless steel
Base	Aluminium
Wear ring	Technopolymer PPS

Shaft Seal

Single seal	Roten
SV - Uniten	
Rotating Assembly	Q1-Silicon carbide
Fixed Assembly	B-Resin impregnated carbon
Elastomers	E - EPDM
Springs	G-AISI 316
Other Components	G-AISI 316

Motor data

Manufacturer	Lowara	Electric voltage	220 V	Speed	2880 1/min	Insulation class	F
Specific design	IE3 Three phase surface motor			Frame size	90	Colour	RAL 5010
Type	PLM90.../322 E3	Electric current	7,97 A				
Rated power	2.2 kW	Degree of protection	IP 55				

Figure B.1: Pump main characteristics

LOWARA
a xylem brand

3SV25FL022T

1016LA31F

Hydraulic data

Operating Data Specification		Hydraulic data (duty point)		Impeller design	
Flow	0.745 l/s	Flow	0.745 l/s	Impeller R	0 mm
Head	110 m	Head	110 m	Frequency	50 Hz
Static head	0 m	MEI >= 0,7		Speed	2900 1/min

Power datas referced to:
Water [100%] ; 277K; 1000kg/m³; 1.57mm²/s
Performance according to ISO 9906 - Annex A

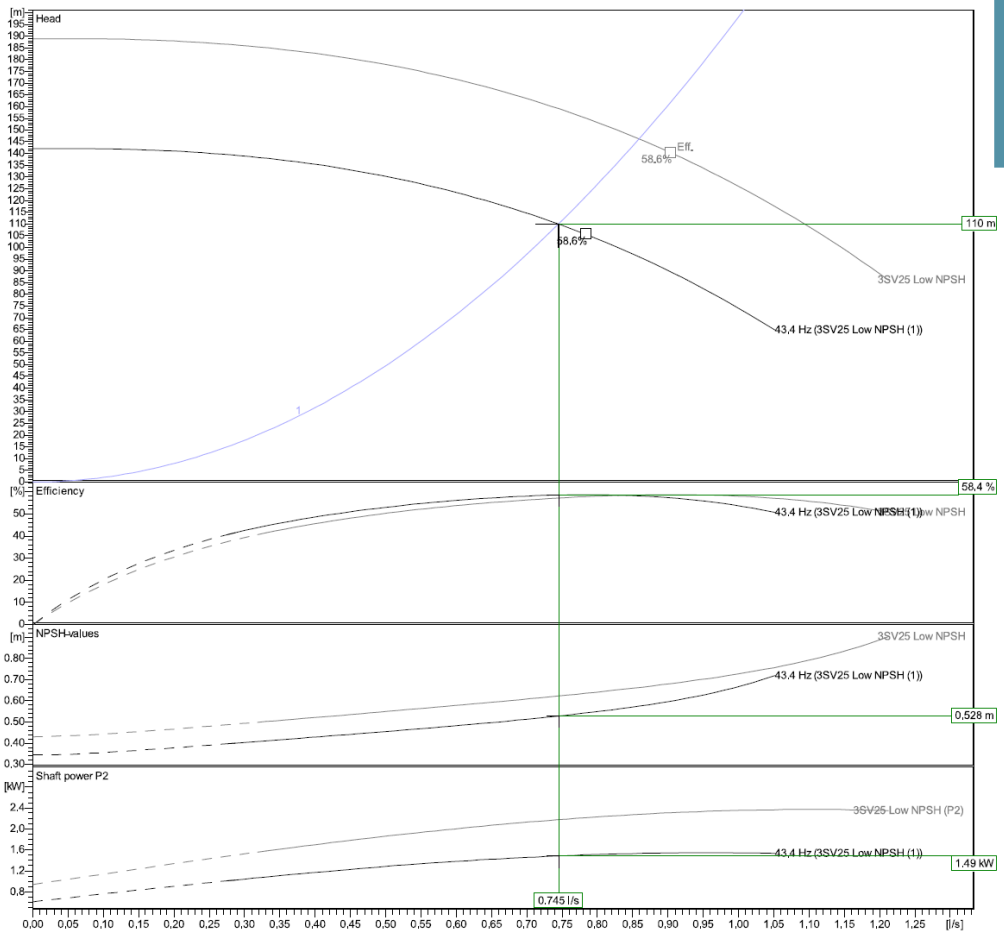

Figure B.2: Pump curves

LOWARA
a xylem brand

3SV25FL022T
1016LA31F

Drawing

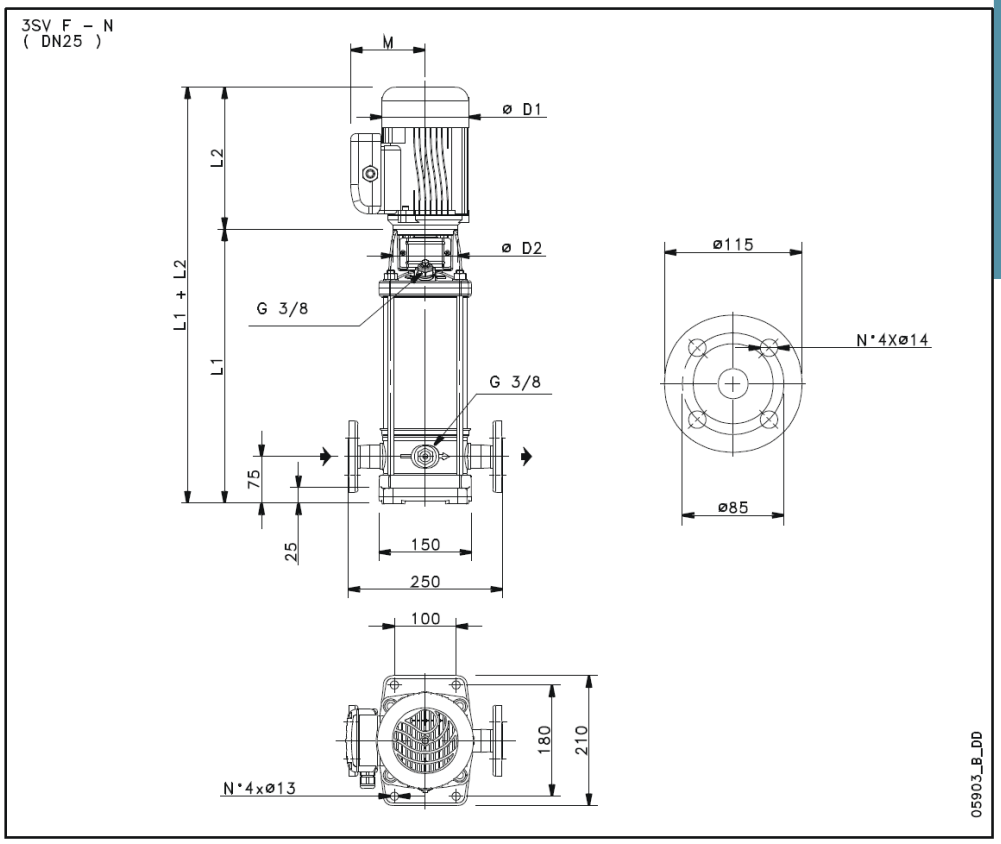

Dimensions mm

D1 D2 L1 L2 M	178 140 738 268 137					Weight 34,8 kg

Figure B.3: Dimensional data